



*Ministry of Higher Education
And Scientific Research
University of Kerbala
College of Engineering
Mechanical Engineering Department*

*Investigation the performance of thermoelectric
generator coupled with solar pond.*

A Thesis

**Submitted to the College of Engineering / University of Kerbala in Partial
Fulfillment of the Requirements for the Degree of Master of Science in Mechanical
Engineering, Thermo-fluid Mechanics**

**By:
Basim Sachit Atiyah
(B.Sc. University of Kufa 2008)**

Supervisors

**Asst. Prof .Dr. Mohammed Hassan Abbood
Dr. Hayder Noori Mohammed**

بِسْمِ اللَّهِ الرَّحْمَنِ الرَّحِيمِ

هُوَ الَّذِي بَعَثَ فِي الْأُمِّيِّينَ رَسُولًا مِنْهُمْ يَتْلُوا عَلَيْهِمْ
آيَاتِهِ وَيُزَكِّيهِمْ وَيُعَلِّمُهُمُ الْكِتَابَ وَالْحِكْمَةَ وَإِنْ كَانُوا
مِنْ قَبْلُ لَفِي ضَلَالٍ مُبِينٍ

صدق الله العلي العظيم

(الجمعة - الآية 2)

Examination committee certification

We certify that we have read the thesis entitled " *Investigation the performance of thermoelectric generator coupled with solar pond* " and as an examination committee, we examined the thesis of the student " *Basim Sachit Atiyah* " in its content and in what is connected with it and that, in our opinion, it is adequate as a thesis for the degree of Master of Science in Mechanical Engineering.

Supervisor

Signature:

Name: Asst. Prof. Dr. Mohammed Hassan Abbood

Date: 13/9/2023

Supervisor

Signature:

Name: Dr. Hayder Noori Mohammed

Date: 13/9/2023

Member

Signature:

Name: Asst. Prof. Dr. Hayder Jabbar Kurji

Date: 13/9/2023

Member

Signature:

Name: Asst. Prof. Dr. Akeel Abbas

Mohammed .

Date: / / 2023

Chairman

Signature:

Name: Prof. Dr. Abbas sahi shafef

Date: / / 2023

Signature:

Name: Asst. Prof. Dr. Hayder Jabbar Kurji

Head of the Department of Mechanical Engineering

Date: 13/9/2023

Signature:

Name: Prof. Dr. Laith shakir Rasheed

Dean of the Engineering College

Date: / / 2023

Supervisors' Certification

We certify that this thesis entitled "*Investigation the performance of thermoelectric generator coupled with solar pond*" was prepared by *Basim Sachit Atiyah* under our supervision at the Mechanical Engineering Department / College of Engineering / University of Kerbala, in partial fulfillment of the requirements for the degree of Master of Sciences in Mechanical Engineering thermo-fluid.



Signature:
Asst. Prof. Dr. Mohammed Hassan Abbood
Date: / / 2023

Signature: 
Dr. Hayder Noori Mohammed
Date: / / 2023

Linguistic certificate

I certify that the thesis entitled "*Investigation the performance of thermoelectric generator coupled with solar pond*" which has been submitted by **Basim Sachit Atiyah** has been proofread, and its language has been proven to meet the English style.


Signature: 

Name: Dr. Ali A. Abdulrasool

Date: 07 / 18 / 2023

Author's comment

I certify that research work entitled "Investigation *the performance of thermoelectric generator coupled with solar pond* " is my own work. The work has not been presented elsewhere for publication. If a material has been used from other sources, it has been properly acknowledged / referred.

Signature: 

Name: Basim Sachit Atiyah

Date: / / 2023

Dedication

I Dedicate This Modest Effort

To my loyal teachers...

To my dear parents...

To my dear wife...

To my children...

To my brothers and sisters...

To All Whom I Love...

Signature: 

Basim Sachit Atiyah

Date: // 2023

Acknowledgments

To begin with, I would like to thank our creator my lord ALLAH almighty.

*Thanks are due to my supervisors **Asst. Prof. Dr. Mohammed H. Abbood, and Dr. Haidar Nuri Mohammad** for their advice, encouragement and supervision.*

Thanks are also due to the head and staff of Mechanical Engineering Department for all the assistance they gave.

I would like to thank all the kind, helpful and lovely people who helped me directly or indirectly to complete this work, and I apologize to them for being unable to mention them by name here.

I would also like to thank my friends for their support and help to complete this work.

Thanks are also due to my family for their patience, support and help to complete this work.

Basim, 2023

Abstract

The sun is regarded as a clean, free, and easily accessible energy source. Solar collectors, solar ponds, and solar desalination devices are just a few examples of the varied uses of solar energy.

In the current study, solar energy was collected and stored in a graded salt solar pond Magnesium sulphate salt was used in this study. Using Square Channel TEG, this energy was recovered from the solar pond and used to generate electricity. experimental test was if adding gravel would increase the amount of heat retained in the pond. Furthermore, concave reflecting mirrors with a thickness of 3 mm were placed to concentrate the intensity of solar radiation on the pond's surface.

The model was using a pyramidal-shaped, inverted pond as this shape is the most common in solar ponds with base area of 0.64m^2 . And surface area of 6.25m^2 , and a depth of 1.35m. The pond walls are inclined at an angle of 60 degrees.

Theoretical findings by using MATLAB version 2014 by entering the required data and equations used in previous research's to calculate the temperatures inside the layers of the solar pond have shown that salt addition improves heat storage in the pond's bottom layer. The amount of solar radiation that is reflected by the mirrors increases the amount of thermal energy that is absorbed through the pond's layers. (plastic and glass) cover that has been placed on the pond's surface reduces thermal energy losses. The quantity of useful energy rose from 2.3 to 22 kilowatts after salt, a cover, mirrors and gravel were added to the traditional pond. These changes also helped the pond's thermal efficiency to rise from 5 to 32 percent. With a mass flow rate of 2 liters per minute and a temperature of $60\text{ }^\circ\text{C}$, TEG's electric power and efficiency was 121.5 W and 12%, respectively.

According to the experimental results, the addition of a plastic or glass cover, reflective mirrors and black gravels increased the operational efficiency of the pond from 3% to 28%. The amount of useful power increased from 2 kW to 20.94 kW. Both power and efficiency achieved 104 W and 9% for TEG, at the bottom layer temperature of $60\text{ }^\circ\text{C}$.

It was found by the obtained results and by the analysis of the error percentage that the theoretical and experimental results are close with an error of 6%.

Table of Contents

Abstract	i
Table of Contents	ii
Nomenclature	iv
Chapter One: INTRODUCTION	
1.1 Background	1
1.2 Solar energy.....	2
1.3 Solar ponds.....	4
1.4 Salts.....	9
1.4.1 Solubility and Specific Heat Capacity of salt.....	10
1.5 Thermoelectric Generator (TEG).....	11
1.6 Advantages and disadvantages of thermoelectric generator.....	13
1.7 Thesis Layout.....	13
1.8 Aim on This Work.....	14
Chapter Two: Literatures Review	
2.1 Experimental Researches	15
2.2 Theoretical Researches	24
2.3 Summary of Literatures Review.....	27
2.4 Scope and Objectives of Present Work.....	31
Chapter Three:Mathematical Modeling and Computational Program....	
3.1 Mathematical Modeling.....	32
3.2 Assumptions.....	33
3.3 Solar Irradiation Calculations in Kerbala city.....	34
3.4 Thermal Analysis of Upper Convective lower.....	36
3.5 The amount of energy reflected by the reflecting mirrors.....	41
3.6 Useful Thermal Energy of Solar Pond.....	41
3.7 Overall Thermal Efficiency of Solar Pond.....	42
3.8 Electric power and Efficiency of TEG.....	43

3.9 Building Computational Program.....	45
Chapter Four: Experimental Work.....	
4.1 Experimental Rig Construction	47
4.2 Thermoelectric Generator TEG.....	53
4.3 Secondary Devices.....	56
4.4 Experimental Measurement Devices.....	57
4.5 Experimental Procedure.....	60
4.6 Experimental Calculations.....	61
Chapter Five: Results, Discussion and Comparison.....	
5.1 Comparison of the experimental and theoretical	63
5.2 Theoretical Results.....	65
5.3 Experimental Results.....	73
5.4 Comparison of the experimental and theoretical.....	80
5.5 Validation with previous work.....	82
Chapter Six: Conclusions and Recommendations.....	
6.1 Conclusions.....	84
6.2 Recommendations.....	84
References	85
Appendices	89

Nomenclature

Symbol	Description	Units
A	Surface area of pond	m ²
A _{TEG}	Area of thermo element	mm ²
B _f	The amount of radiation falling	W/m ²
C	Salt concentration	%
C _p	Heat specific	KJ/Kg. C
G _f	The amount of radiation reflected	W/m ²
H _o	Daily global solar radiation on the solar pond surface	W/m ²
H _x	Solar radiation that enters deep into the layers of the pond	W/m ²
H _{ex}	The extraterrestrial daily solar radiation on a solar pond	W/m ²
H _u	Solar radiation inside upper zone	W/m ²
H _n	Solar radiation inside middle zone	W/m ²
H _L	Solar radiation inside lower zone	W/m ²
hc	Convection heat transfer coefficient	W/m ² .k
I	Current of TEG	A
I _{on}	Constant irradiation intensity	W/m ²
I _{SG}	Solar constant	W/m ²
I _o	Hourly global solar radiation on the solar pond surface	W/m ²
k	Thermal conductivity of layer	W/m. k
L	Length of thermo element,	mm
L _f	The reflector's length	m
ML _f	The side length of the reflector	m
m _s	Mass of water	Kg
N	Number of couples	---
n	Day for year	Day
$\frac{n}{N}$	The ratio sunshine duration	---

Pa	Partial pressure	mmHg
P_{TEG}	Electrical power generated	W
Q_u	Useful energy	W/m ²
Q_{cond}	Conduction heat transfer	W/m ²
Q_c	Convection heat transfer from upper zone	W/m ²
Q_r	Radiation heat transfer from upper zone	W/m ²
Q_{loss}	Heat losses	W/m ²
Q_{ext}	Heat extraction from pond	W/m ²
SM_f	The reflector's projection area	m ²
T	Absolute temperature.	°C
T_{sky}	Sky temperature	K
T_a	Ambient temperature	°C
T_h	Hot junction temperature	°C
T_c	Cold junction temperature	°C
Δt	Time period	Hour
U_f	The amount of solar radiation incident	W/m ²
V	Voltage of TEG	V
v	Volume	m ³
x	Thickness	m
ZY_f	The front side of the reflector's projection area	m ²
ZT	Figure of merit	---

Greek Symbols

Symbol	Description	Units
ρ_{Ω}	Electrical resistivity of thermo element material	cm
η_{TEG}	Efficiency of TEG	%
ρ_S	density of the brine	
α_p	Seebeck coefficient of P type TEG leg	W/m. K
α_n	Seebeck coefficient of N type TEG leg	W/m. K
θ_f	The angle between ZY_f and the reflector	°
α_f	The angle between the horizon and the incident light	°
v	Wind speed	m/s
α	Seebeck coefficient of TEG	$\mu V/k$
δ	The angle of solar declination	°
ω_S	The angle of sunset hour	°

Abbreviation

Symbol	Description
LCZ	Lower Convective Zone
MgSO ₄	Magnesium Sulfate
NCZ	Non-Convective Zone
NaCl	Sodium Chloride
Na ₂ CO ₃	Sodium Carbonate
TEG	Thermoelectric Generator
UCZ	Upper Convective Zone

Chapter One

Introduction

CHAPTER ONE

INTRODUCTION

1.1 Background

Renewable energy is turning to be a more crucial source of energy result to the increase in the price of crude oil and the growth in greenhouse gas emissions from the burning of fossil fuels. The vast majority of our electricity is produced by fossil fuels so renewable energy production offers humanity a long-term future because there is only a finite amount of fossil fuels that cannot meet the huge consumption of large population growth. Figure 1.1 shows the global carbon dioxide emissions from 1850 to 2030. This is because fossil fuels are used to cover our energy needs. Global warming is mostly brought on by carbon dioxide emissions into the atmosphere that result from human activity. To protect the earth for future generations, dependence on fossil fuels must be reduced. The production of power from renewable energy is more environmentally beneficial. Instead of the fossil fuels, renewable energy sources can meet all of our energy needs.

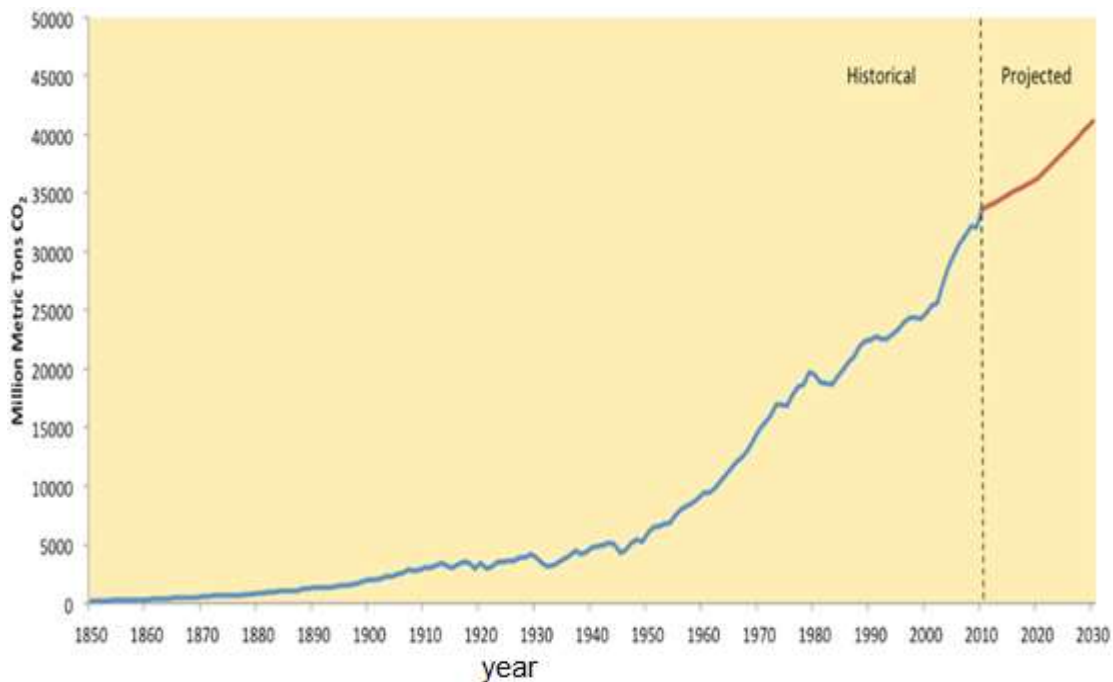
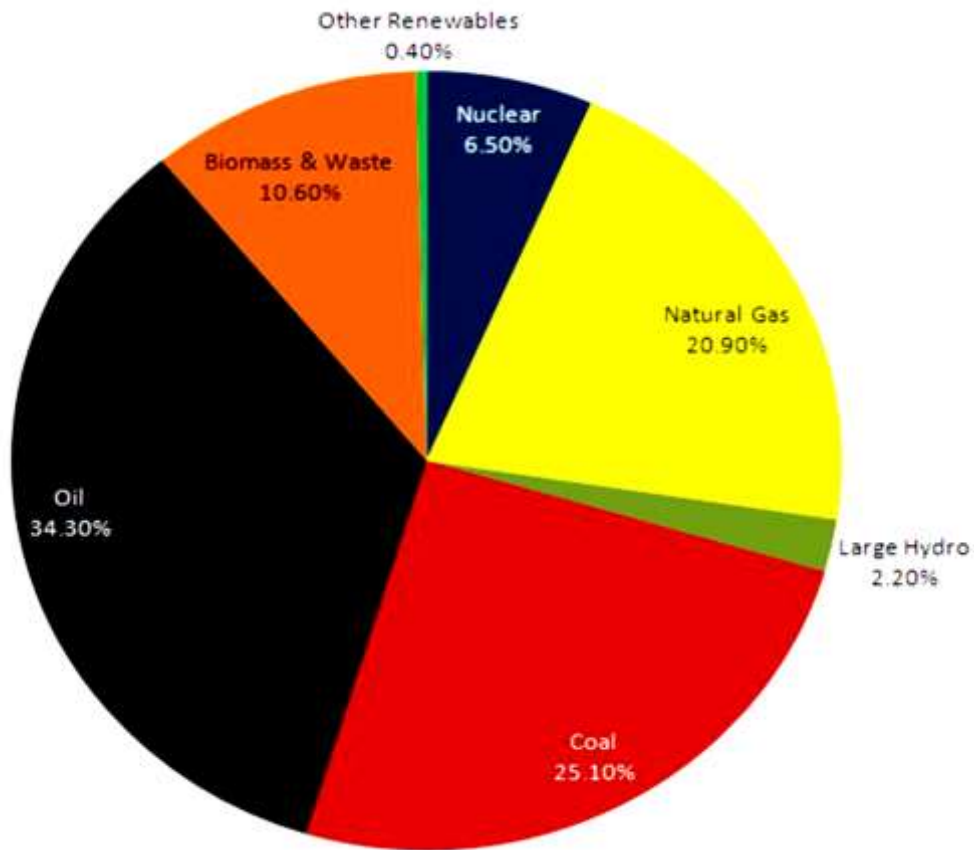


Figure 1.1 (Oak Ridge) National Laboratory's (Carbon Dioxide) Information Analysis Center (World Energy Outlook, 2012) [1]

Figure 1.2 shows that fossil fuels providing 81 percent of world energy generation, while renewable energy sources providing just 19 percent of global energy generation.



Energy Resources (TWh)	1973 (%)	2004 (%)	2010 (%)
Coal	38.3	39.6	40.6
Natural Gas	12.1	19.5	22.2
Nuclear Energy	3.3	15.6	12.9
Oil	24.7	6.6	4.6
Total Amount of Nonrenewable Energy Resources	<u>78.4</u>	<u>81.3</u>	<u>80.3</u>
Hydro Energy	21.0	16.4	16.0
Other	0.6	2.3	3.7
Total Amount of Renewable Energy Resources	<u>21.6</u>	<u>18.7</u>	<u>19.7</u>

Source: Prepared using International Energy Agency data.

Figure and table 1.2 Energy Generation on a Global [1]

Fossil fuels currently account for most of our electricity needs. There are various ways that renewable energy sources can satisfy our energy needs. One of the primary sources of renewable energy is solar energy. Solar energy can be thought of as an endless supply of energy that can never run out. Using solar energy has positive effects on the economy, society, politics, and technology. Solar energy generation has advanced significantly during the past ten years, particularly in wealthy nations. This illustrates how popular this technology is becoming. Most of the energy produced in Europe, the United States, and the Asia-Pacific are produced by Japan and China, with Germany leading the pack, followed by Spain and Italy. Any energy source's advantages must be assessed in terms of their immediate and long-term effects on the environment and human life, besides their economic value. Most developing countries are in Africa and the Middle East, with some countries in Asia and South America. Lack of advanced technologies and financing are delaying the full use of this energy [2].

The following are some advantages of using concentrated solar energy:

- 1- the absorber device is made of expensive materials while the light is reflected into it using considerably less expensive materials.
- 2- reduces the absorber surface area and, as a result, expenses .
- 3- it makes it possible to reach significantly higher temperatures (over 500 °C).
- 4- important when storing thermal energy in solar ponds that are used to produce electricity.

1.2 Solar ponds

Solar ponds are a potential choice now that there has been a repeated emphasis on eco-friendly energy generation and storage technology. Most solar thermal energy systems used today produce heat by using solar radiation to raise the temperature of water in a collector before pumping it to an external storage tank. These two qualities are combined in a solar pond, which is a simple, low-cost method of generating and storing heat. A low-cost solar collector with a large thermal storage capacity is a solar pond with a salinity gradient. Solar

ponds have long been a simple and cost-effective way to get solar energy that can generate power instead of fossil fuels. The thermoelectric generator (TEG) is characterized by its ability to operate at lower temperatures, such as thermal energy from solar ponds, although the method still requires a temperature difference on both sides of the thermoelectric generator [2].

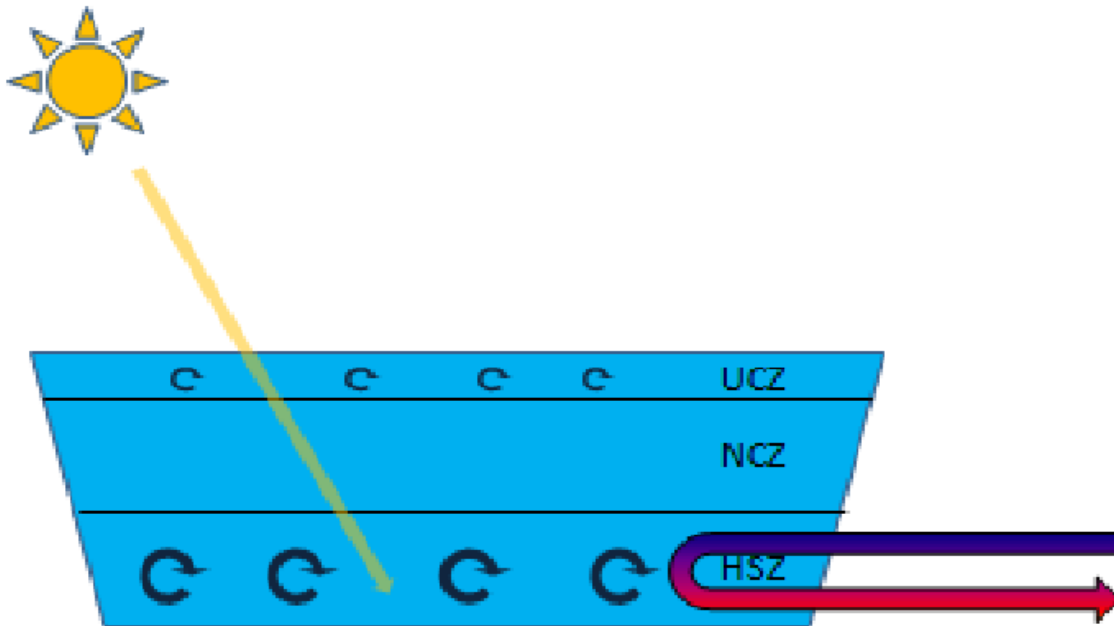


Figure (1.4) A solar pond with a salt gradient in a simplified diagram [2]

Solar ponds exist in a range of sizes and shapes, but they all have the same function: capturing solar energy and storing it for use at a later time. Because of its lower density, heated water by solar radiation would typically rise to the pond's surface and transfer its heat to the surrounding air through convection and evaporation, allowing the water to remain at a temperature close to that of the surrounding air. The idea behind solar ponds is to stop water from evaporating and convecting away its heat content into the atmosphere. In shallow solar ponds, this is accomplished by covering or separating the water. In salinity gradient solar ponds, it is accomplished by sprinkling the water with salt or brine without mixing it. By increasing the density of the heated water and preventing it from rising to the surface, even at temperatures close to boiling, this results in stable zones with variable salt concentrations. The salt water can now be pumped away or a heat exchanger can evaporate

or heat liquid using the hot salt water to extract the heat from the bottom layer. Salt-gradient solar ponds also have the advantage of being able to create both fresh and salt water, which is helpful in hot and dry conditions. Overall, salt-gradient solar ponds could be a low-tech solution for producing heat, electricity, and possibly fresh water in developing and even industrial countries. This is because energy storage is becoming more and more important due to renewable energy sources have low energy densities and unstable availability [4].

1.3.1 Solar Ponds Classification

Solar ponds are divided into two types: convective and non-convective ponds, as shown in figure (1.5).

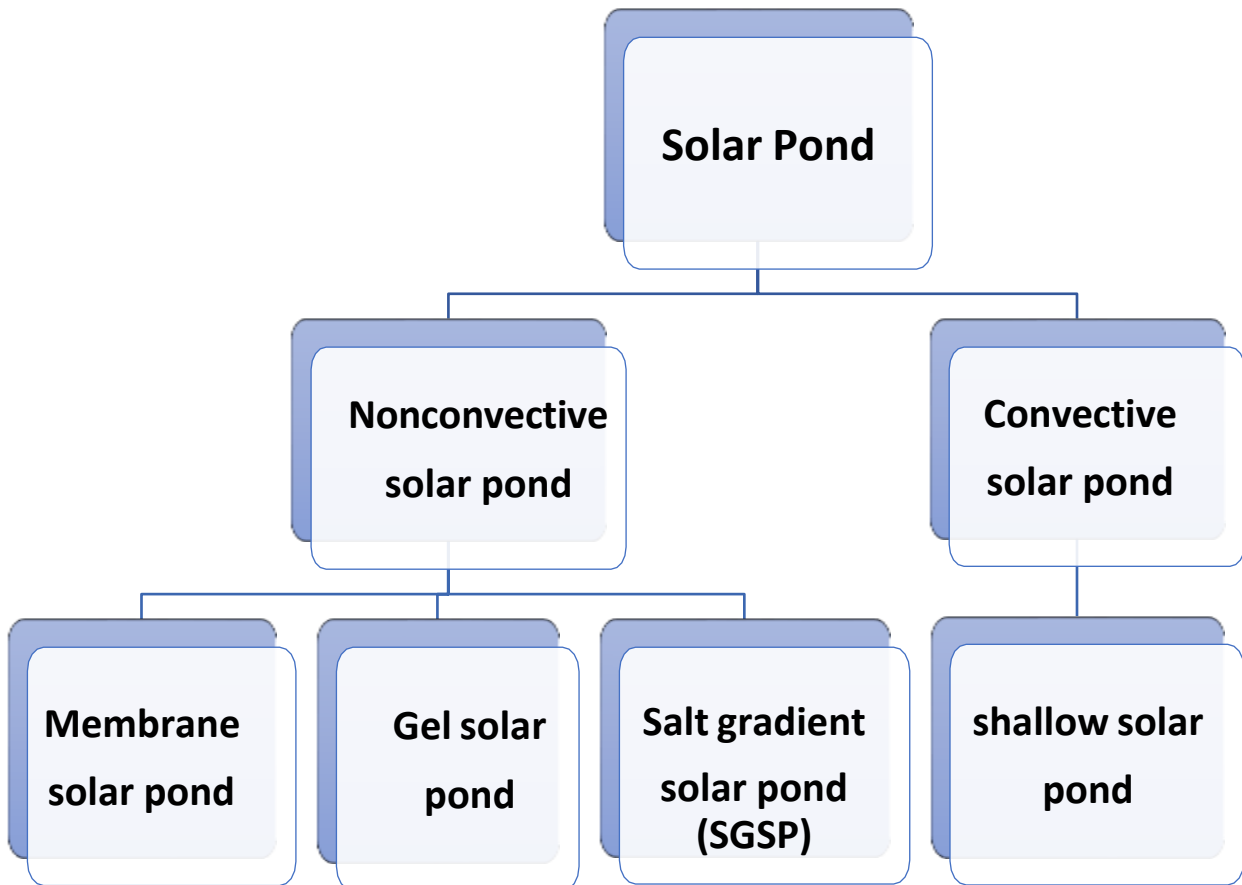


Figure (1.5) Schematic Diagram of the Solar Ponds Classification [2].

1.3.1.1 Convective Solar Pond

There is no evaporation of the pond water in this form. As a result, heat loss will be decreased. The small solar pond illustrated is the greatest example of this sort of pond. It's a basin of salt-free water that's covered with a translucent plastic or glass sheet to keep the water from evaporating while allowing convection to happen. This style of pond has a black liner to absorb the maximum amount of solar radiation while also preventing water leaks. Solar radiation is used to heat the water during the day in this sort of pond, and the stored heat is recovered at night by transfer the heated water to an external tank. The reason this sort of pond does not develop is that some of the heat is lost when the hot water is moved to the exterior tank [3].

1.3.1.2 Non-Convective Solar Pond

The type of solar pond is determined by the properties of the brine (water and additives). No convection occurs at the pond surface with this form, since there is no connection between the water's surface and the surrounding air. The two main types of non-convective ponds are membrane ponds and salt gradient ponds. The first type is distinguished by a translucent membrane that divides the pond's layers and lets sunlight pass through. The second form of solar pond, known as a salinity gradient solar pond, comprises three layers of water with varying salt concentrations. Because of the density that salt gives the water, the most concentrated layer of salt sinks to the bottom of the pond. To enhance the ability to absorb sunlight, heat is produced when the energy from the sun's rays is absorbed by the water's surface. The bottom of the pond heats and reaches temperatures above 90 degrees Celsius. [4]. The lowest layer of the solar pond, where the salt is collected, is the densest layer. It has the highest temperature of the other layers. The bottom layer of the pond may provide thermal energy that a heat exchanger can harvest and use for a variety of purposes. The third type of non-convective solar pond is the gelatinous pond, which has a layer of gel on its upper surface to prevent water from evaporating and maintain a high pond temperature. This suggests that the maximum amount of thermal energy will be stored, according to [4]. Another approach for reducing or preventing heat losses from the bottom layer of the pond is to replace the middle layer with a gel that acts as a thermal insulator, [5]. The salinity

gradient solar pond and the gel solar pond are depicted in figures (1.6) and (1.7), respectively.

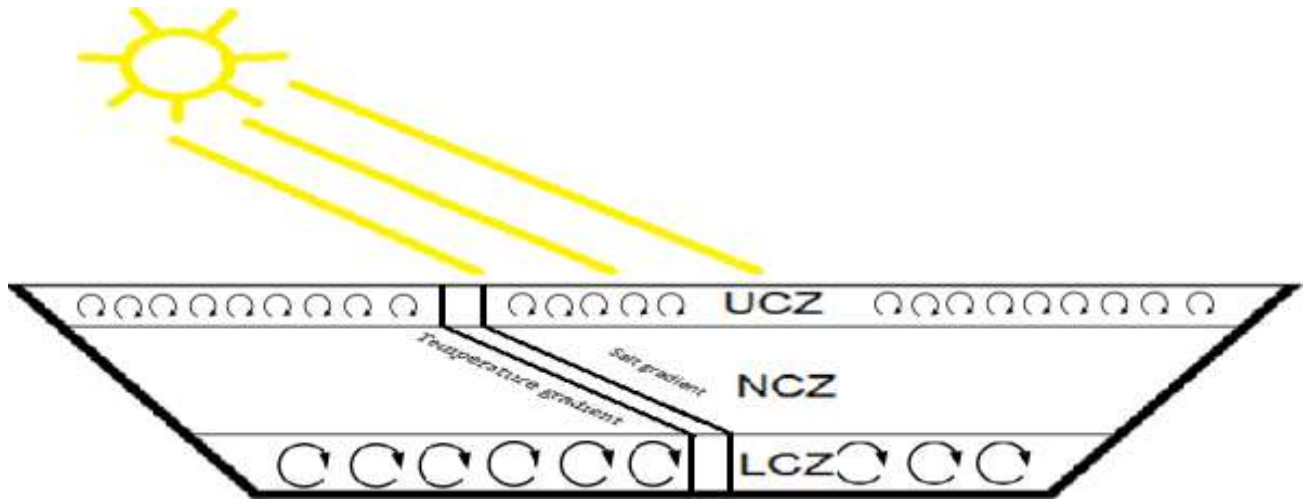


Figure (1.6): The salinity gradient solar pond [5].

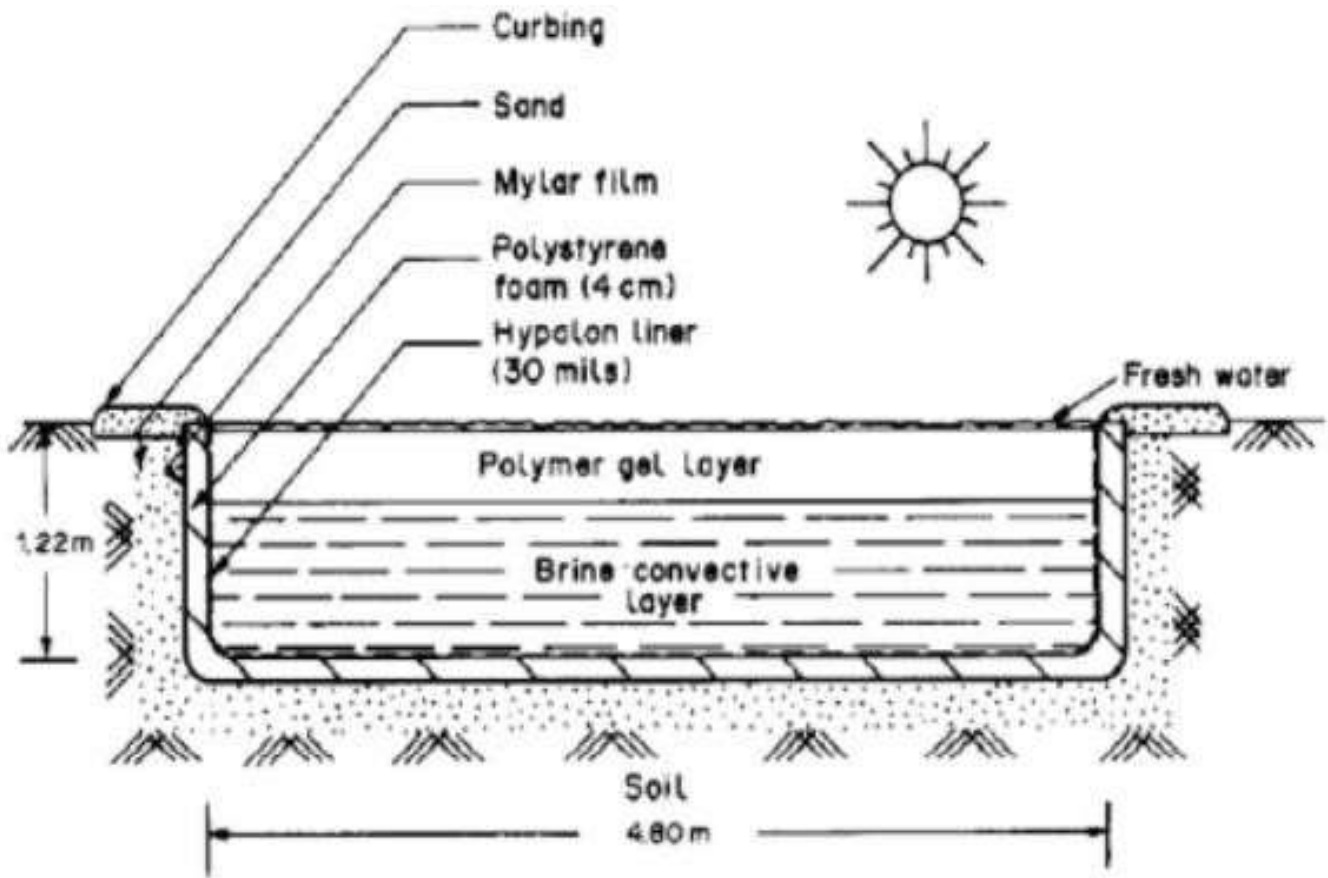


Figure (1.7): Gel Solar Pond [5].

1.3.2 Advantages of Solar Pond

The following are some of the benefits of a solar pond [6]: -

1. Low running costs.
2. Feasibility of construction,
3. High thermal storage capacity due to the property of the brine inside the pond.
4. Low temperature applicability for a wide variety of applications,
5. The salt used may be recovered and returned to the pond with all its advantages.
6. Low construction costs for solar ponds.

1.3.4 Disadvantages of Solar Pond

1. Any hole in the liner leads to leakage of the salty pond water and thus to the pollution of the surrounding soil
2. Wind, especially in arid places, can damage pond surfaces and increase evaporation rates [6].

1.4 Salts

Many factors, both external and internal, affect the performance of a solar pond, including dust, salt, wind speed, ambient temperature, layer thickness, and more. The purpose of the brine is to limit the movement of heat between the layers and save it in the bottom layer of the pond. This is done based on the properties of the brine to reduce the load caused by the high temperature in the pond bottom area [7]. To reach a specified solution density, a salt's solubility in water must be high. The solubility of the salt should not be affected by temperature fluctuations in the solar pond. The salts should have no detrimental consequences on the human health or the environment. They must also be inexpensive and always available [7]. The parameters of several salts used in solar ponds are listed in Table (1.1). (sodium chloride, sodium Sulfate and magnesium Sulfate).

Table (1.1) Properties of Some Salts Used in Solar Ponds [8].

Salt Name	Molecular formula	Density g/cm ³	Solubility in water g/100 ml	Specific heat J/ kg. k	Potential risks
Sodium chloride	NaCl	2.16	36.3	88	NO
Sodium Sulfate	Na ₂ SO ₃	1.46	49.7	117	NO
Magnesium Sulfate	MgSO ₄	2.66	35.1	126	NO

1.4.1 Solubility and Specific Heat Capacity of salt

Salt performs a full homogeneity process between its atoms and molecules since it dissolves in water. Here salt is the dissolved substance and water is the solvent, [19]. The positive sodium ion and the negative chloride ion together form sodium chloride salt. The salt dissolves quickly in water because positive sodium ions attract negative chloride ions, and positive water ions attract each other.

As the salt dissolves in the water, the water's thermal properties will change. Fresh water molecules, which resemble polymer chains, conduct heat far more quickly. The amount of thermal energy needed to raise one kilogram of water by one degree will decrease consequently, which will cause a decrease in the specific heat capacity. Seventy-seven percent of the salts in the seas and oceans are sodium chloride, which is stable at 60 degrees Celsius [8].

1.5 Thermoelectric Generator (TEG)

Scientists are focusing on enhancing energy-harvesting power generators. Thermoelectric generators have proved their ability to convert thermal energy directly into electric power. TEGs are ecologically friendly, operate silently since they lack mechanical motors or spinning parts. They may be made from several materials, including silicon, polymers, and ceramics. TEG modules will revolutionize the conversion of thermal energy to electrical energy in the future. TEG functioning requires no specific heat source; heat transfer from gas, liquid and radiation can all be used to power them. When linked to an external load, the TEG module may generate thermoelectric power [9]. The Seebeck effect, which turns heat into electricity, and the Peltier effect, which turns electricity into heat, gives thermoelectric power sources their name. The electron is a thermoelectric generator's functional component. A TEG is hence silent, safe for the environment, and devoid of moving parts. TE generators are as dependable as PV and may operate for an average of 10 to 30 years without experiencing serious technical issues [10]. The fundamental building block of a thermoelectric (TEG) is a series electrical connection between two n- and two p-type semiconductor thermoelements. The module is made up of many main structures sandwiched between two ceramic plates and electrically coupled in series but heated in parallel [11]. The output power and conversion efficiency of semiconductors, which are used to make modern thermoelectric converters, are superior to those of metal alloys. The fact that semiconductors are often no ductile crystalline solids makes it difficult to construct the thermocouple junction. The quality of thermoelectric materials used for the Seebeck effect or Peltier effect cooling (refrigeration) is determined by three intrinsic material properties: electrical conductivity, Seebeck coefficient, and thermal conductivity. Both the cooling and power generation processes include the passage of electrical current. High electrical conductivity materials are hence useful. A significant Seebeck coefficient is necessary because a significant generated voltage per unit temperature gradient is desired [40]:

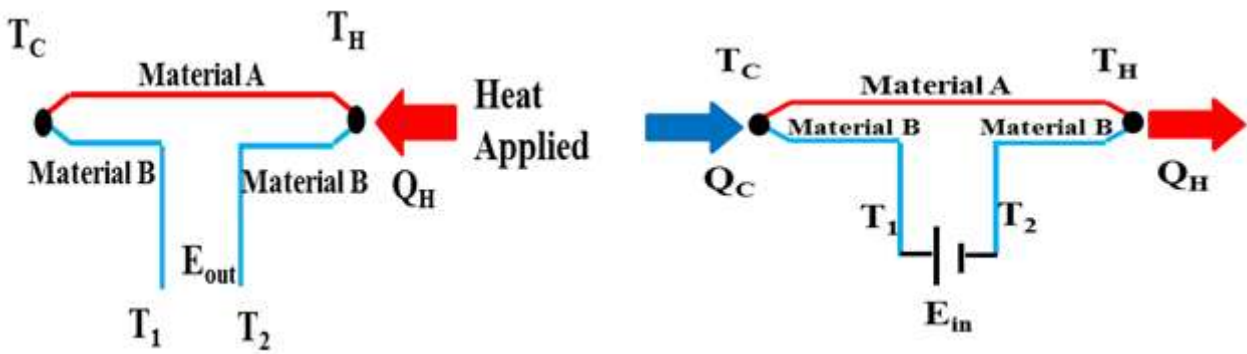


Figure (1.9) Illustrative representation of: a. Seebeck effect b. Peltier effect [12].

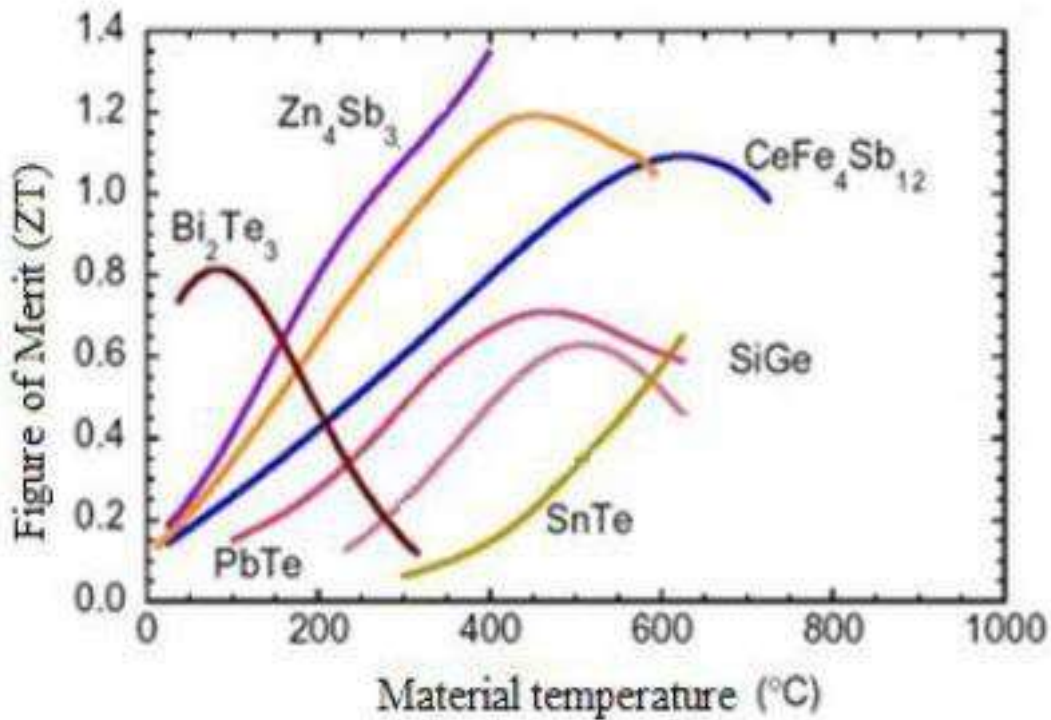


Figure (1.10) Relation between ZT of the Thermoelectric module materials and temperature [13].

The number of thermocouples, the cross-sectional area, and the length of the thermal element are all factors in thermoelectric engineering. For various temperature differences, the conversion effectiveness of the thermoelectric module versus the length of the thermoelectric elements depends on the properties of thermoelectric materials. When the heat source is cheap or practically free, as in the case of waste heat recovery or

energy harvesting, a long thermal element is needed for higher conversion efficiency, whereas a relatively short thermal element is needed for greater power output [13].

1.6.1 Advantages of thermoelectric generator [14].

- 1.Solid-state electronics that don't use liquids for cooling or fuel.
- 2.Are completely static.
- 3.Working in challenging conditions.
- 4.More trustworthy.
- 5.Do not require prolonged upkeep.
- 6.Environmentally responsible.

1.6.2 Disadvantages of thermoelectric generator [14].

TEG compounds are expensive because they include rare elements, and their normal efficiency is only about 5-8%.

1.7 Thesis Layout

- Chapter 1 (Introduction)

A review of the energy sources, the techniques used to collect them, and the function of the devices connected to the solar pond and thermoelectric generator.

- Chapter 2 (Literature Review)

It includes a review of previous research on the topic of the solar pond, thermoelectric generator and the factors affecting its efficiency.

- Chapter 3 (Theoretical Part)

It presents the software used to apply mathematical relationships to calculate the temperatures within the pond layers and thermoelectric generator and the useful energy and efficiency generated by the pond.

- Chapter 4 (Experimental Work)

It introduces the stages of solar pond constructing and connect it to the thermoelectric generator, as well as the experimental work and rig testing steps.

- Chapter 5 (Results and Discussion)

It includes of the findings and a discussion, and comparison between of theoretical and experimental results.

- Chapter 6 (Conclusions and recommendations)

The thesis conclusions presented, and the recommendations for future research are suggested.

1.8 Aim on This Work

The main objective of this project is to investigate the performance of a solar pond electric power generation system using thermoelectric generators in the holy city of Karbala, Iraq, and to generate electric power from it experimentally. Also it studies the possibility of increasing the utilization of solar energy by using salts and reflective mirrors. Here are the desired objectives of this work:

- TEG heat exchanger design suitable for very low driving temperature differences.
- Knowing the effects on the performance of TEG due to the uneven distribution of temperatures.
- Comparison of generation system performance with and without cover, reflecting mirrors and gravel.
- Developing a mathematical model (by using MATLAB) of solar pond system to generate energy by using TEG with natural convection heating.

Chapter Two
Literature Review

Chapter Two

Literature Review

This chapter presents and explores previous work and research on solar ponds and their use for thermal energy storage and conservation. The basics and improvements related to thermal energy storage in solar ponds and their great benefit in using electric power generation, water desalination plants, and other applications are described.

2.1 Experimental Researches

A solar pond with a surface area of 12.25 m² and a depth of 2 m was constructed by **Bezir et al (2008) [15]** in Turkey. The results of providing a leather workshop with hot water with and without covers were similar, but reflectors during the day increased the heating area, and these reflectors are foldable and work at night as a cover to reduce heat loss. According to the principle, there is a direct relationship between the size of the solar pond and its efficiency. Variable air temperature values are derived from analytical functions and used in theoretical model simulations. They identified the parameters that affected the solar ponds. It was discovered that the cover has no effect on the performance of the solar pond when it is used only at night, as it acts as a layer that prevents the heat entering the pond from escaping. But when utilized as reflectors, covers are incredibly effective. When compared to the uncovered condition using covers plus reflectors, the temperature of the LCZ of the solar pond increases by approximately 25%.

The solar ponds' upper and bottom halves can range in temperature by up to 40°C **Singh. et al (2012) [16]**. studied gradient solar pond power generation at low temperatures and on a small scale in Malaysia. Experimental hot and cold water heaters created from a solar pond that served as an energy storage device could generate 9.56 W of power at 15.67 V and 0.61 A at a temperature differential of 100 °C to 16 °C. Even when there is a slight temperature differential, TEG still produces voltage. These findings show that small-scale solar power generation applications are best suited for electric motors which are small in size.

Singh. et al (2012) [1]. Study brackish solar pond which is one type of solar collector that has the capacity to store thermal energy for an extended period of time at a cheaper construction cost. Temperature up to 80°C, it can capture and store solar energy. Experimental research has been done on a system that uses gravity-assisted heat pipes, such as a thermal siphon, to transfer heat from the bottom region to the hot surface of the thermoelectric modules. Investigation of the performance of a solar pond producing electricity for thermal generators (TEG) is done by placing eight TEGs on each disc in a TEG arrangement. To ensure efficient heat conduction across the TEGs, the discs are made from 1 mm thick aluminum plates. Hot water is kept at 12.7, 29.4 and 37.7°C, while cold water is kept at -3.8°C. Specifically, the results were 0.85, 3.46, and 5.30 watts. The results show that TEGs can generate electrical energy by using the heat from the Salinity Gradient Solar Pond. The designed experimental devices can deliver a maximum power of 5.30 W at 13.4 V and 0.24 A with a temperature difference of 23.8 °C. The results of the research in the current work indicate that there is a great potential for generating electrical energy from small solar ponds through a simple and passive device that includes thermal cells.

Tundee et al. (2014) [18]. Presented a study focused on the use of thermoelectric and thermal siphon devices in combination to generate electricity from solar ponds. The study's aim is to establish the effectiveness of thermophones in heat transfer by constructing a solar pond with a 7 m² surface area and a 1.3 m depth. The temperature of the aquarium was controlled between 40 and 100 degrees Celsius using a heater, and 16 thermoelectric cells were connected to the condenser to create an experimental siphon. Cold water was used to cool the condenser. The ideal temperature for heat exchange in an evaporator is 70 °C. The greater the temperature difference between the upper layer and the lower layer of the solar pond since the lower layer acts as a heat source. Thus the heat transfers through the thermoelectric generator and the greater the voltage generated. Data was collected every 10 minutes. 1st August 2010. The highest voltage obtained from the thermoelectric generator is 234.25 mV.

Singh et al. (2014) [19], constructed a graded salt solar pond in Malaysia. The proposed system is capable of producing electricity even on cloudy days or at night as the brackish solar pond acts as a heat storage system. The goal is to use thermoelectric generators to produce energy from the heat of the solar pond. In this experiment, hot water in the lower layer of the pond and cold water in the upper layer are used to generate energy using a thermoelectric generator system. Thermoelectric generators can operate at very low temperature differences and can be a good candidate for replacing organic order cycle engines for power generation. The temperature difference in the solar pond can be used to drive thermoelectric generators to produce electricity. The results obtained showed great potential for this system to generate power from low temperature for power supply systems in remote areas. A tube with square cross-section surrounded by 60 TEG and immersed in water inside the bottom layer of the pond, the water flows into the tube at a rate of 1.75 and 10 kg/min, respectively. Voltage difference, TEG, temperature difference, and flow rate all have a linear connection with each other. The power output rate of the TEG increases with the increase of the temperature difference between the two sides of the TEG.

Assari et al (2015) [20], study examined various solar pond designs at two salinity levels. To improve the solar pond's effectiveness, two alternative solar ponds (rectangular and circular) were built over the three-month summer trial period. The pond's surface was covered with plastic. Where the findings indicated that using plastic sheeting to cover the pond's surface caused the water's temperature to rise. The modest shadow area that was created in the rectangular pond is what caused this discrepancy. The findings showed that the maximum temperatures of the rectangular and circular solar ponds were 74°C and 71°C, respectively, with respect to the shade regions generated in both ponds. The glazed plastic top keeps heat from escaping the pond, which helps keep solar ponds sustainable and easy to maintain. At the conclusion of the test, this resulted in a 13 °C temperature difference between the UCZ in the solar ponds and the ocean, resulting in a smaller top-to-bottom temperature differential. It was determined that the dusty weather decreased the temperature in the sun ponds and had a detrimental impact on the solar ponds' ability to generate energy.

In the research of **Qarroot. (2015) [21]**, an experimental shallow solar pond (SSP) with an area of $1 * 1 \text{ m}^2$ and a depth of 20 cm was built in July 2015. Solar evaporation ponds are very suitable especially for the disposal of brackish water from inland desalination plants in arid and semi-arid regions due to Solar abundance. Almost all forms of salt production require evaporation of the brine so that it eventually produces salt crystals. In this study, three cases of a solar pond were tested: the first was a solar pond without using any mirror, the second was using a solar pond using one reflective mirror, and then a solar pond using two reflective mirrors over a period of five days. The mirrors were installed using a manual system to control their movement according to the different angles to become more effective by reflecting and increasing the thermal energy on the surface of the brine inside the evaporation pond. The researcher concluded that using two mirrors is more effective than using one. and, the use of mirrors reduces the required area of land by collecting solar energy and reflecting it using mirrors directly on the surface of the pond.

Singh (2015) [22], discussed an experimental result with a thermoelectric generator and primary heat exchanger for generating electricity from a solar pond in Malaysia using a square steel conduit 50 mm x 50 mm x 600 mm with TEGs mounted and arranged in rows of 10 TEGs occupying an area of 40 mm x 400 mm on each side of the square duct. Electricity can be generated up to 7.02 Watts by 40 TEG. Square duct and acrylic tube were used to recreate LCZ and UCZ solar pond conditions using hot and cold water. Hot water temperature ranges from 40°C to 90°C. The intake and exit on each end of a 90 mm diameter acrylic tube allowed cold water to enter the heat exchanger. The acrylic tube has a length of 500 mm. The LCZ and UCZ solar pond conditions were replicated using hot and cold water flowing through the square channel and acrylic tube. An adaptable hot water provided the hot fluid. The range of the water's temperature was 40 °C to 90 °C. A pump was used to pump the water into the square channel and out of it so it could return to the tank. The rate of water flow was measured by a flow sensor at the inflow. Tap water was used to supply the cold water that went into the acrylic tube. The result shows that the proposed approach is more suitable for small-scale solar applications.

Balaji. (2016) [23]. Conducted an experimental study on a solar pond (that had dimensions of 0.25 m² and a depth of 0.5 m) in India. This study creates a salt mixture that has a high capacity for absorbing solar energy and a good capacity for storing it so that it may be converted into heat for technologies for producing electricity and desalinating water. The salts, sodium sulfate and sodium carbonate, were chosen as two types with strong solar energy absorption and storage capacities. According to the results of the experimental investigation of the solar pond, mixing these two salts results in a temperature rise of 47 to 60 degrees Celsius in 10 days with an efficiency of 18.68 percent.

Sathish et al (2017) [24]. built a square solar pond in India with dimensions of 1.7 m² and 0.5 m in depth. The walls are made multi layers of plywood and are angled at a 45-degree angle. The interior is insulated with 2 cm of thick polyethylene, while the exterior is covered with 4 mm of thick glass. The goal of the experiment was to compare the energy storage capacities of salt and gravel. Sodium chloride salt was used in the experiment, followed by gravel. The temperature was measured, and it was discovered that salt had a higher heat absorption capacity, reaching 65 C compared to gravel's 45 C. The experiment's temperature shift over time can be seen in the solar pond's temperature distribution with salt (NaCl). At 10 o'clock, when the temperature is almost at its maximum, the temperatures are measured. It is possible to see how the temperature increases over time until it reaches a constant state. About five days later, the solar pond has attained reliable operating conditions. On the sixth day, the temperature reaches a maximum of 62°C, which may be located within the summit of the LCZ. In general, the model accurately predicts the reported temperature trend, which shows that temperatures rose with depth and peaked at the top of the LCZ. The midsection of the UCZ has the largest temperature error, which is approximately 1.7°C. According to the time and depth of the solar pond, the temperature variation keeps growing. The upper convective zone's (UCZ) temperature is consistent with the ambient temperature. The temperature in the non-convective zone (NCZ) continues to rise with passing hours and sun energy. The salt (NaCl) that is held in the lower convective zone (LCZ), where the high temperature is attained, is used for other purposes.

A brackish solar pond was constructed in the Dead Sea area over a period of 3 months using salty seawater as brine by **Al-whoosh et al (2017) [25]**. The volume of the pond is 5 m^3 . The pond's bottom and sides were insulated by two layers of glass-wool with a thickness of $1 \times 10^{-3} \text{ m}$, and a black thermal plastic with a 3 mm thickness was used to offer a maximum amount of sun radiation. Using extremely precise sensors with an accuracy of $0.1 \text{ }^\circ\text{C}$ for a temperature range of $0\text{-}120 \text{ }^\circ\text{C}$, the pond temperature was measured at several levels spaced 0, 15, 30, 60, 90, and 120 cm from the surface to the lower strata of the pond. Every 30 minutes, the temperature was recorded using a data logger. A portable conductivity meter was used to test salinity, and daily computer transfers of the measured data were made. The experimental results showed that the bottom layer had a higher temperature and reached a maximum temperature of $85 \text{ }^\circ\text{C}$ after 100 hours of operation. Desalination plants operating in temperatures below $100 \text{ }^\circ\text{C}$ can make use of this heat to produce electricity. The thermal insulation of the pond succeeded in keeping the boundary insulated and allowing the thermal energy stored in the lower area to be continuously extracted during the day. The cost of salt represents 45% of the total cost of the solar pond, so building ponds near the Dead Sea is a cheaper alternative.

To test the electrical and thermal performance, an experimental study was conducted by **Goswami, et al (2019) [26]** on a 4 m^2 surface area saline gradient solar pond. The goal of the experiment was to examine the variables affecting the solar pond's performance over the course of 30 days, including both sunny and rainy days, salt concentration (C), thermal conductivity (K), density (ρ), specific heat (Cp), and the shape of the solar pond. Ethylene propylene diene monomer, a dark substance that absorbs sunlight, coats the interior of the pond. To act as insulation and lessen heat loss, glass wool applies to the exterior. A reflector was used to raise the temperature of the bottom region. In a range, K reduces as pond depth rises. Compared to water, salt has a greater K value. The heat absorption reaction takes place inside the solution when the internal temperature drops, but it cannot spread because of the drop in K. This leads to the conclusion that the salt content and the thermal conductivity K

are strongly connected. The experiments are conducted during the period of August-September 2018 in Rupnagar, Punjab (30.9659°N, 76.5230°E).

Goswami and Ranjan (2020) [27], conducted an experimental investigation to use a 4m² by 1m deep solar pond insulated with black ethylene and covered with propylene to charge a 12V battery. In the lower zone, sodium chloride is used as salt, and its concentration is 24.01 percent, whereas upper zone contains the normal water with the lowest salt concentration of 0.28%. To increase the concentration of solar radiation, a stainless steel reflector with an octagonal shape was built. Two thermosyphons fabricated of copper sheets of 1 mm thickness are installed inside the pond to transport heat from the lower to the upper portion of each thermosyphon. As the thermal conductivity of glass wool is very low, the outer surface of the solar pond is insulated with glass wool. This will enhance the temperature gain in the solar pond. When the radiation intensity was 976 W/m², and when TEG material, made of bismuth semiconductors, was used for the purpose of converting thermal energy into electrical energy, the temperature of the bottom layer of the pool reached 55 degrees Celsius. Then a potential difference of 1.5 volts was obtained. The H Horiba meter measures salt concentrations up to 10% across several layers directly, while salt concentrations above this limit are estimated by diluting the brine.

Abbood et al (2020) [28], designed an experimental model of a solar pond in Karbala, Iraq, to heat water. The surface area of the pond is 7.29 m² at a depth of 1 m, and its walls are inclined at an angle of 45 degrees. The experiment was conducted in 2020. Two types of salt were used in this work: sodium chloride and potassium chloride. The pond was gradually filled with water, starting with a layer of 0.3 m thickness LCZ that had 10.7% sodium chloride salt added to it. This layer's concentration was raised until the saturation point, or maximum percentage of 26%, was attained. After that, three levels of the NCZ layer were added, each with a thickness of 0.2 m and varying salt concentrations ranging from 2% to 4%, increasing with depth. The UCZ layer, which was 0.1 m thick and salt-free, was then applied. The pond was left for four days to stabilize the temperature inside its

layers. The experimental results showed the efficiency of sodium chloride salt at a concentration of 25% in raising the water temperature in the pond to 44 °C, compared to 40 °C using potassium chloride salt. The useful energy and experimental thermal efficiency of the solar pond were 28.2 MJ and 11.6%, respectively.

Abbood et al (2021) [9]. studied the work of a graduated solar pond with a surface area of 7.29 m² using sodium chloride salt at a concentration of 6.98%. To build a conventional salinity gradient solar pond, sodium chloride salt was added to the bottom layer of the pond at a rate of 75 g/l of water. The lowering of the water's specific heat allows the temperature to rise more quickly, which is the main advantage of adding salt to water. Changes in the temperature of the solar pond should not have an impact on the solubility of salt, which would then have an impact on the performance of the pond. Any salt must have a high solubility in water to obtain the appropriate solution density. Experiments were performed with and without reflecting mirrors and a solar tracking system to increase the concentration of solar radiation on the surface of the pond. It was conducted in Iraq in Karbala (32.55°N, 43.97°E). The results showed that the maximum temperature of the lower layer of the pond with mirrors and a tracker is about 30 degrees Celsius. It was concluded that the use of reflective mirrors alone improves the useful energy, thermal efficiency, and heat storage of solar ponds by 4.6%, 35.5%, and 22.4%, respectively. Whereas using mirrors and trackers together improves solar pond by about 23.8%, 51.7%, and 44.7%, respectively.

2.2 Theoretical Researches

Aramesh et al (2017) [3]. Conducted a theoretical study to determine the quantity of energy produced by a solar pond over long periods of time rather than for instantaneous measurements. Particularly in small ponds, the impact of shadowing is apparent on the pond's ability to store energy. Therefore, for various layers of the pond, these mathematical equations may precisely forecast the quantity of energy entering the body of water. The

results indicate that the theoretical and experimental values are in good agreement with each other when calculating the energy efficiency of the low convective zone of the real pond. The energy efficiency testing data and theoretical results in January, May, and August are respectively 9.68% and 11.38%, 17.54% and 18.92%, and 28.11% and 30.94%. As a result, the modified relations can serve as a useful guide when estimating pond performance prior to construction.

Rizvi. et al. (2015) [29] studied the theoretical part of his dissertation using computer programs about the effect of using deferent technologies, for example placing a cover on the surface of the pond and reflectors on the sides of the solar pond, can increase the efficiency of the solar pond and the amount of radiation entering the pond. The maximum water temperature was around 65°C, an increase of about 28% compared to the normal condition (without the use of a cover on the pond deck and reflectors).

Solar ponds with a salinity gradient can be utilized to store heat by absorbing sun energy. Many industrial applications that call for low-grade heat can then be powered by heat. **Monjezi (2016) [30].** studied theoretically the performance of a solar pond using a computer program. The model includes novel approaches for simulation of both the Heat Storage Zone (HSZ) and the Upper Convective Zone (UCZ) where in addition to convective, evaporative, and radiative heat losses, the cooling effect of adding fresh water to the surface of the pond is taken into account. The top 1 cm of the pond absorbs 22.4% of the incoming radiation in the form of long-wavelength radiation, which causes a rapid rise in the UCZ's temperature. This hot zone then steadily descends to the Non-Convective Zone (NCZ) and, eventually, the High-Stability Zone (HSZ). According to the findings, it would take 65 days for the lower zone water temperature to reach the boiling point if the solar pond were to be begun. This presumption is in line with other studies' experimental findings. While the pond's top layer will require roughly 47 liters of new water daily. It was discovered that the lower zone resistance to heat loss from the layers above it increased with temperature.

Prasad, (2016) [31], conducted a computational simulation using a computer program to comprehend the behaviour of a solar pond and the direction of heat diffusion based on assumptions. The findings showed that the lower layer has a greater temperature (around 53 °C), whereas the upper layer is only about 35 °C. The findings also revealed that the pond's thermal efficiency is at 24%.

Sinha (2018) [32], conducted a study using computer program to model a solar pond with a surface area of 10 km² and a depth of 3 m that would generate roughly 15 megawatts of electrical energy. A Salt Gradient Solar Pond (SGSP) is a sizable body of saltwater with the distinction that a certain salinity profile is fabricated and kept constant. Thermal energy is delivered to SGSP by incident solar radiation. The design capacity of thermal and electrical power generation determines the size of SGSP. SGSP typically has depths between 2 and 5 meters and an area between 2 and 12 kilometers. In this study, salts of MgCl₂, NaHCO₃, and NaCl were used to lessen convectional heat loss. The lower region had the highest salt concentration, while the salinity in the higher region was regulated at roughly 5%. The findings showed that a corrugated surface at the pond's bottom might raise the water temperature in the storage region to roughly 100 °C.

This study simulates how well a mathematical model of the solar pond performs in terms of capturing and storing thermal energy in the lowest layer of the city of Karbala (32.616° N, 44.025° E). **Mahdi (2019) [4]**, built a mathematical model to simulate the performance of a solar pond to collect thermal energy in the city of Kerbela, Iraq. It was discovered that a number of factors influence the amount of stored energy. The location of the pond and the amount of incident radiation from the earth are the most important factors. Fortran software was used to calculate the incident of solar radiation on the surface of the pond. Then the finite difference method was used to calculate the water temperature. The results showed an agreement with previous meteorological data. The maximum temperature of the lower layer of the pond reached 90 C and the solar radiation exceeded 7 kW/m². According to the

results, it could be concluded that the city of Kerbela is suitable for making a solar pond and using it in many applications.

In order to better understand the effects of relative varied conditions on thermal performance enhancement of solar pond, the thermal performance of solar pond for various conditions was numerically explored in this article using the discrete ordinates method. **Sogukpinar (2019) [34]** used COMSOL software to investigate the operation of a salinity gradient solar pond with a square surface area and to calculate the energy generated by it. In order to verify the simulation accuracy of the heat transfer model, the seasonal temperature change of the solar pond was estimated for the entire one-year period beginning in March. According to the results, summertime temperatures were calculated to be approximately 55 °C. While wintertime lows ranged from 20 to 30 °C and spring and fall highs between 30 and 40 °C. These results show that the solar pond system is an effective system for providing hot water for many applications, including electric power generation.

2.3 Summary of Literatures Review

Table (2.1): Summary of Literatures Review

Experimental Researches

	Ref.	Researcher and Year	Investigation scope	Finding
1	1	Bezir et al (2008)	Reflectors and covers	Increase the heating area by 25%
2	4	Singh. et al (2012).	The thermoelectric generator system is designed to generate power from solar ponds.	powered by the hot and cold water from the salinity gradient. Maximum power of 9.56 W which was obtained at 15.67 V and 0.61 A when the temperature difference of 100 °C was maintained across 16 thermoelectric cells.

Chapter Two: Literature Review

3	5	Singh. et al (2012).	thermosiphon – thermoelectric module will be most suitable for small-scale applications of solar ponds for power generation.	maximum power of 5.30W which was Obtained at 13.4 V and 0.24 A at temperature The 75 °C difference was maintained across 16 cells thermometers
4	7	Tundee et al, (2013).	solar ponds and mixture of thermosiphon and thermoelectric units.	The voltage generated by the thermoelectric cells is dependent on the temperature difference between the hot and the cold sides of the thermoelectric cells. The highest voltage of 234.25 millivolts.
5	8	Singh et al (2014)	Thermoelectric generators to produce electricity through hot water in LCZ and cold water in the UCZ of the solar pond	Maximum power of 34.42 W which was obtained at 55.16 V and 0.62 A.
6	12	Assari et al, 2015.	Solar pond shape design.	Reducing the shade area in a rectangular pond increases the temperature of the pond by 4.2%.
7	13	Qarroot, 2015.	Reflecting mirrors and evaporation rate	Increasing the number of reflective mirrors reduces the surface area required for the pond

Chapter Two: Literature Review

8	14	Singh et al (2015).	A solar pond that uses a thermoelectric generator and a simple heat exchanger to produce energy	A maximum of 7.02 W of electrical power output was obtained from a simple heat exchanger with 40 TEG.
9	18	Balaji 2016	The type of salt used in the solar pond	Experiment with sodium sulfate and sodium carbonate salts. The maximum temperature is 60°C within 10 hours, and the efficiency is 18.68%.
10	22	Sathish et al, 2017.	Sodium chloride salt and black gravels	Experiment with sodium chloride salt and black gravels . The percentage of increase in temperature by using salt instead of black gravels was 16.2%.
11	21	Al-whoosh et al, 2017.	Salt concentration and thermal insulation in the pond.	Increase the thickness of the thermal insulation for a pond. Temperature max 85°C after 100 hours of operation.
12	27	Goswami and Ranjan (2019)	salinity gradient solar pond to investigate the electrical and thermal performance.	Thermal conductivity, density and specific heat depend strongly on the salinity and their dependence on the temperature is relatively weaker. TDS and EC depend on both salinity and temperature.

Chapter Two: Literature Review

13	28	Goswami and Ranjan (2020).	Solar pond and two-phase thermosiphon toward thermoelectric power generation	The maximum temperature gradient across the thermoelectric system was found as 23.57 °C, and the corresponding open-circuit voltage was obtained as 1.435 V.
14	29	Abbood et al (2020)	Salinity gradient solar pond for water heating	The experimental results showed the efficiency of sodium chloride salt at a concentration of 25% in raising the water temperature in the pond to 44 °C.
15	30	Abbood et al (2021)	Using a solar tracking system to raise the efficiency of solar pond for water heating	It was concluded that the use of reflective mirrors alone improves thermal efficiency of solar ponds by 35.5%, Whereas using mirrors and trackers together improves them by about 51.7%.

Theoretical Researches

Seq.	Ref.	Researcher and Year	Boundary conditions	Modification Method and Results
------	------	---------------------	---------------------	---------------------------------

Chapter Two: Literature Review

1	20	Aramesh, 2017	The effect of shading on the performance of the solar pond.	Shading significantly affects the energy storage performance of the pond by 2.83%.
2	15	Rizvi, 2015	Use reflectors as covers on the surface of the pond.	The percentage of temperature increase using both the cap and reflectors was 28%.
3	16	Monjezi, 2016	The pond surface area for the water evaporation is 100 m ² .	The upper layer requires 47 liters of fresh water per day to compensate for evaporation.
4	17	Prasad, 2016	The temperature difference of the layers of the solar pond.	The temperature of the lower layer reaches 52°C and the efficiency of the thermal pond is 23.9%.
5	23	Sinha, 2018	The type of salt used in the solar pond.	The temperature in the storage area is up to 100°C using a corrugated surface at the bottom of the pond.
6	25	Mahdi, 2019	Conditions surrounding the pond.	The temperature reached 90 degrees Celsius in the simulation program, and the solar radiation exceeded 7 kW/m ² .
7	26	Sogukpiner, 2019	The effect of thermal insulation on the amount of heat lost.	The temperature of the pond reached about 55 C° during a period of 420 days

2.4 Scope and Objectives of Present Work.

In previous studies, the performance of solar ponds of different designs, the components of those ponds, the salts that were used, the thermal properties of those salts, and other components associated with the ponds such as reflectors or the type of cover used on the

Chapter Two: Literature Review

surface of the pond were studied, in addition to other researches that studied the solar ponds and linked them to a thermoelectric generator to produce electrical energy and calculate amount of energy generated.

In the current work, the performance of a salt-gradient solar pond (with magnesium sulfate salt in different concentrations) will be studied with the use of reflective mirrors and plastic cover on the surface of the pond or glass and the addition of gravel to improve the efficiency of the solar pond. The hot water from the pond was directed through a square-section pipe surrounded by a thermoelectric generator to generate power. This work will be carried out experimentally and theoretically in the holy city of Karbala, Iraq.

CHAPTER THREE

***MATHEMATICAL MODELING AND COMPUTATIONAL
PROGRAM***

Chapter Three

Mathematical Modeling and Computational Program

This chapter is divided into two main sections. The first section includes mathematical modeling of solar pond system. In this section, theories of sunlight falling on the surface of a solar pond and the mathematical relations of its performance are presented. The analyzes of thermal energy transfer through the pond layers (upper, middle and lower layer) are also explained. In addition to the mathematical relations for calculating energy loss, the thermal energy conserved in the solar pond is presented in this section. Besides, the mathematical relationships for finding the useful energy, overall efficiency of the pond and temperature distribution within the three layers of the solar pond are presented. TEG to explore the possibility of using TEG to generate energy from a solar pond. TEG can operate even in low temperature conditions and is suitable for power generation using low-grade heat from a solar pond. While the second section of this chapter is an explanation of the computational program used in this study, which is the MATLAB program.

Design Considerations for Solar Ponds

The solar pond's surface area.

The heat exchanger tubes' length.

Salt's accessibility and affordable cost.

Appropriate pond placement for sun radiation.

The liquid that is utilized to transfer the pond's heat.

The relative humidity and wind speed.

Maintain excellent transparency to the solar pond's surface.

The solar pond's form.

3.1 Mathematical Modeling

The solar pond performance affected by two parameters which are the quantity of solar radiation entered into the pond and the quantity of energy leaved it via surface area. The heat transfer behavior inside the layers of solar pond can be described by building a

mathematical model for those layers. This model can be obtained by applying the energy equilibrium principle of the pond body.

The water molecules at the pond surface are heated by the incident sunlight. The hot part of water molecules transfers into the mid layer of the solar pond. In the same scenario, the heat moves to the bottom layer of the pond. Knowing that the heat transfers inside the three pond layers by the heat conduction process.

Figure (3.1) displays the heat transfer inside the three pond layers.

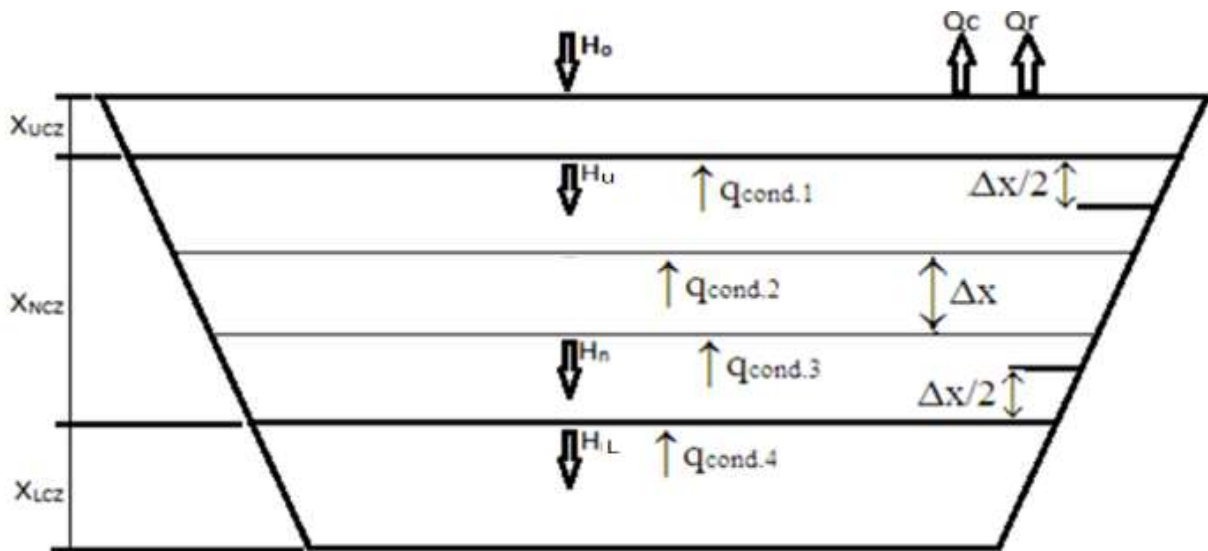


Figure (3.1): Heat Transfer into the Three Layers of Solar Pond

3.2 Assumptions

In the theoretical aspect of this study, the following assumptions will be taken into account: -

1. The heat transfer through the layers of the solar pond is one-dimension.
2. The energy losses from the base and walls insulated of solar pond are negligible.
3. The solar pond surface can be considered as a horizontal surface.

4. The quantity of solar radiation which reaches to the lower layer is totally absorbed by a brine of the solar pond.
5. The physical properties of used salts (specific heat capacity, thermal conductivity, and density) are constant.
6. The losses due to the evaporation of water can be disregarded.
7. The refractive index of brine may be considered as a constant value since the difference in its value in each layer of the pond is small.

3.3 Solar Irradiation Calculations in Karbala city

In the recent years, the data of solar irradiation are usually measured and recorded for almost any region in the world. The solar irradiation estimates and predictions are often required to obtain a good approximation of incident radiation. The solar radiation path in the atmosphere is seasonally various depending on the position of a solar pond so, the sun's altitude, and daily sunshine period and azimuth angle will be also various. This may be due to the earth's rotation or/and the angle of deviation. This might have a direct impact (positively or adversely) of the amount of incident radiation on the pond surface and, consequently, on the solar pond's performance.

The dust and fog in the atmosphere reflect a slight part of the solar radiation which enters the atmosphere and the residual part falls on the earth's surface.

The quantity of the solar radiation arriving into the solar pond (H_x) can be found at any depth (x) in the pond as follows [3]: -

$$H_x = H_o \left\{ 0.36 - 0.08 \ln \left(\frac{x}{\cos \theta_1} \right) \right\} \quad \dots (3.1)$$

Where: (H_o) is the quantity of global incident solar radiation on the solar pond surface and θ_1 is the light refraction angle inside the solar pond. H_o can be found by the following equation [6]: -

$$H_o = \left[0.29 \times \cos(\varphi) + 0.52 \times \left(\frac{n}{N} \right) \right] H_{ex} \quad \dots (3.2)$$

Where: φ is the latitude angle and its value is 32.55° for Karbala city, $\left(\frac{n}{N} \right)$ is the percentage of the sunshine period and H_{ex} is the incident daily solar radiation on the solar pond.

The light refraction angle (θ_1) can be found by the following equation [25]:

$$\cos\theta_1 = 1.333 \cos\theta_2 \quad \dots (3.3)$$

Where: θ_2 is the direct radiation incidence angle on the surface of pond.

H_{ex} can be determined by the following equation [3]: -

$$H_{ex} = \frac{24}{\pi} \times I_{on} \times \left[\cos(\varphi) \cos(\delta) \cos(\omega_s) + \frac{2\pi\omega_s}{360} \sin(\varphi) \sin(\delta) \right] \quad \dots (3.4)$$

Where: I_{on} is the daily intensity of constant irradiation and depends on the days number of the year. δ is the angle of solar declination and ω_s is the angle of sunset hour.

The incidence angle (θ_2) can be calculated as follow [6]:

$$\cos \theta_2 = \cos(\varphi) \cos(\delta) \cos(\omega) + \cos(\varphi) \cos(\delta) \quad \dots (3.5)$$

Where: ω is the hour angle which can be found at noon depending on the local time (h). ω in the morning be negative and in the evening be positive.

The angle of solar declination (δ) can be found by [30]:

$$\delta = 23.45 \sin \left[360 * \frac{283+n}{365} \right] \quad \dots (3.6)$$

Where: n is the number of days in the year.

The angle of hour (ω) can be determined by [25]:

$$\omega = 360 * \frac{(h-12)}{24} \quad \dots(3.7)$$

The daily intensity of the constant irradiation (I_{on}) can be calculated by the following equation [25]:

$$I_{on} = 1367 \times \left[1 + 0.033 \times \cos \left(360 \times \frac{n}{365} \right) \right] \quad \dots (3.8)$$

The angle of sunset hour (ω_s) can be calculated by the next equation [6]:

$$\omega_s = \cos^{-1}(-\tan\varphi \times \tan\delta) \quad \dots (3.9)$$

The percentage of absorbed radiation, H_x , decreases as we go deeper into the layers of the solar pond to a certain depth, x . The value of H_0 is different from H_x because the value of the refractive index in air is different from the value in water.

Table (3.1) contains the monthly input quantities for Karbela city in April month. These quantities are the average daily ambient temperature (T_a), wind velocity (v), relative humidity (Υ), and the percentage of sunshine interval ($\underline{n} / \underline{N}$) [35].

Table (3.1) Weather Data for the City of Karbala in Year of 2022 [43].

Month	T_a (°C)	Υ (%)	v (m/s)	$\underline{n} / \underline{N}$
April	23.8	28	4	0.69

3.4.1 Thermal Analysis of Upper Convective lower

The thermal energy entered (E_{in}) into the water body of the pond equals the energy kept in it (E_{stored}) plus the energy leaves (E_{out}) from it as shown in figure 3.2.

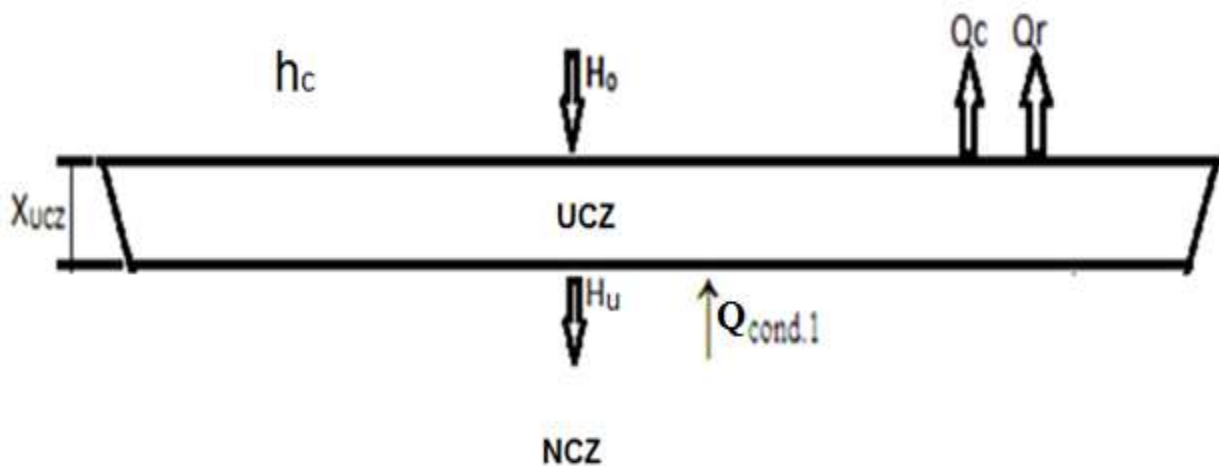


Figure (3.2): Thermal energy equilibrium for the upper zone of the solar pond

Then the equation of the thermal energy equilibrium for the upper layer of the solar pond (UCZ) is as follows [25]: -

$$E_{in} = E_{out} + E_{stored} \quad \dots (3.10)$$

Where: -

$$E_{in} = H_o + Q_{cond.1} \quad \dots (3.11)$$

$$E_{out} = H_u + Q_{loss} \quad \dots (3.12)$$

$$E_{stored} = \frac{\partial T}{\partial t} * \rho_{UCZ} * Cp_{UCZ} * x_{UCZ} \quad \dots (3.13)$$

By substitution the three equations (3.11, 3.12 and 3.13) in Eq. (3.10), the following equation is obtained [3]:

$$[H_o + Q_{cond.1}] = [H_u + Q_{loss}] + \left[\frac{\partial T}{\partial t} * \rho_{UCZ} * Cp_{UCZ} * x_{UCZ} \right] \quad \dots (3.14)$$

where: H_u is the quantity of sun light absorbed by the upper pond layer, which is considered the direct light for the mid layer and is computed by H_x Eq. (3.1) and x is the thickness of the upper layer (x_{UCZ}). ρ_{UCZ} is the density of the upper layer solution. Cp_{UCZ} is the brine specific heat (Brine) and x_{UCZ} is the thickness of the upper pond layer (UCZ).

Solar radiation and temperature are variable, so we will use the transient solution method for the mathematical modeling.

By deriving Eq. (3.14), the temperature distribution for the upper pond layer can be gotten as follows [30]:

$$[H_o + Q_{cond.1}] = [H_u + Q_{loss}] + \left[\left(\frac{(\partial T(\Delta t) - \partial t(\Delta T))}{\Delta t^2} \right) (\rho_{UCZ} * Cp_{UCZ} * x_{UCZ}) \right] \quad \dots (3.15)$$

Where: -

$$Q_{cond.1} = \frac{k * (T_2^t - T_1^t)}{\frac{\Delta x}{2}} \quad \dots (3.16)$$

By substitution the two equations (3.15 & 3.16) in Eq. (3.14) and multiplying it (Eq. (3.14)) by $(\Delta t / (\rho_{UCZ} * Cp_{sol} * X_{UCZ}))$, the finite difference equation for the water temperature of upper pond layer at the time (t+1) can be obtained as follows [6]:

$$T_u^{t+1} = T_u^t + \frac{\Delta t}{\rho_{UCZ} * Cp_{UCZ} * X_{UCZ}} \left[(H_o - H_u) + \frac{K_{UCZ}(T_u^t - T_a^t)}{\frac{X_{UCZ}}{2}} - Q_{loss}^t \right] \quad \dots (3.17)$$

Where: Δt is the difference of time between two readings. Q_{loss}^t are the heat losses from the solar pond surface at the time (t) due to the heat convection (Q_c) and the heat radiation (Q_r). The losses of water evaporation are very small comparing with the losses of heat convection and radiation and therefore can be neglected.

The following equation represents the heat losses from the pond surface [30]:

$$Q_{loss} = Q_c + Q_r \quad \dots (3.18)$$

Convection losses are affected by the ambient temperature and wind speed. The following equation is to find these losses per square meter of surface area of the solar pond, as follows [30]: -

$$Q_c = h_c * (T_u - T_a) \quad \dots (3.19)$$

where: h_c is the coefficient of heat convection and T_u is the upper convective zone temperature, which can be found by [30]: -

$$h_c = 5.7 + 3.8v \quad \dots (3.20)$$

Where: v is the wind velocity.

The heat radiation losses are associated with the heat transfer between the upper pond layer and the sky. Then these losses are functions of the upper zone temperature and the sky temperature. By assuming that the solar pond acts as a black body and thus the equation of heat radiation losses is written as [31]: -

$$Q_r = \sigma \times \epsilon * A * [(T_u + 273)^4 - (T_{sky} + 273)^4] \quad \dots (3.21)$$

where: T_{sky} is the sky temperature and can be found by the following equation [4].

$$T_{sky} = T_a - (0.55 + 0.061^2 \sqrt{P_a})^{0.25} \quad \dots (3.22)$$

where: P_a is the water vapour partial pressure in the air and can be found as follows:

$$P_a = (\gamma) \exp\left(18.403 - \left(\frac{3885}{T_a}\right)\right) \quad \dots (3.23)$$

where: γ is the relative humidity, σ is Stefan Boltzmann's constant which equals $5.673 \times 10^{-8} \text{ W/m}^2 \text{ K}^4$ and ϵ is the water emissivity which equals to 0.83 [31].

3.4.2 Thermal Analysis of Mid Convective layer

By the same scenario of the upper convective zone (section (3.4.1)), the energy equilibrium equation for the mid zone of the solar pond (NCZ) is taken as [31]: -

$$(H_u + Q_{\text{cond}3}) = (H_n + Q_{\text{cond}2}) + \left(\frac{\partial T}{\partial t}\right) (\Delta x * \rho_n * C_{p_{\text{sol}}}) \quad \dots (3.24)$$

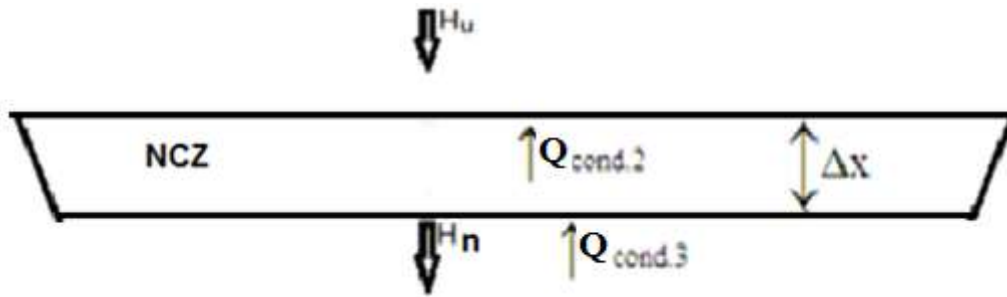


Figure (3.3): The thermal energy equilibrium of the mid zone of the solar pond

where: - $(H_u + Q_{\text{cond}3})$ represents the thermal energy entering into the mid zone, $(H_n + Q_{\text{cond}2})$ is the thermal energy departing from it (the heat losses) and $\left(\frac{\partial T}{\partial t}\right) (x_{\text{ncz}} * \rho_n * C_{p_{\text{sol}}})$ represents the thermal energy stored in this zone. Knowing that H_n is computed by Eq. (3.1) and Δx in that equation equals the thickness of mid layer.

Figure (3.3) show the thermal energy equilibrium of the mid zone of the solar pond. Also, in the same scenario of section (3.1.3), the water temperature finite difference equation of the mid zone of the solar pond (NCZ) can be obtained as follows.

$$T_n^{t+1} = T_n^t + \frac{\Delta t}{\rho_{\text{ncz}} * C_{p_{\text{ncz}}} * X_{\text{ncz}}} \left[(H_n - H_u) + \frac{K_{\text{ncz}} (T_n^t - T_u^t)}{X_{\text{ncz}}} \right] \quad \dots (3.25)$$

3.4.3 Thermal Analysis of Lower Convective layer

Similarity to the upper convective zone (section (3.4.1)), the energy equilibrium equation for the lower convective zone (LCZ) is [32]: -

$$H_L = Q_{\text{cond.4}} + \left(\frac{\partial T}{\partial t} * \rho_{\text{LCZ}} * C_{p\text{LCZ}} * X_{\text{LCZ}} \right) \quad \dots (3.26)$$

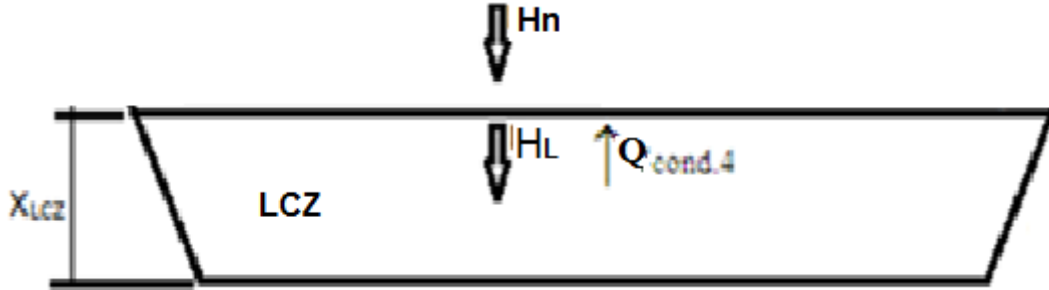


Figure (3.4): Thermal energy equilibrium of the lower zone of the solar pond

where: H_L is the thermal energy entering into the lower convective zone and is computed by eq. (3.1) knowing that x in that equation is the thickness of the lower layer. $Q_{\text{cond.4}}$ is the thermal energy leaving from the lower zone $\frac{\partial T}{\partial t} * \rho_{\text{LCZ}} * C_{p\text{LCZ}} * X_{\text{LCZ}}$ is the thermal energy stored in the lower zone of the solar pond and which represents the useful thermal energy which can be used in many of applications.

The thermal energy which leave the lower zone (losses) is the energy moved from this zone to the mid zone as shown in figure (3.4). These thermal losses can be calculated by applying [30].

$$Q_{\text{cond.4}} = -K_{\text{LCZ}}A \left. \frac{\partial T_n^t}{\partial x} \right| \quad \dots (3.27)$$

The difference of brine temperature of the pond lower zone (LCZ) can be determined by the next equation [32].

$$T_L^{t+1} = T_L^t + \frac{\Delta t}{\rho_{\text{LCZ}} * C_{p\text{LCZ}} * X_{\text{LCZ}}} \left[(H_L) + \frac{K_{\text{LCZ}}(T_L^t + T_n^t)}{X_{\text{LCZ}}/2} \right] \quad \dots (3.28)$$

3.5 The amount of energy reflected by the mirrors [45].

The amount of solar radiation reflected from mirrors into the solar pond is calculated by the following equations:

$$U_f = \frac{G_f}{L_f^2} \quad \dots(3.29)$$

Where L_f is the reflector's length, G_f is the amount of radiation reflected toward the pond by the reflector, and U_f is the amount of solar radiation incident on one square meter of the pond per second. The following equation of G_f :

$$G_f = SM_f * B_f \quad \dots(3.30)$$

where B_f is the amount of radiation falling on one square meter of ground per second (measured during the experiment). SM_f is the reflector's projection area and perpendicular to the incident light and given as:

$$SM_f = ZY_f * L_f \quad \dots(3.31)$$

where ZY_f is the front side of the reflector's projection area and perpendicular to the incident light and given as:

$$ZY_f = ML_f * \cos \theta_f \quad \dots(3.32)$$

where ML_f is the side length of the reflector and θ_f is the angle between ZY_f and the reflector, and is given as:

$$\theta_f = 90^\circ - (180^\circ - \alpha_f - \beta_f) = -90^\circ + \alpha_f + \beta_f \quad \dots (3.33)$$

where β_f is the controlled angle with horizon and α_f is the angle between the horizon and the incident light reaching the horizontal surface per second and given as:

$$\alpha_f = 90^\circ - \theta \quad \dots (3.34)$$

Where θ is zenith angle.

3.6 Useful Thermal Energy of Solar Pond

The useful thermal energy of the solar pond (Q_u) can be determined by the following equation [25]: -

$$Q_u = M_s C_{p_s} \Delta T / \Delta t \quad \dots (3.29)$$

where: M_s is the brine mass of the solar pond, Cp_s is the heat capacity of the pond brine and ΔT is the average temperature difference between the lower zone and ambient Δt is time.

The brine mass of solar pond (M_s) can be obtained by the following equation: -

$$M_s = \rho_s * V_{LCZ} \quad \dots (3.30)$$

where: ρ_s and V_{LCZ} are the density and volume of the brine of the lower convective zone of the solar pond respectively. $V_{LCZ} = 0.650 \text{ m}^3$ and ρ_s is determined by Equation (3.31) **Duffie** [34].

$$\rho_s = \rho_w * (1 - C) + \rho_{salt} * C \quad \dots (3.31)$$

The heat capacity of the pond brine (Cp_s) can be found by the next equation (3.32)

Duffie [34]: -

$$Cp_s = [(\rho_w * Cp_w * (1 - C) + \rho_{salt} * Cp_{salt} * C)] / \rho_s \quad \dots (3.32)$$

where: C is the salt concentration in the solar pond water. Cp_w and ρ_w are the heat capacity and the density of the pond water and equal 997 kg/m^3 and $4.18 \text{ kJ/kg.C}^\circ$ respectively. ρ_{salt} and Cp_{salt} are the density and the heat capacity of the pond salt and equal 1329 kg/m^3 and $2.572 \text{ kJ/kg.C}^\circ$ for the MgSO_4 .

3.7 Overall Thermal Efficiency of Solar Pond

The solar pond thermal efficiency (η) can be calculated by division of the useful energy (Q_u) on the quantity of incident sun light on the pond surface (I) as follows [32]: -

$$\eta = Q_u / I \quad \dots (3.35)$$

The incident sun light on the pond surface (I) can be found by the following equation: -

$$I = I_0 * A \quad \dots (3.36)$$

where: A is the solar pond surface area.

3.8 Electric power and Efficiency of TEG

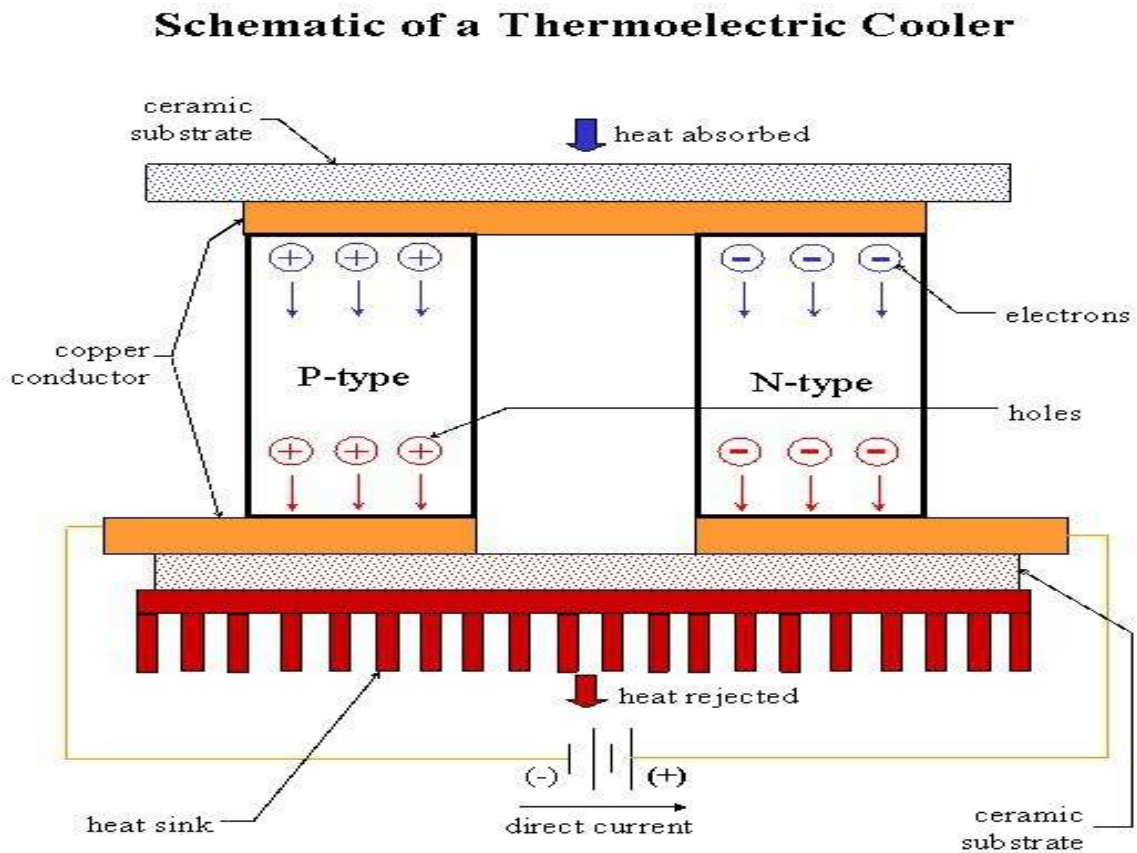


Figure 3.1 Schematic diagram of the thermoelectric generator TEG [36].

Thermoelectric power sources are characterized by the conversion of heat into electricity with Seebeck effect, which is called (TEG). The working part of a thermoelectric generator is the electron. Thus a TEG produces no noise, is environmentally friendly, with no moving parts. The basic structure of thermoelectric (TEG), or the basic building block, consists of n-type and p-type semiconductor thermo elements connected electrically in series by a conducting strip (usually copper or aluminum). The module consists of a number of the primary building connected electrically in series but thermally in parallel and incorporated between two ceramic plates [36].

Modern thermoelectric converters are made of semiconductors, which have better conversion efficiency and output power than metal alloys. The implementation of the

thermocouple junction is complicated by the fact that semiconductors are generally no ductile crystalline solids. Electrical conductivity, Seebeck coefficient, and thermal conductivity are three intrinsic material qualities that define the quality of thermoelectric materials used for generating electric power via the Seebeck effect or via the Peltier effect [37].

The electrical power generated from TEG is given as [28]

$$\mathbf{P}_{\text{TEG}} = IV \quad \dots (3.36)$$

$$\mathbf{V}_{\text{TEG}} = \alpha\Delta T \quad \dots (3.37)$$

where:

$$\alpha = (\alpha_p - \alpha_n) , \Delta T = (T_h - T_c) ,$$

T_h and T_c represent the hot and cold junction temperature respectively. α_p and α_n are the Seebeck coefficient of P and N type TEG leg respectively.

For TEG containing N number of couples, the following equation can be used for open circuit and short circuit relations.

$$\mathbf{V}_{\text{TEG}} = 2N\alpha\Delta T \quad \dots (3.38)$$

$$\mathbf{I}_{\text{TEG}} = (\alpha/\rho) (\mathbf{A}_{\text{TEG}}/L) \Delta T \quad \dots (3.39)$$

Electrical resistivity of thermo element material, ρ Ω cm. Area of thermo element, \mathbf{A}_{TEG} mm². Length of thermo element, L mm.

The thermoelectric power is related to dimensionless figure of merit given [38].

$$ZT = \alpha^2 \sigma T/k \quad \dots(3.40)$$

where α is the Seebeck coefficient of TEG, σ and k are the electrical and thermal conductivity respectively and T is the absolute temperature.

For calculating the efficiency of TEG, the following equation is used [38].

$$\eta_{\text{TEG}} = \frac{T_h - T_c}{T_h} \left[\frac{(1+ZT)^{0.5} - 1}{(1+ZT)^{0.5} + \left(\frac{T_c}{T_h}\right)} \right] \quad \dots(3.41)$$

3.9 Building Computational Program.

In the present work, the computational program software which was used for solving the heat transfer equations inside the solar pond layers is MATLAB (2014 version). This is to calculate the useful thermal energy and the overall efficiency of the solar pond. But before that, the solar radiation and the brine temperature of the solar pond layers are calculated.

Nine computational codes were constructed each code represents a certain test case. The first code is for the normal case of solar pond (without adding improvers). The second, third, fourth and fifth codes are for the first, second, third and fourth days of the uncovered saline solar pond respectively. The sixth, seventh, eighth and ninth codes are for the first, second, third and fourth days of the covered saline solar pond respectively. In each code, the equations which represents the case of this code are supplied into the program. The constants as the local latitude, the local time, the solar constant ...etc. and many variable into the program.

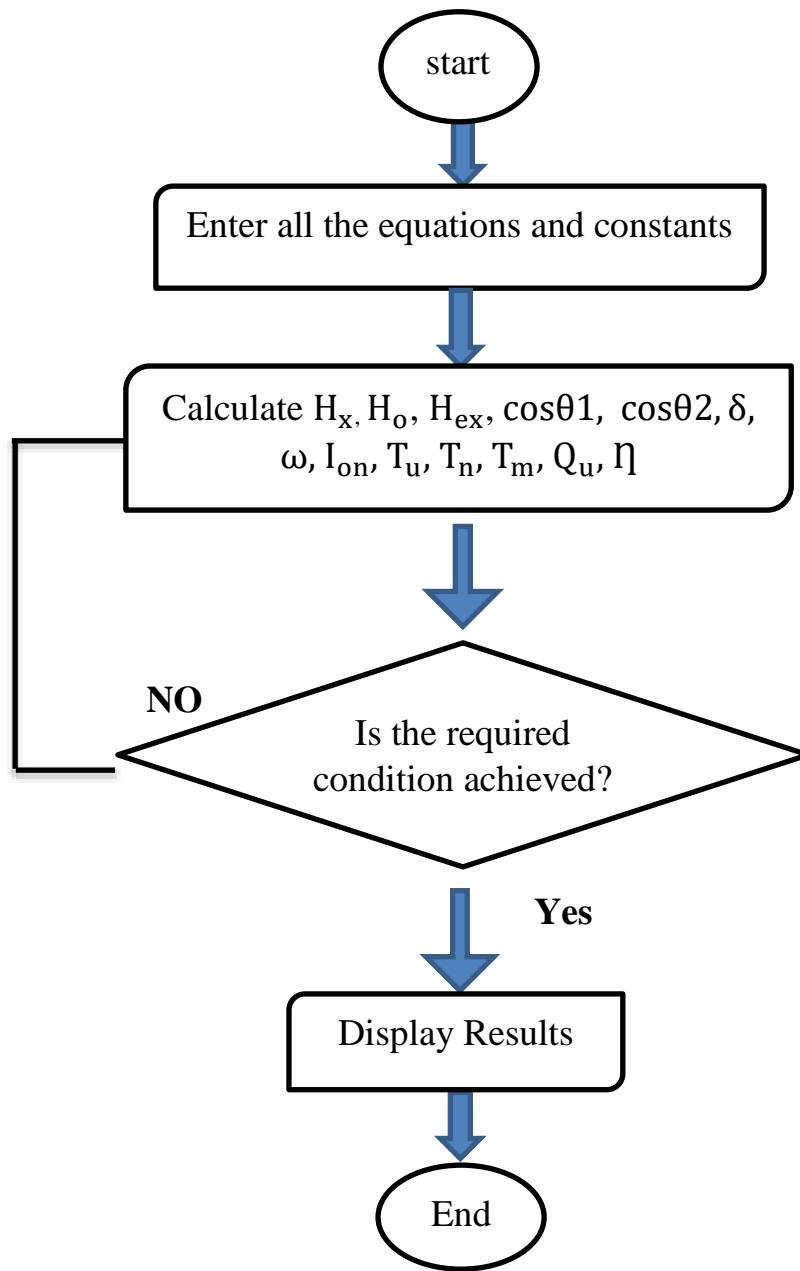


Figure (3.5): The Flow Chart of the Computational Program

CHAPTER FOUR
EXPERIMENTAL WORK

Chapter Four

Experimental Work

The construction of the solar pond, its measurements, and the materials (gravel and magnesium sulfate salts) added to the pond water are all covered in this chapter. Thermocouples, flow meters, and other measuring tools are illustrated. The modification items (reflector mirrors, plastic covers, and glass covers) used to enhance the solar pond's efficiency are described. It describes the steps involved in carrying out tests. It has also been explained how to produce electrical energy from the hot water produced by the solar pond using semiconductors (thermoelectric generator). Experimental reading of solar radiation, wind speed, voltage and current of TEG are done. The calibration of the experimental measuring tools used in this work has been presented.

4.1 Experimental solar pond

Solar pond mainly consists of a basin containing brine or any other solution that retains heat for use in other applications. The pond in this work consists of a basin in the shape of a pyramid with its head cut off towards the bottom, its base area is 0.64 m^2 and its surface area is 6.25 m^2 . The basin contains a brine with a depth of 1.35 m. The walls of the basin are inclined at an angle of 60° . The walls of the pond are lined with thermal insulation material, and the walls themselves are made of wood. These dimensions and specifications were chosen after a review of research similar to the idea of the project, and they were worked on with some changes, the purpose of which is to study the impact of these changes on the work of the pond. The experimental system schematic diagram is displayed in Figure (4.1).

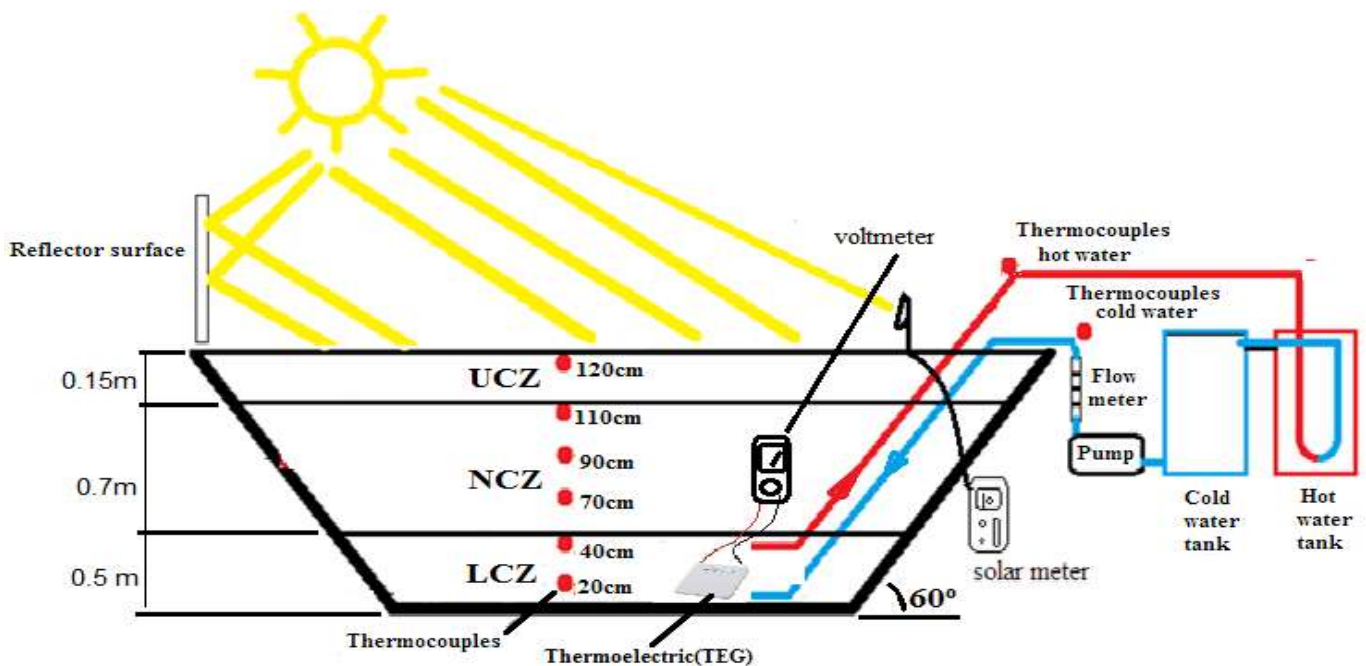


Figure (4.1) Schematic Diagram of Experimental Rig

4.1.1 Solar Pond Construction

The solar pond was built with a salt gradient and a pyramidal design in the city of Karbala (32.55N and 43.97E). The pond's bottom has a 0.64 m² area, its depth is 1.35 m, and its surface area is 6.25 m². A 60-degree tilt can be seen in the pond's walls. "Knowing that the hierarchical shape of the solar pond was chosen to accord to **Sayre** [19].

The construction of the solar pond is as following:

The first step was to create a metal frame out of steel strips with a 90-degree cross section. The pond bearing frame was created by welding these strips together. First layer of the pond body was then constructed from hardwood panels that had been screwed to the steel frame. On these panels, a heat insulator polyurethane (K=0.063 W/m.C)(2 layers, each 5 cm thick) was then put in place to stop heat loss.

Figures (4.2, 4.3) depict the construction process for the solar pond and the foam layers used to insulate heat and the finished design of the pond.

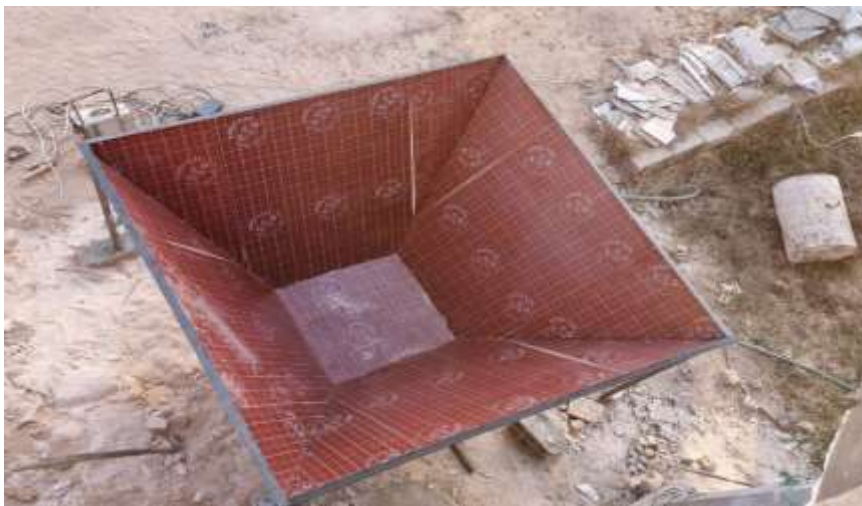


Figure (4.2) Steps of the solar pond construction

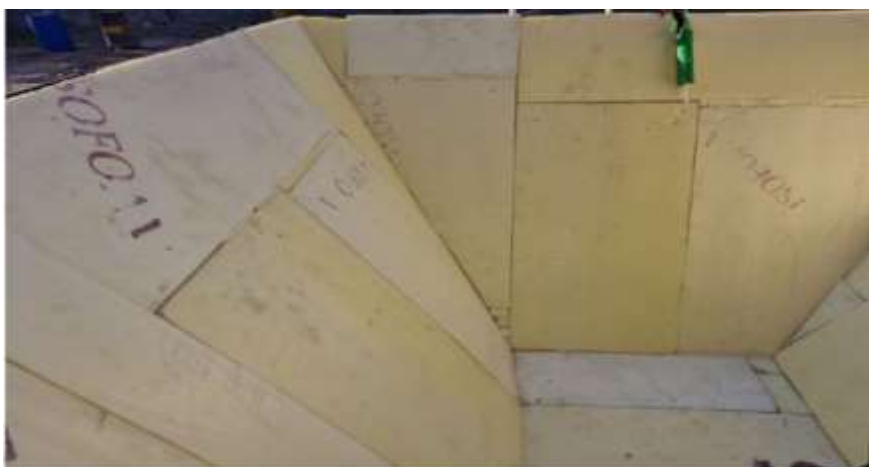


Figure (4.3): Layers of polyurethane as insulate material

4.1.2 Solar Pond liner

The solar pond's liner was chosen to be a synthetic polymer (polyamide 6.6). It is *lightweight*, waterproof, and simple to install, among other positive traits. The liner's purpose is to keep water from leaking out of the pond. The inside walls of the solar pond were covered with three layers of the synthetic polymer, as shown in figure (4.4). Each layer of the liner is 0.5mm thick. Figure (4.5) shown the inside layer was covered with black epoxy to boost the solar pond's ability to collect solar radiation.



Figure (4.4): Solar pond liner



Figure (4.5): inside layer of solar pond with black epoxy.

4.1.3 Salts

For the purpose of selecting the appropriate quality of salt for the pond, experiments were conducted on 9 beakers filled with 100 mm of water were used in the solar pond during the month of March 2022, when the average solar radiation was 1133 W/ m^2 . In each beaker, an amount of each of the three types of salts are magnesium sulfate, sodium carbonate and sodium chloride were used in different concentrations, namely 30%, 70%, and 100%. Then the thermocouples are inserted into the vials and placed facing the sun, and a reading is taken every half hour. With contrition of 100%, a rise in the temperature of the flasks containing magnesium sulphate salt was observed. This indicates that this salt is the best among other used to absorb the largest amount of solar radiation and maintain temperatures for a longer period. As shown in figure (4.6) the test take from 10:00 to 14:00 and it repeat in next day.



Figure (4.6) Experimental of Salts High Heat Absorption.

The magnesium sulphate salt was used in this solar pond. In addition, it is stable at high temperatures and has suitable solubility. The properties of the salts used in the pond (magnesium sulphate) are shown in Table (4.1).

Table (4.1): Properties of salts [44].

Salt Name	Molecular formula	Density kg/m³	Solubility in water g/100 ml	Specific heat J/ kg. k	The potential risks
Magnesium sulfate	MgSO ₄	2660	35.1	1255	NO
Sodium carbonate	Na ₂ CO ₃	2540	21.5	1123	No
Sodium chloride	NaCl	2160	36.3	8812	No

4.1.4 Layers of Solar Pond

The upper layer is a thermal layer containing pure water or low salinity, with a thickness of (0.15 m), chosen with this thickness to pass the largest possible amount of solar radiation to the next area.

The second (middle) layer is an area with a salt gradient. It is assumed to be divided into three layers according to the degree of salinity in each layer. The degree of salinity in this layer varies vertically and increases towards downward.

Samples were taken from this layer at different depths, and the concentration of salt was measured. The salt concentration ranged between 2% and 4%.

The third (lower) layer is the storage and convection area. With a thickness of 0.5 meters, it contains the highest salt concentration, which reached 28%, after taking samples for testing. The function of this layer is to collect solar radiation as thermal energy based on the property of the brine in storing heat. These three layers are shown in Figure 4.7.

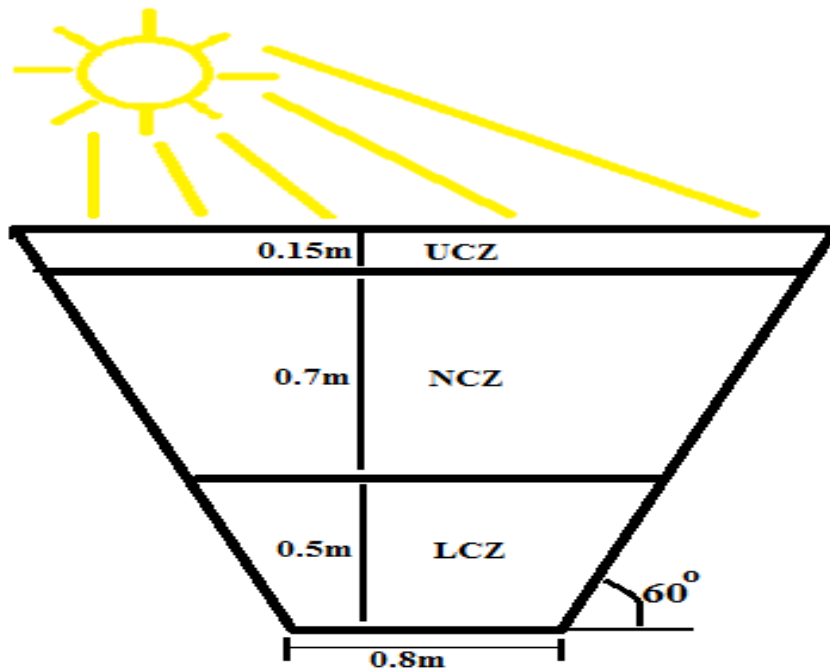


Figure (4.7): Layers of the solar pond.

4.1.4 Reflective Mirrors 60°

Mirrors consist of a thin layer of glass that reflects light. They are fixed on polyethylene with a thickness of 3 mm. The function of these mirrors is to focus the solar radiation on the surface of the solar pond. Reflecting mirrors were used in the present work, which is an oval concave reflector as shown in Figure (4.8).



Figure (4.8) Reflective Mirrors.

The quantity of heat that the dish directs toward the solar pond. Many factors affect how much heat is concentrated on the solar pond by the elliptical reflector.

1. Dimensions of the main dish.
2. The cleanliness of the reflective layer (dust collection).
3. the heat absorption potential of the endothermic metal.

4. The presence of condensed drops of water vapour in the air on the surface of the reflective layer during the early hours of the day.

The mirror is moved around its horizontal axis manually using a graduated ruler. Two sets of this type were installed on either side of the pond. The first set was placed on the southeast side of the pond, facing the sun. This group works from the morning until noon, and then its effect fades in the afternoon. The second set was placed on the southwest side of the pond to reflect solar radiation towards the surface of the pond from noon until sunset.

Table (4.2) Properties of the Semiconductor Material of Used

Seebeck coefficient			Electrical resistivity		Electrical Resistance (Ω)	Thermal conductivity		Thermal Conductance (W/K)
p-type conductance ($\mu\text{V/K}$)	n-type ($\mu\text{V/K}$)	Combined $\times 10^3$ ($\mu\text{V/K}$)	p-type ($\mu\Omega\text{m}$)	n-type ($\mu\Omega\text{m}$)	6.0	p-type (W/(m K))	n-type (W/(m K))	0.2
140.0	-188.5	41.1	6.0	29.5			1.3	

4.2.1 Experimental Set Up for Thermoelectric(TEG):

It is constructed from a square aluminium tube that is 50 mm by 50 mm in dimension and 1 mm thickness. A circular copper tube was put into the square channel to allow the water to exit. The copper tube has a thickness of 2 mm and an outer diameter of 13 mm. circular copper tube and the square channel must be placed together in order for the cold water to flow through this tube and be supplied to the ice and water tank. The gap was 13.5 mm in size. Cold water from the ice and water tanks is pumped into the square channel using four pipes on either side of the four channels. The outside square channel is linked to the TEG. Thermal glue with a high conductivity and low heat resistance is used to join TEGs together. according to Figure 4.10.



Figure (4.10) Solar Pond Liner.

The length of this section is longer than that of LCZ section of Solar pond (about 600 mm) while the length of the LCZ is 500 mm to exploit as much pond heat as possible.

Each side is connected to 15 TEGs, each measuring 40 x 40 mm, and all are connected in series. An external square channel contains 60 TEG in the four aspects. The rest of the outlet tubes are insulated to stop heat transfer to the interior of the tubes from the NCZ section of the solar pond.

The entire structure is located vertically in the solar pond. Cooling water flows through the cavities of the structure. Heat is transferred from the LCZ section of the solar pond via the TEG to the cooling water flow gap. This leads to the temperature differences required for the power generation of TEG. The figure (4.11) below shows the square channel and the thermoelectric associated with it.



Figure (4.11) Preparation of the Experimental Square Channel TEG.

4.3 Secondary Devices

4.3.1 Water Pump

It is the device used for pumping pure water into the square channel. It works with a constant voltage. A maximum water flow rate is produced by this device at 4 L/min, as shown in figure 4.12. It has two valves to control the flow rate of water.



Figure (4.12) Water Pump

4.3.2 Water Tank

A water tank with dimensions of (50 * 100) cm made of plastic, as in the figure (4.13), was used, insulated from the outside to keep the water inside at a low temperature, containing ice granules at a temperature of (0-2.9 degrees Celsius) to feed a square aluminium channel with A thermoelectric generator is connected to it. This is to exchange thermal energy with hot water in the lower layer of the solar pond.

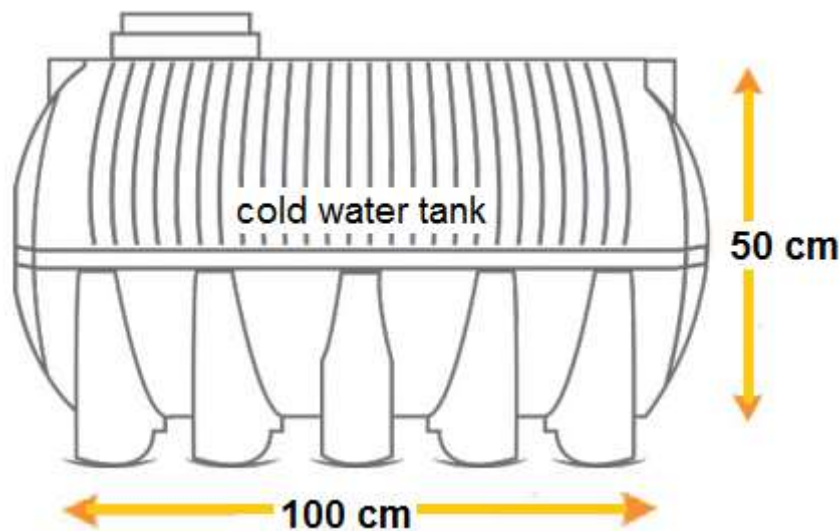


Figure (4.13). Water Tank

4.4 Experimental Measurement Devices

During the period of the experiment, several measurement tools were used to gauge a few of the variable factors. To evaluate the effectiveness of the solar pond, these elements include the temperature, radiation level, and salt content. According to the book No. M/54, these devices were calibrated in the Ministry of Science and Technology's Department of Renewable Energy on January 14, 2022.

4.4.1 Temperature Measurement

In this work, two devices were used to get temperature readings, namely the thermometer and the thermometer (Extech TM500). The first was used to record the temperature of the water. Where 10 thermocouples were installed: 7 inside the solar pond at different depths; two at the entrance and exit of the square channel. And one on the ground near a pond to measure the ambient temperature. While the thermometer is used to show the temperature readings (data show) that are measured by the thermocouples. It displays and stores up to 12 values of temperature. The temperature readings range of this device is from -20 to $+250^{\circ}\text{C}$ with an error ratio of $\pm 0.4\%$ ($\pm 0.5^{\circ}\text{C}$). The recorded data is stored on the SD card. Figure (4.14 a1 and a2) show the thermocouples and the thermometer, respectively, and figure (4.15) shows locations of the thermocouples.

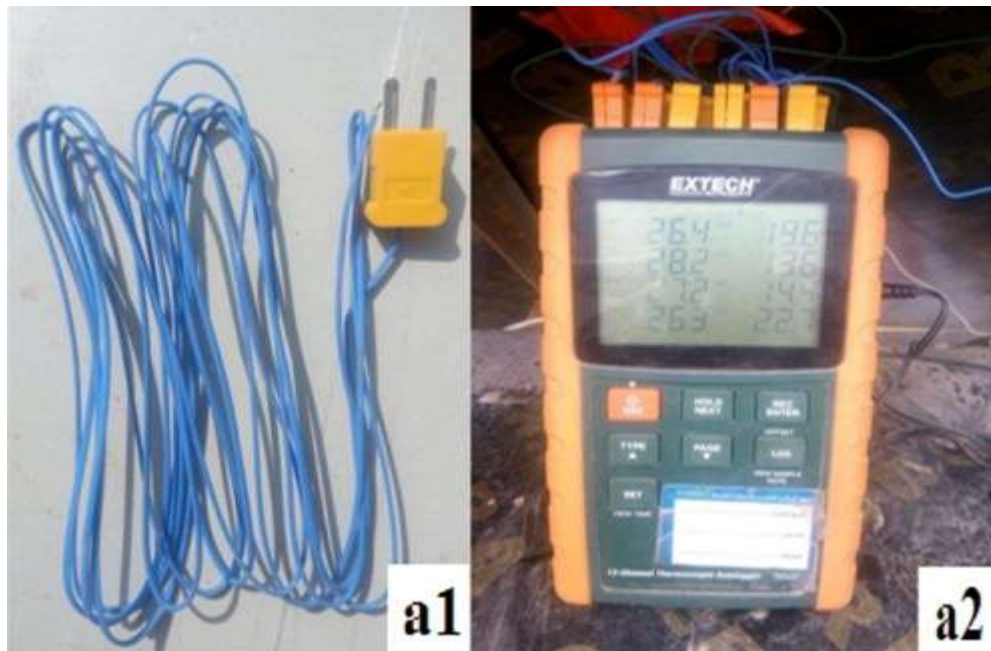


Figure (4.14): (a1) Thermometer and (a2) thermocouples

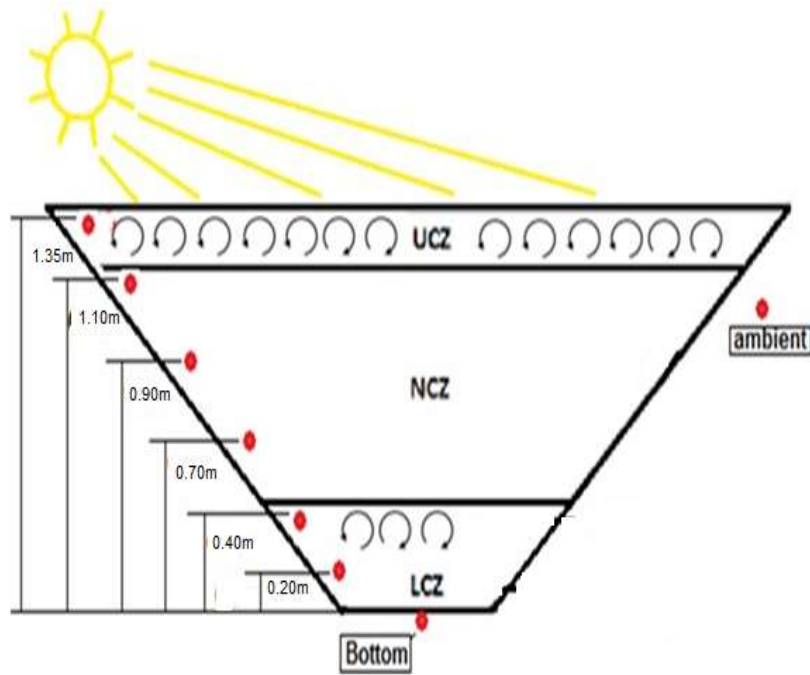


Figure (4.15): Locations of the thermocouples.

4.4.2 Solar Power Meter

A device for measuring direct solar radiation is the solar power meter (TES-132 data logging). When sunlight strikes the object, it is focused on its thermal system, which turns the heat into an electrical signal that can be measured in watts per square meter. A figure illustrates this (4.16). With a manufacturing error rate of 0.4% to 0.50%, the greatest radiation range that may be detected by this instrument is 2000 W/m². The devices were calibrated by the Renewable Energy Directorate in Ministry of Science and Technology and according to Appendix (A).



Figure (4.16): Solar Power Meter

4.4.3 Flow Meter

It is a device that is used to measure the amount of fluid going through the pipe or the fluid flow rate, as illustrated in figure (4.17). The range of the counter flow is (0.5 to 4) L/min. Control valves regulate the flow rate.



Figure (4.17) Flow Meter

4.5 Experimental Procedure

The current experiment was run over the course of two months in 2022. Every beta test runs from 8 a.m. to 7 a.m. the next day. The experimental effort started by examining the impact of salt type and concentration on the functionality of the solar pond. Three different salts were chosen (Sodium chloride salt, sodium carbonate salt, and magnesium sulfate salt). using three fixed concentrations (about 100%, 70%, and 30% of the saturation limit). An experiment was conducted to find out each salt's heat capability. Each beaker is filled with 100 ml of water with the addition of magnesium sulfate salt, which is the salt used in the solar pond, and it was chosen with a concentration of 100% of the saturation limit, which is a percentage that was approved from previous researchs. At the rate of 400 grams per 1 liter of water.

4.5.1 Steps to Operate the Solar Pond:

1. During a period from 27.3.2022 - 1.4.2022 normal pond without salt.
2. Then, magnesium sulfate salt was added from 2.4.2022 - 10.4.2022.
3. An Aplastic cover was placed for a period from 11.4.2022 - 15.4.2022.

4. A plastic cover and a reflective mirror were placed for the period from 16.4.2022 – 25.4. 2022.
5. A cover was placed over glass, a reflective mirror, and black gravels inside the pond for the period from 25.4.2022 – 10.5.2022.
- 6.

Table (4.3) Experimental steps.

No. of test	Date	work
1	27.3.2022 - 1.4.2022	Normal Pond Without Salt
2	2.4.2022 - 10.4.2022	Magnesium Sulfate Salt Was Placed
3	11.4.2022 - 15.4.2022	A Plastic Cover Was Placed
4	16.4.2022 – 25.4. 2022	A Plastic Cover And A Reflective Mirror Was Placed With Reflective Surfaces
5	25.4.2022 – 10.5.2022	A Cover Was Placed Glass, Reflective Mirror And Black gravels Inside The Pond

The following steps can be used to characterize the experimental process of the current work:

1. Fill the solar pond layers with pure water completely, insulating its three layers with an insulate material.
2. Measure the water temperature of the solar pond using thermocouples.
3. Add 400 grams of the magnesium sulfate salt ($MgSO_4$) per 1 liter of water (a concentration of around 28%) into the lower zone (LCZ) of the solar wait until the salt dissolves in the water and the brine becomes homogeneous.
4. Installing a plastic cover on the solar pond and measuring the water temperature.
5. Installing reflective mirrors on the sides of the solar pond with the plastic cover and measuring the water temperature.
6. Installing reflective mirrors on the sides of the solar pond with the glass cover; placing black black gravels at the bottom of the pond; and measuring the water temperature.
7. Feed the square channel with cold pure water at a temperature of about (0–3) °C at a volume flow rate of (0.5, 1 and 2) L/min, and measure the voltage and current generated by the thermoelectric because of the temperature difference between the solar pond and the cold water. Passing inside the square channel is the temperature of the water.

knowing that a tube was used to inject salt into the different layers of the solar pond.

Chapter Five
Results, Discussion and Comparison

Chapter Five

Results, Discussion and Comparison

Theoretical and experimental findings are given, examined, and contrasted in this chapter. The effects of providing a cover to the pond's surface and the impact of reflecting mirrors on performing a standard solar pond devoid of salt and a solar pond with a salt gradient are among the experimental findings. The production of electricity is a completing by using semi-metals (thermoelectric generator) and the temperature differential between the outer layer and the lower layer. These tests are all carried out independently. This will enhance the solar pond's useable energy and thermal efficiency, among other features. Magnesium sulfate salt and a plastic cover were used in the experiments on the solar pond with a salinity gradient. The previous experiments were repeated with a glass cover and gravel added to the solar pond.

5.1 comparison between the experimental and theoretical results

A comparison was made between the experimental and theoretical temperatures of the lower layer of the solar pond with the addition of salt, cover, reflective mirrors, and gravel. A clear increase in temperatures can be observed in the theoretical results, due to the low value of energy losses from the solar pond due to the influence of external factors on the performance of the solar pond, as a case Loss-free ideal. From the theoretical results, the lowest and highest temperatures were 58 and 66 °C, respectively. While it was 57 and 61 °C in the experimental results. As shown in Figure (5.1). The difference in maximum temperatures between theoretical and experimental results was 4 °C. In the theoretical case, there are no losses due to external factors such as the influence of wind, shade, and clouds that cause a decrease in the ambient temperature, In the experimental case, all of the aforementioned factors have an impact on the performance of the solar pond. The error percentage between theoretical and experimental results was 6%, which is acceptable in view of research's similar to the current work.

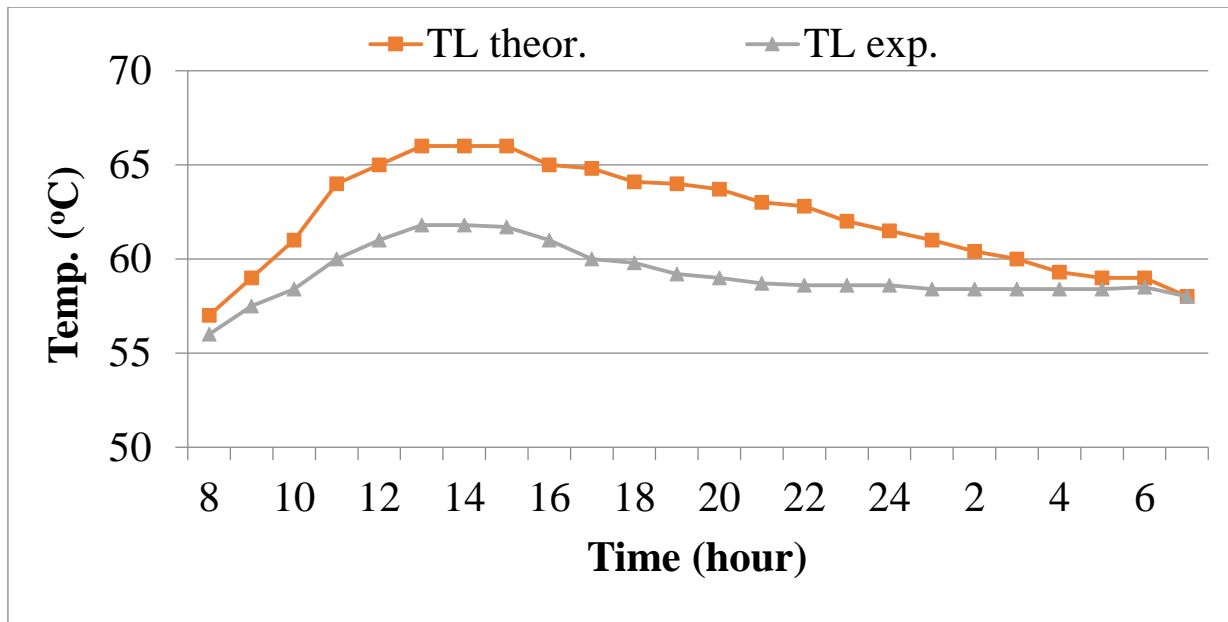


Figure (5.1) Comparison of the experimental and theoretical temperatures for the solar pond's lowest layer

In Figure (5.2), the useful energy of the salinity gradient solar pond with the addition of a cover, reflecting mirrors and gravel, are compared between the theoretical and experimental results. Reading the useful energy, there is an increase of 90% between the performance of the regular pond and the pond the actual equipment and additives such as salt, gravel and reflective mirrors. This indicates the extent to which these additives affect the performance of the solar pond and improve its productivity.

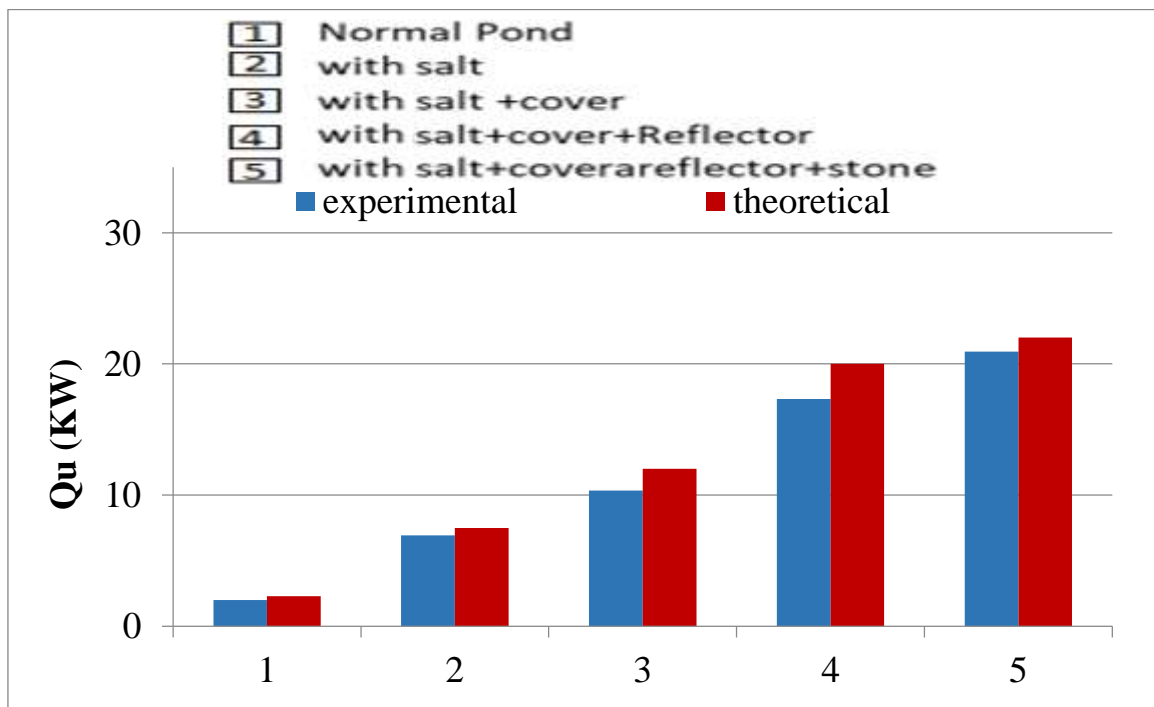


Figure (5.2) Comparison of the experimental and theoretical of the useful energy.

5.2 Theoretical Results

MATLAB program is used to calculate the results theoretically and compare them with experimental tests. In the program, the properties of magnesium sulfate salt with a concentration of 28% are used, with two different types of coverings that use plastic and glass, in addition to pebbles and reflective mirrors. The percentage of deviation in the experimental results was shown by comparing the experimental and theoretical results.

5.2.1 Solar Pond Temperature

The normal pond (NP) and the salinity gradient pond with the addition of cover and reflective mirrors are two examples of the ponds where special equations were applied using the Matlab program to get the following results, which show the water temperatures in the pond layers in four different cases.

When exposed to sunlight, water can absorb this radiation and convert it into heat energy, which it then stores within its layers. The water temperatures in the salt-free pond over a 24-hour period are shown in Figure(5.3). The results showed that the water temperature begins to rise during the day, reaching its maximum at one o'clock after noon with more radiation entering the water. This temperature gradually decreases when the water temperature decreases in this experiment to reach its lowest value of 10 Celsius at five o'clock in the morning. The temperature rose to a maximum of 32 Celsius when the solar radiation value was 1000 W / m^2 before it gradually decreases due to changes in the angle of sunlight hitting the surface of the pond.

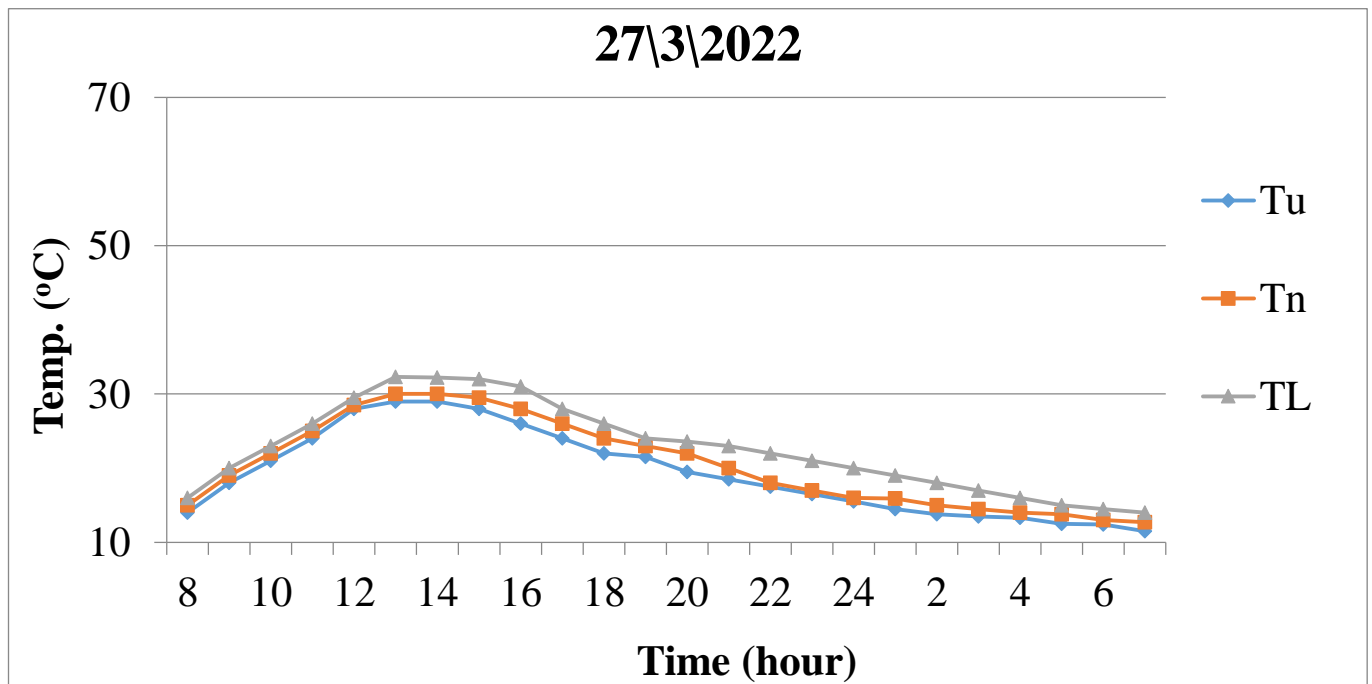


Figure (5.3) Temperature layers of the normal solar pond

The amount of solar radiation on the surface of the solar pond for the day of the experiment when using salt reached its maximum degree of 1005 W / m^2 . Figure (5.4) shows the high temperature of the ponds to reach 41.8Celsius degree one o'clock after noon, especially in the lower layer. The effect of salting water causes this to happen because the brine has the property of storing heat and preventing its loss to the surrounding. This results in a brine solution that absorbs solar energy and converts it into thermal energy inside the pond. The percentage increase in the temperature of the salt basin compared to the natural basin was 24%.

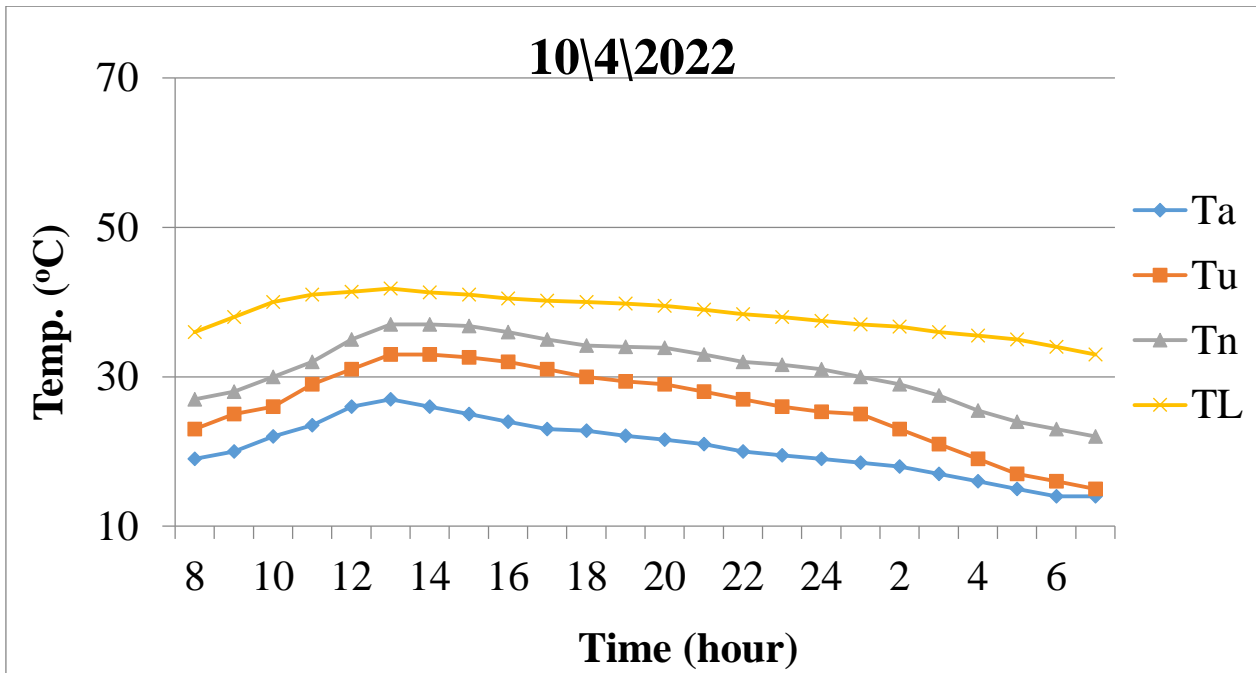


Figure (5.4) Temperature layers of the salty solar pond

Figure (5.5) shows the effect of covering the surface of the solar pond with plastic, in contrast to the previous case, where the salt gradient pond was left open to the elements. The graph shows a clear increase in the amount of radiation that reaches the surface of the pond, and the temperature of the bottom layer of the pond with 1010 W / m^2 and $47 \text{ }^\circ\text{C}$, respectively when the temperature was at the morning of the day at eight o'clock in the morning $42 \text{ }^\circ\text{C}$. Compared to the normal pond and the salt pond without cover, the percentage increase in temperature of the salt pond with cover was 31% and 10%, respectively. This is due to the cover's effect on the amount of heat inside the pond.

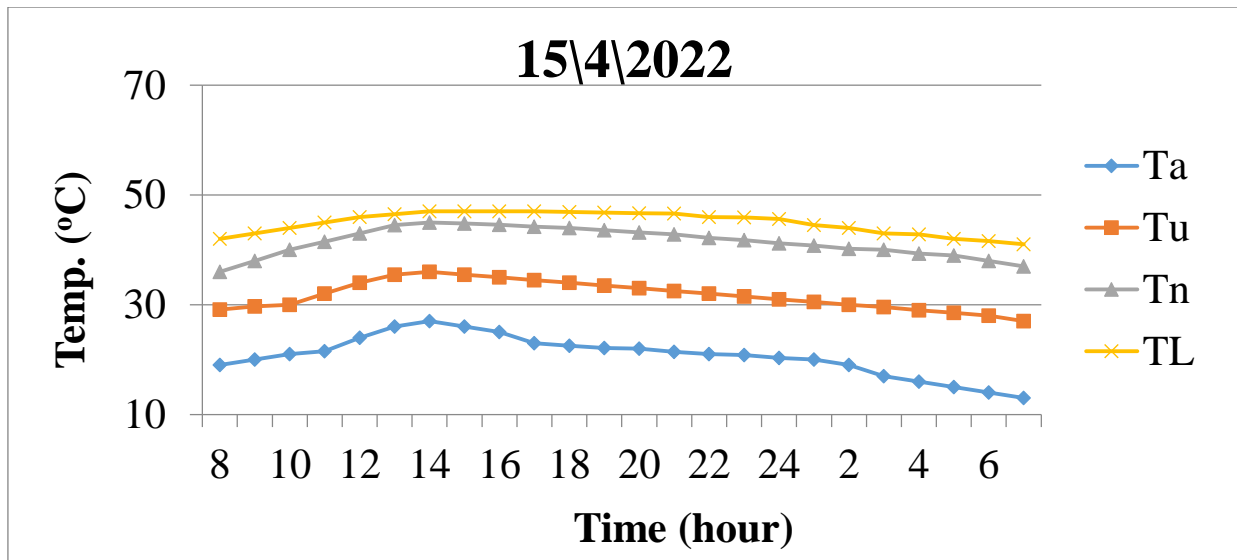


Figure (5.5) Temperature layers of the covered salty solar pond

Any increase in the amount of radiation falling on the surface of the pond shows an increase in the thermal energy stored in the pond because the amount of solar radiation on the surface of the pond affects the amount of thermal energy stored in the layers of the pond. Here comes the role of reflective mirrors on the sides of the pond, which increase the amount of radiation by diverting sunlight away from its surface towards the surface of the pond. At eight o'clock in the morning, the temperature was 58 Celsius degrees, and at one o'clock in the evening, the largest amount of radiation was reached, 1113 watts / m². When the temperature reached 65 Celsius degrees, this can be shown in Figure (5.6). The pond temperature increased by 28% over the previous case. These percentages show an increase in the efficiency of the pond when using salt, cover and reflectors together because the reflective mirrors increased the amount of radiation concentrated on the surface of the pond and thus increased the temperature inside and the cover prevents the escape of heat outside the surface of the pond.

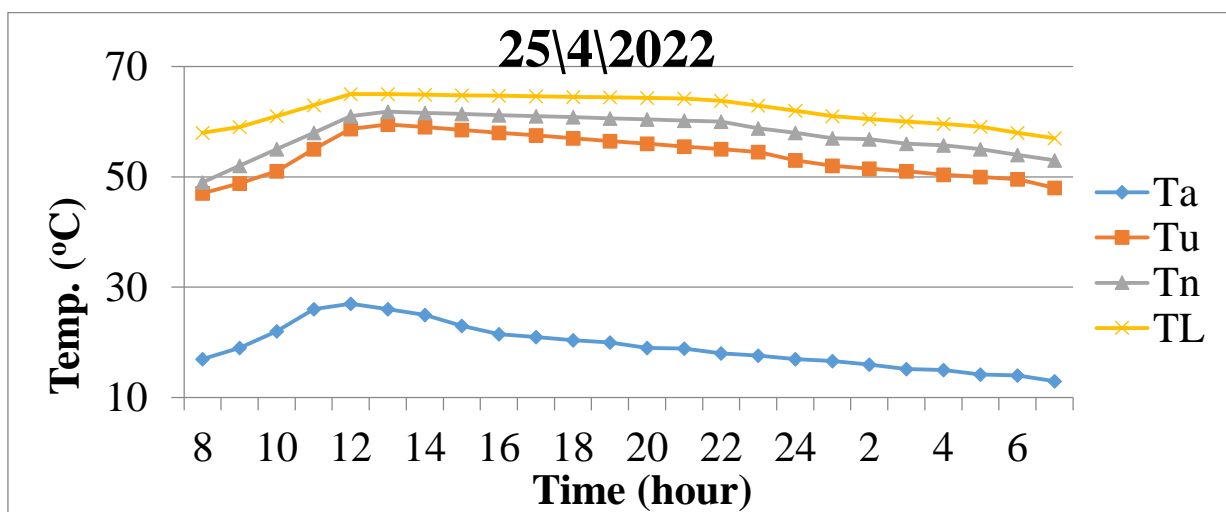


Figure (5.6) Temperature layers of the covered salty solar pond with the reflectors.

The amount of solar radiation on the surface of the solar pond for the day of the experiment when using salt, glass cover, reflector, and gravel. It reached its maximum value of 1155 W/m^2 . In Figure (5.7), a slight rise in temperature of 1 Celsius degree was observed after gravel was added to the bottom of the pond to verify its effect on raising the temperature of the solar pond. High air temperature may also cause the pond temperature to rise. The pond temperature, in this case, was 66 Celsius degree, percentage increase over the previous case that amounted to 0.15%. Results from the graphs below indicate that the effect of gravel on solar pond performance is comparable to the effect of salt on a pond. Therefore, regardless of the added cost of using the pond, there is no point in adding black gravels to it.

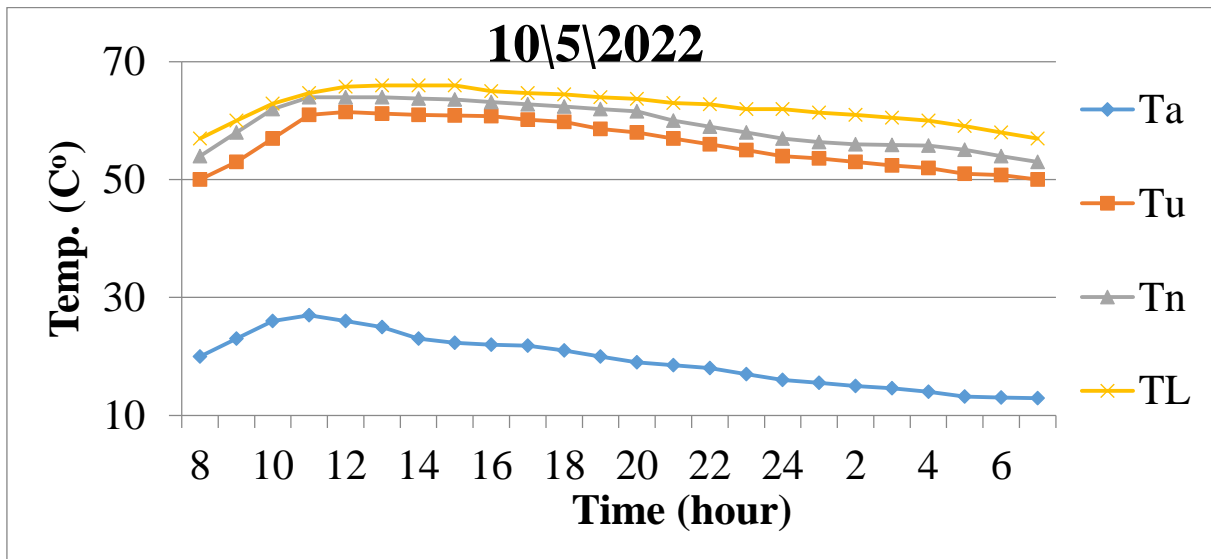


Figure (5.7) Temperature layers of the covered salty solar pond with the reflectors and black gravels .

5.2.2 Useful Energy of Solar Pond

Figure (5.8) presents the theoretical results for the useful energy of a solar pond with a normal pond and salinity gradient pond using with additional appliances and equipment. The pond temperature has increased since the reflective mirrors and cover were added, so more energy will be produced. This is because there is a direct relationship between it and temperature. Theoretical results show that the pond has a useful energy of 2 kilowatts. By adding salts, the useful energy reached 7.5 kilowatts, with an increase of 73%. The increase in radiation that affects the surface of the pond and adding salts, reflective mirrors, cover, and gravel, the useful energy 22 kW with a percentage increase of 89% compared to the normal pond.

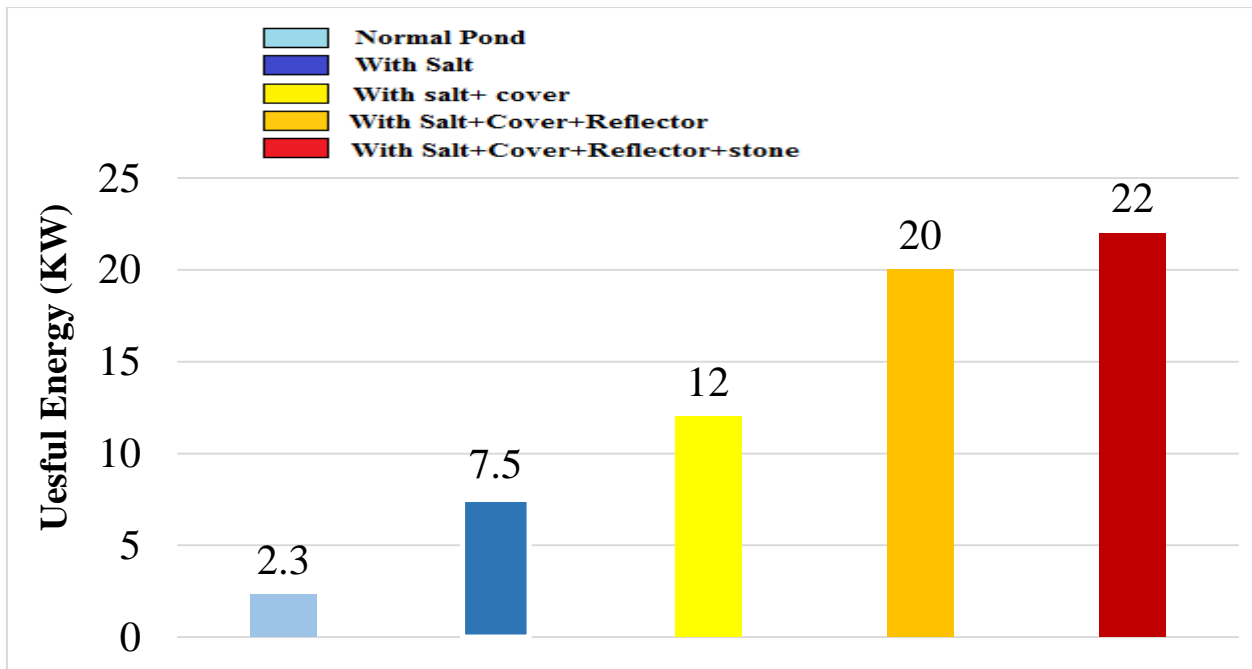


Figure (5.8) Useful Energy of Solar Pond with different conditions

5.2.3 Overall Thermal Efficiency of Solar Pond

The efficiency results of the conventional pond and the solar pond with a salinity gradient are shown in Figure (5.9). The pond's efficiency has significantly increased and reach to 32%. This is because of including gravel, cover, and reflective mirrors. This method improves the ponds' effectiveness. It increases the solar pond's useful energy, which is directly related to the solar pond's thermal efficiency. By doing improvements to the solar pond, efficiency rose from 5% to 32%.

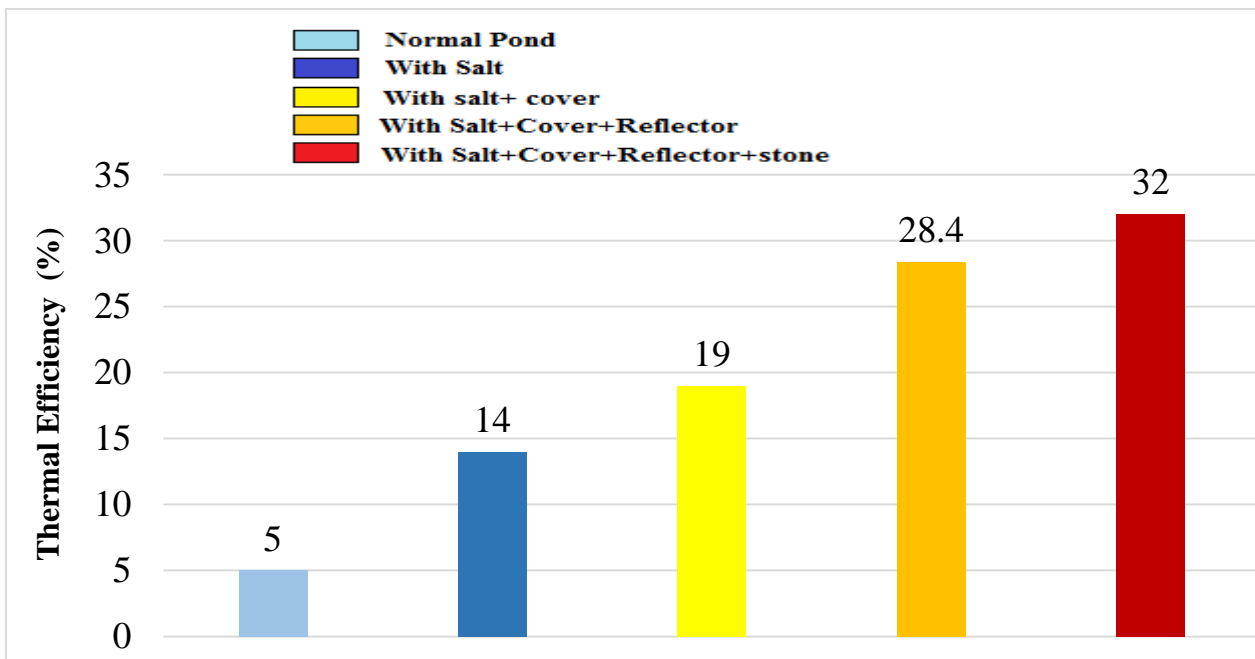


Figure (5.9) Overall Thermal Efficiency of Solar Pond with different conditions

5.2.4 Power of TEG

Figure (5.10) shows the current generated by TEG due to the difference in temperature and for three flow rates of water through tubes in contact with the electrodes with a value of 1.1 A at the flow rate 2 L/min and the temperature of the flowing water 20 Celsius degree. It should be noted that when the flow rate rises, the current value also rises, reaching 1.5 A at the temperature 60 Celsius degree of the water flowing at a rate of 2 L/min. The reason for this increase is that all TEG slides operate with the same productivity because all the water that comes into contact with the TEG at high velocity.

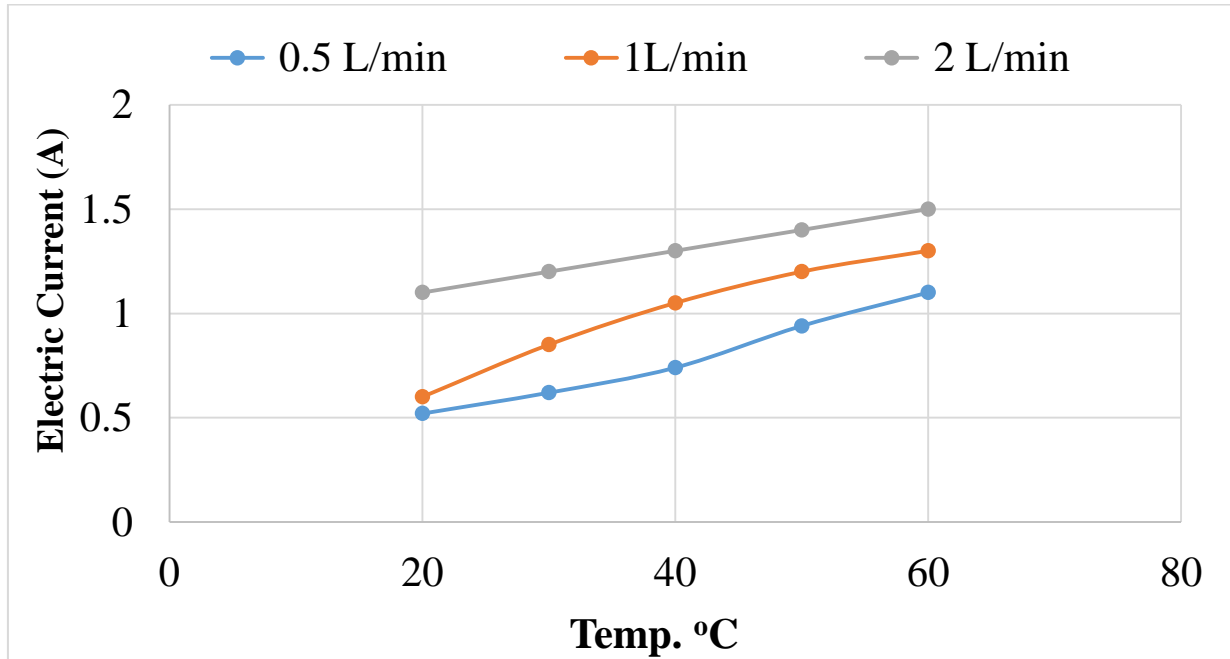


Figure (5.10) Electric Current Resulted from Solar Pond.

Figure (5.11) exhibits behaviour that is similarity that of the previous graph in terms of the cause. The graph shows the electrical potential difference (TEG) for three distinct water flow rates. The highest value of the voltage was 81 volts, when the value of the flow rate was 2 L/min, with an increase of 0.18% from the original flow rate 0.5 L/min, where the value of the voltage was 66 volts.

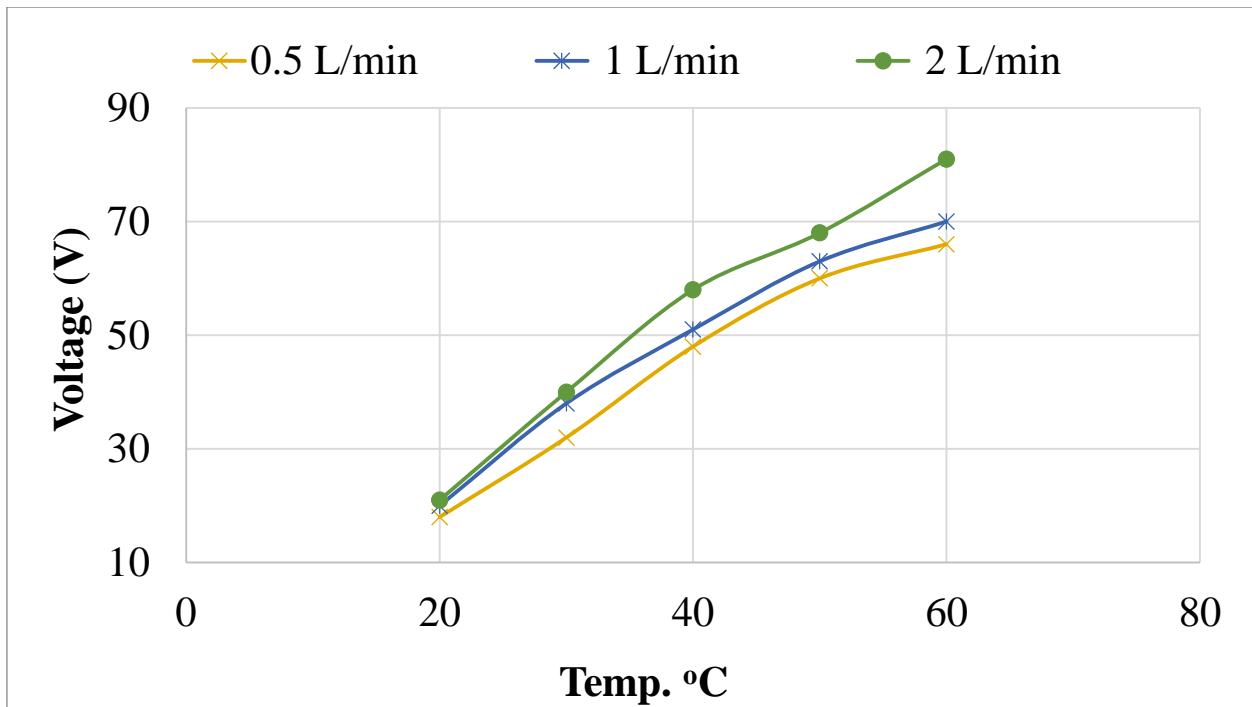


Figure (5.11) Voltage Resulted from Solar Pond.

The highest electric potential difference that can be obtained with a flow rate 2 L/min. in the same direction, calculating the electric potential difference and the current resulting from the passage of hot and cold water on both sides of the TEG at three flow rates results in the production of the electric power generated by (TEG), where it reached its maximum value of 121.5 watts, at a flow rate of 2 l/min. With an increase of 40% from the lowest flow rate of 0.5 L/ min, with a power of 72.6 watts, is shown in Figure (5.12).

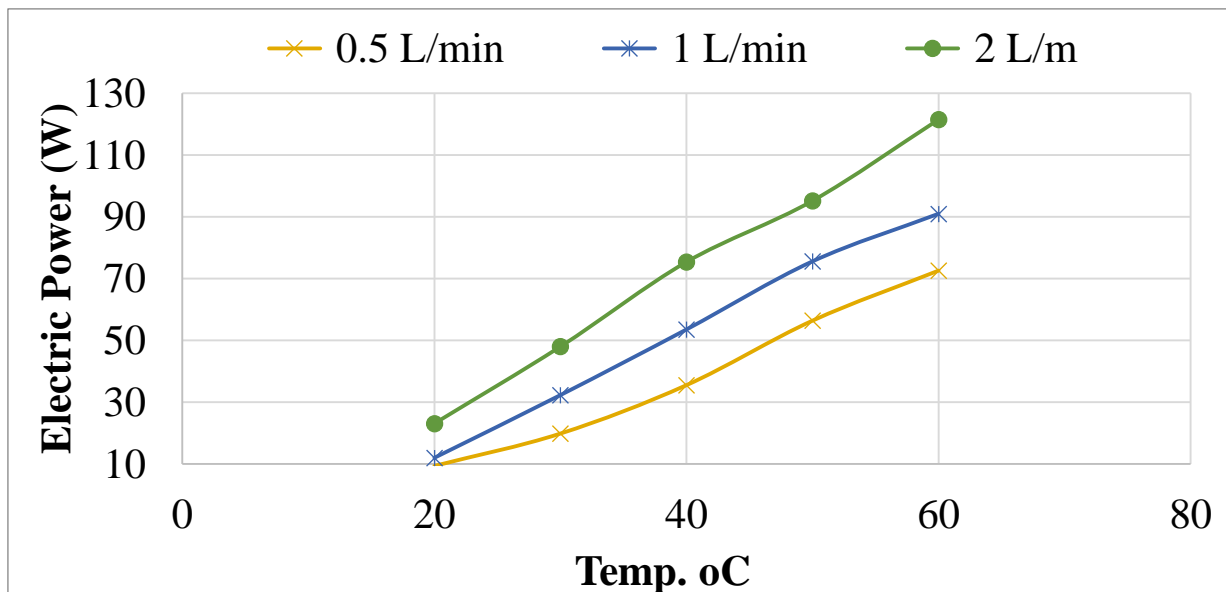


Figure (5.12) Electric Power Resulted from Solar Pond.

5.2.5 Electric Efficiency of Thermoelectric

The electrical energy generated by the work of the TEG is calculated from three flow rates to determine the electrical efficiency of the TEG, as shown in Figure (5.13). The electrical efficiency was 9%, when the flow rate was 0.5 L/min and increased to 12% at the flow rate 2 L/min. It can be seen that increasing the mass flow rate increases the thermal efficiency.

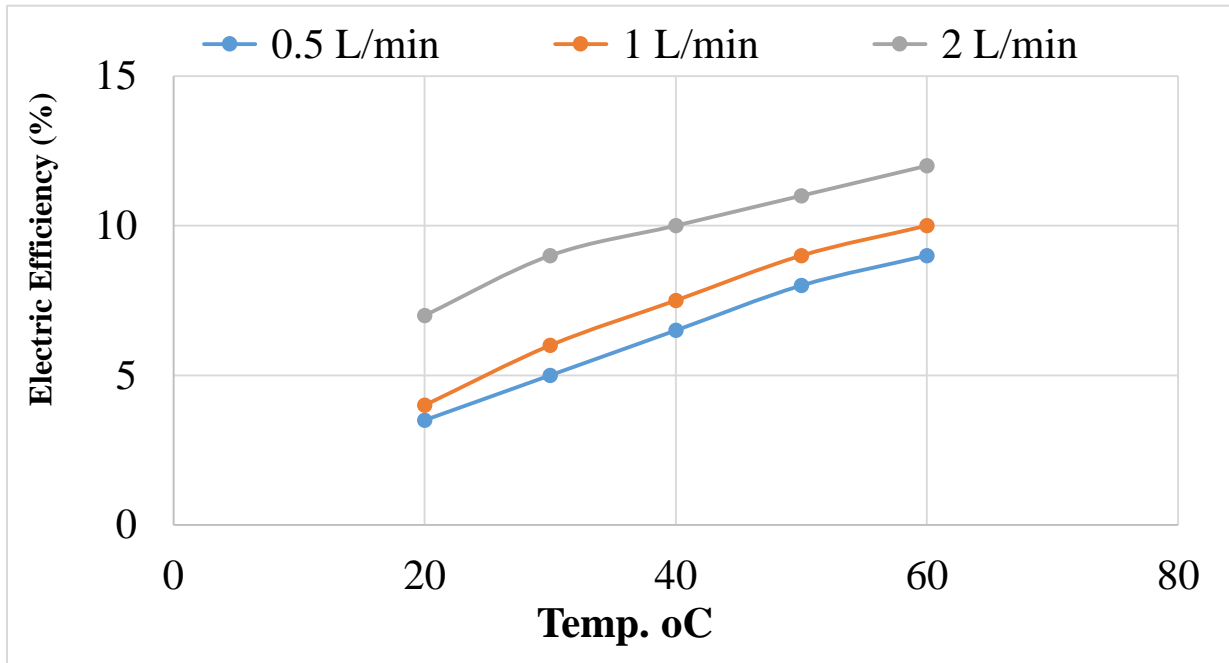


Figure (5.13) Electric Efficiency of Thermoelectric.

5.3 Experimental Results

In the experimental part, the solar pond's temperature and the surrounding air temperature are both monitored. Then, the solar pond's thermal efficiency and useful energy are computed.

5.3.1 Solar Pond Temperature

Figure (5.14) shows the ambient temperature of the traditional solar pond without additions, as well as the temperatures of the three layers of the pond. The behaviour of the pond can be observed to between the experimental and theoretical, where the temperature inside the pond begins with the increase in the temperature of the surroundings and the amount of radiation that falls on the surface of the pond, then the temperature begins to decrease as the sun goes down and the amount of radiation reaching the solar pond decreases. The temperature was at the beginning of the day, specifically at eight o'clock in the morning 20.8 Celsius degree, and, then rise to 25.7 Celsius degree at one after noon.

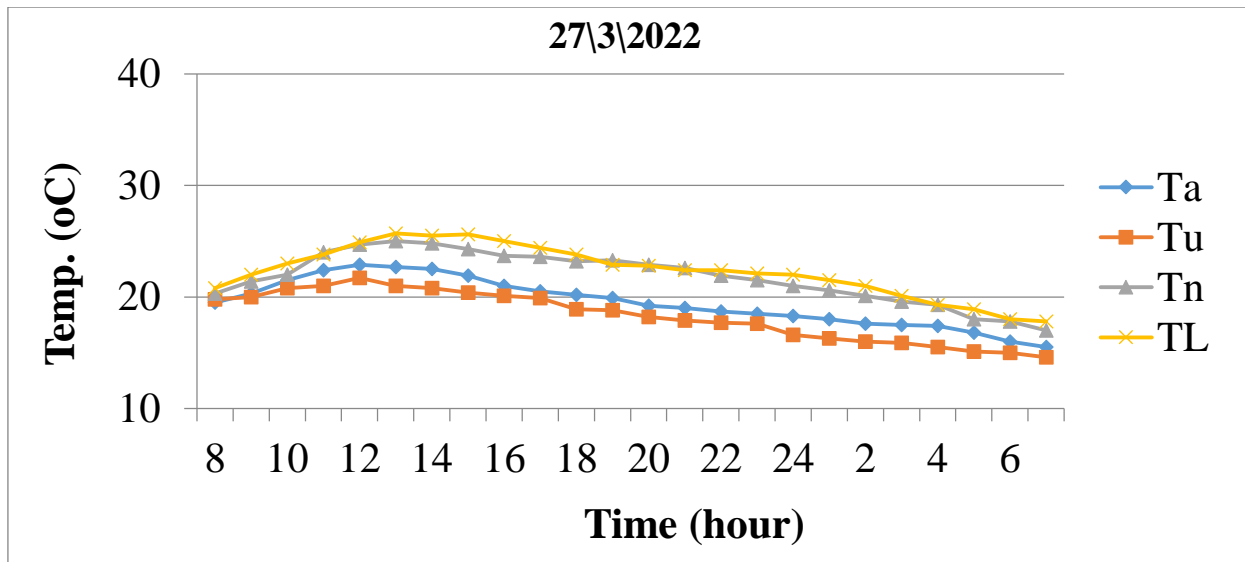


Figure (5.14) Temperature layers of the normal solar pond.

According to the results, as shown in figure (5.15), the maximum value of the water temperature for a typical solar pond was attained at around 1 PM. On the date 27/3/2022. With utilizing salts, it begins at 11:00 AM and lasts until 4 PM. This is can be due to the water has a high specific heat capacity (4.18 kJ/kg C), which makes it a slow conductor of heat. As a result, it takes longer to reach its maximum temperature than salt because of its poor heat capacity. Because of this, adding salt to water causes the salt ions to interact with the water molecules, resulting in a salty combination that has a lower heat capacity (about 1.2 kJ/kg. C) than water in a container. To put it another way, because the hydrogen bonds in the resultant mixture are weaker than those in water alone, it takes less time to reach the maximum temperature.

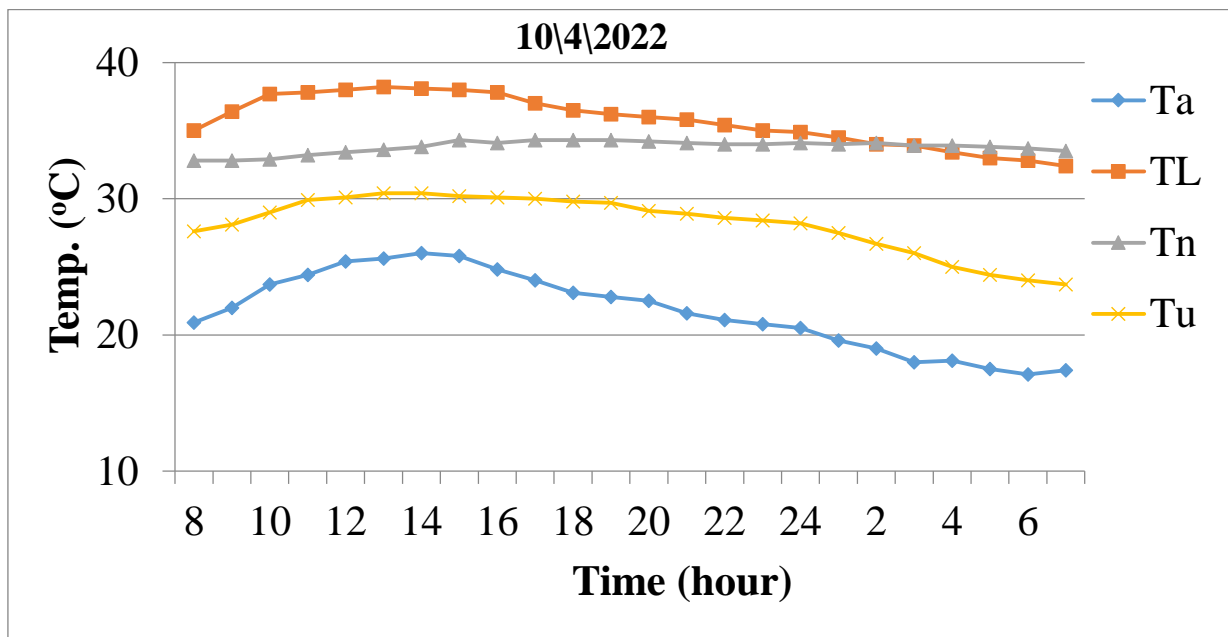


Figure (5.15) Temperature layers of the salty solar pond.

from the previous figure. The temperature of the salt pond was 38.2 C at 1:00 PM, with a percentage increase of 33% compared normal pond, as the maximum temperature in it reached 25.7 Celsius degree at the same time of the day.

Result of covering the solar pond’s surface with plastic are seen in Figure (5.16). The graph shows a discernible rise in pond temperature at the lowest zone, reach 45.1 C With a percentage increase of 43% from the normal pond case. The cover impact on the pond’s functionality accounts for this, as it significantly reduces water evaporation and heat loss from the pond.

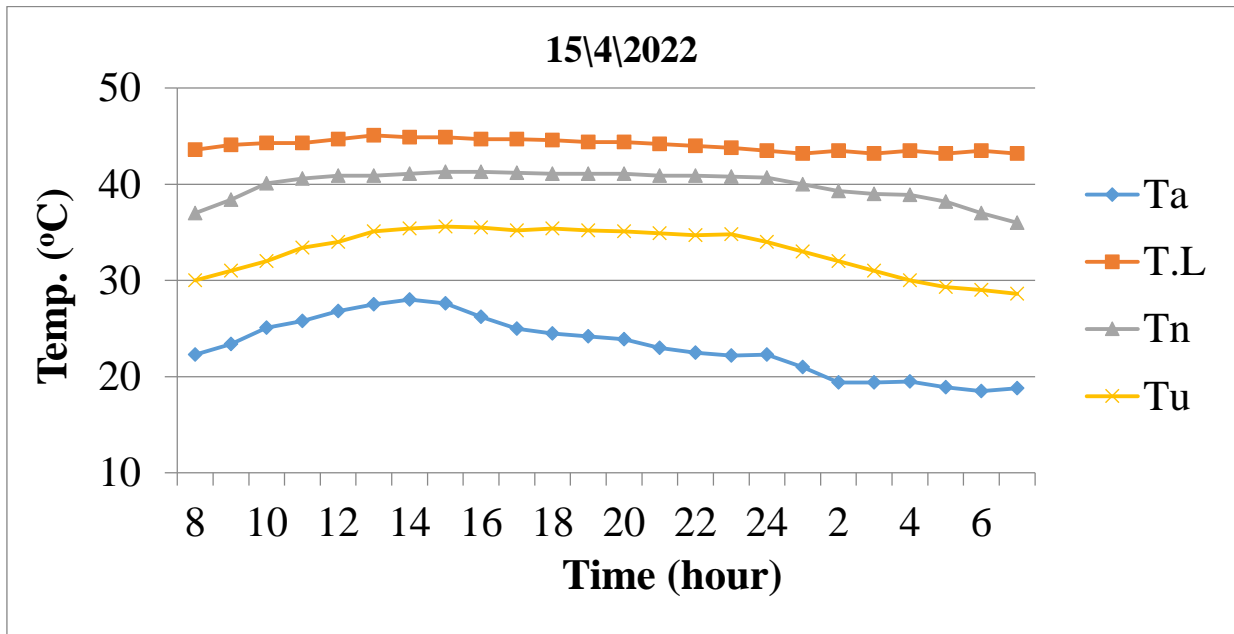


Figure (5.16) Temperature layers of the covered salty solar pond.

Increased thermal energy stored in the pond is shown by an increase in the radiation emitted on the pond’s surface. This is where the reflective mirrors on the pond’s sides come into effect, increase the amount of radiation by reflecting the sun’s rays that hit its surface toward the pond’s surface, the temperature reach 59.2 Celsius degree due to the effect of reflective mirrors, and the increase was by 56% compared to that of the normal pond, as illustrated in Figure (5.17).

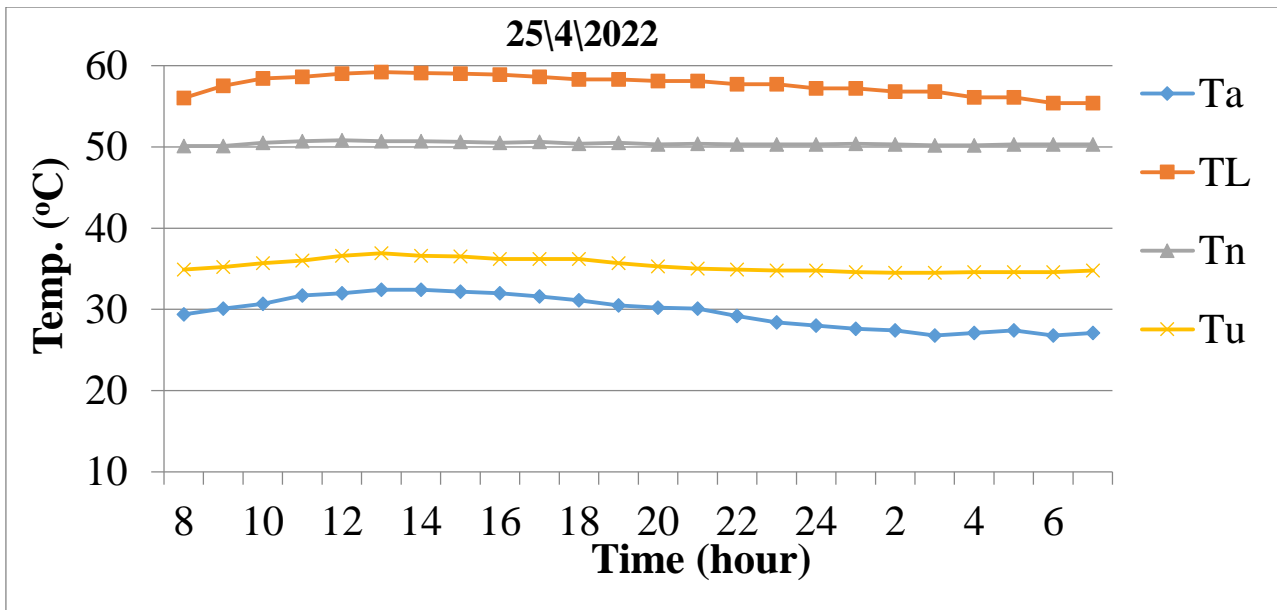


Figure (5.17) Temperature layers of the covered salty solar pond with the reflectors.

The increase in the thermal energy stored in the pond is shown by the increase in the radiation emitted on the surface of the pond 919 W/m^2 . Mirrors and glass cover increase the amount of radiation that hit the surface of the pond. In addition black gravels, the temperature reaches 61.9 degrees Celsius due to the effect it, an increase of 58% compared to in the normal pond as shown in Figure (5.18). It was concluded through the results that the effect of adding gravel is small on the performance of the pond compared to the effect of salt on the pond in terms of the high temperatures of the layers of the solar pond. Therefore, adding gravel to the pond would not be feasible besides the increased cost of using it.

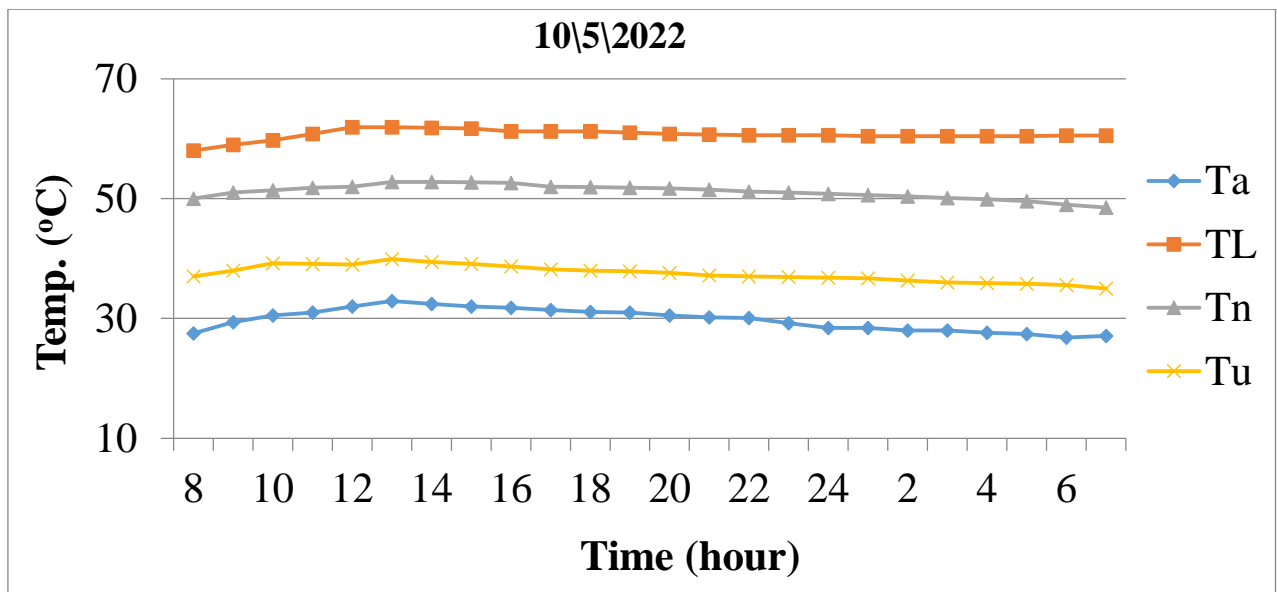


Figure (5.18) Temperature layers of the covered salty solar pond with the reflectors and black gravels .

5.3.2 Useful Energy and Thermal Efficiency of Solar Pond

The outputs of the solar pond useful energy for the four cases (normal, with salt, with cover and reflective mirrors) are shown in Figure (5.19). Comparing the salinity-graded pond results with the typical pond results shows that salt, cover, and mirrors can enhance the produced energy of a solar pond. Naturally, this happens because the usable energy depends on the temperature difference, and since the use of these methods raises the temperature of the pond, the useful energy will undoubtedly also rise. The percentage of increase in useful energy between the normal pond and the salt-gradient pond reached 88%. The reason for this is due to the large temperature difference between the normal pond and the salt gradient pond.

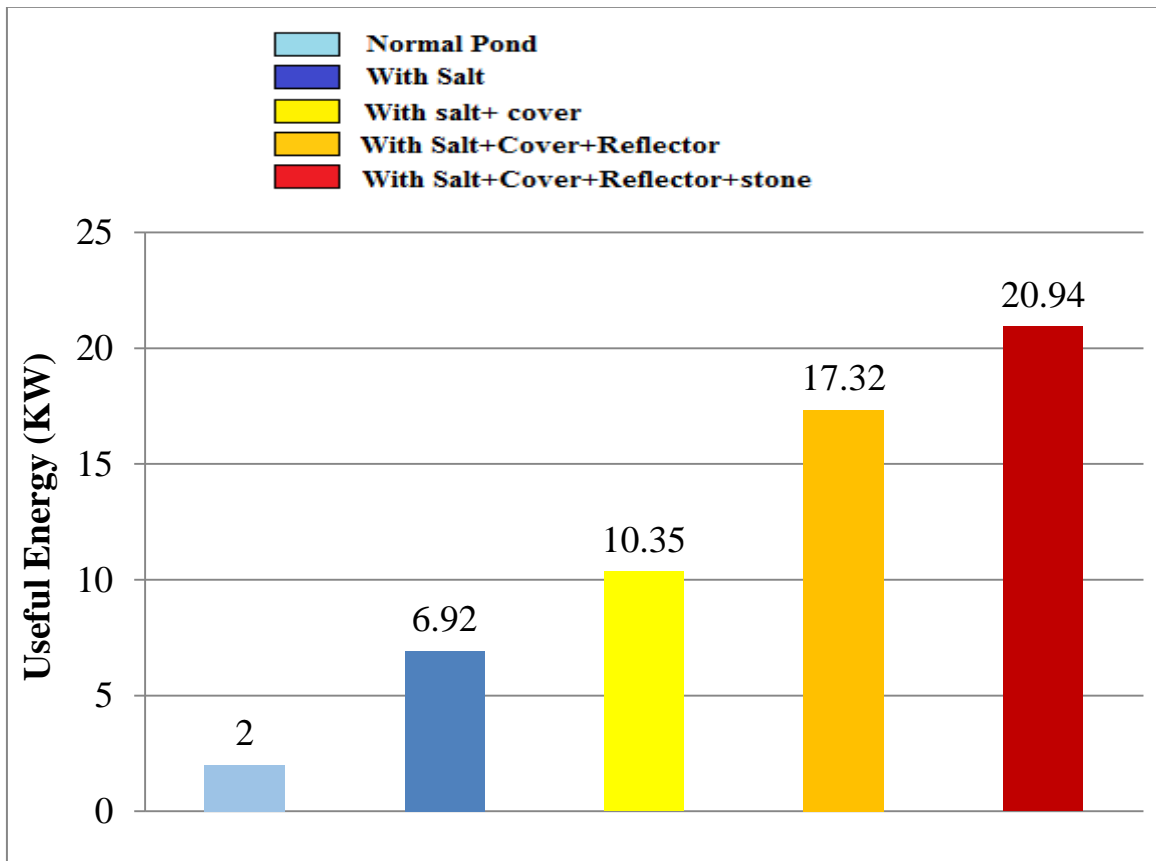


Figure (5.19) Useful Energy of Solar Pond

The experimental findings of the thermal efficiency of solar ponds with a regular pond and a salinity gradient pond with various methodologies are shown in Figure (5.20). According to the findings, these methods can improve the solar pond's thermal efficiency. This occurs because the thermal efficiency is determined by dividing the useful energy by solar radiation. The thermal efficiency will undoubtedly increase as these technologies increase the useful energy of the solar pond. The outcomes also showed that the solar pond's thermal efficiency is increased by using cover and reflective mirrors.

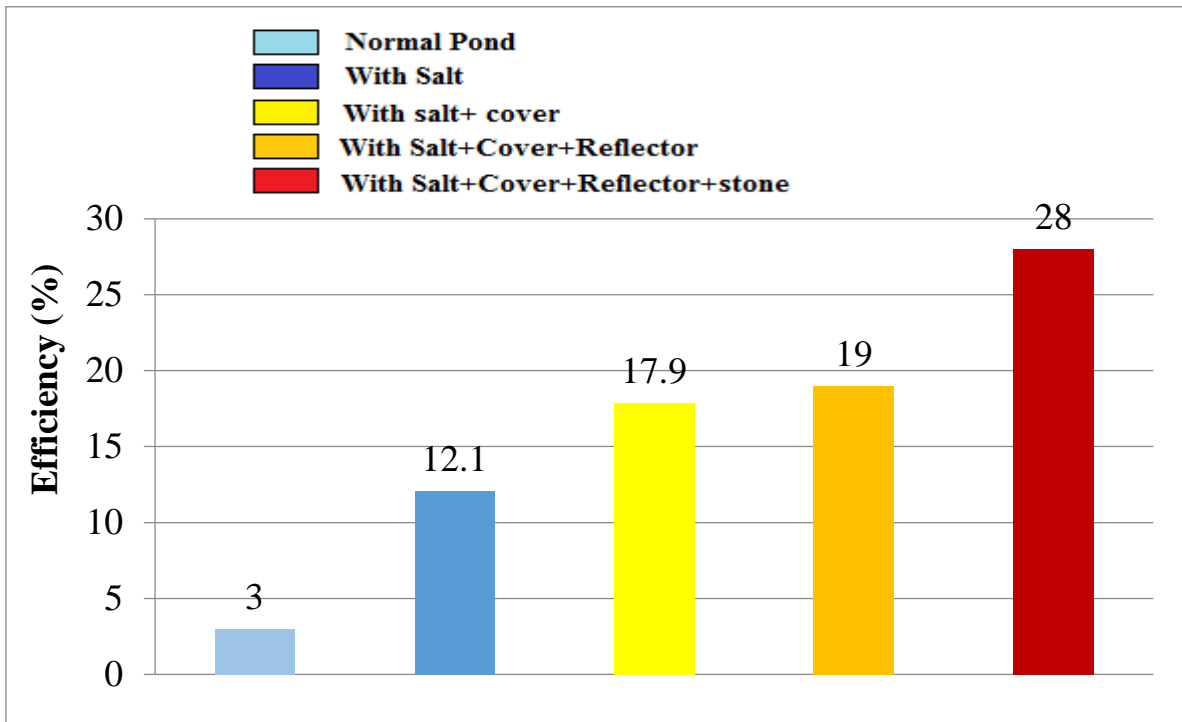


Figure (5.20) Thermal Efficiency of Solar Pond.

5.3.3 Power Resulted from Solar Pond

The current produced by TEG because of temperature differences and for three water flow rates through the tubes in contact with the electrodes is shown in Figure (5.21) (TEG). It should be noted that when the flow rate rises, the current value also rises. The reason for this increase is that all the (TEG) chips operate at the same productivity and all the water in contact with the (TEG) at highest velocity.

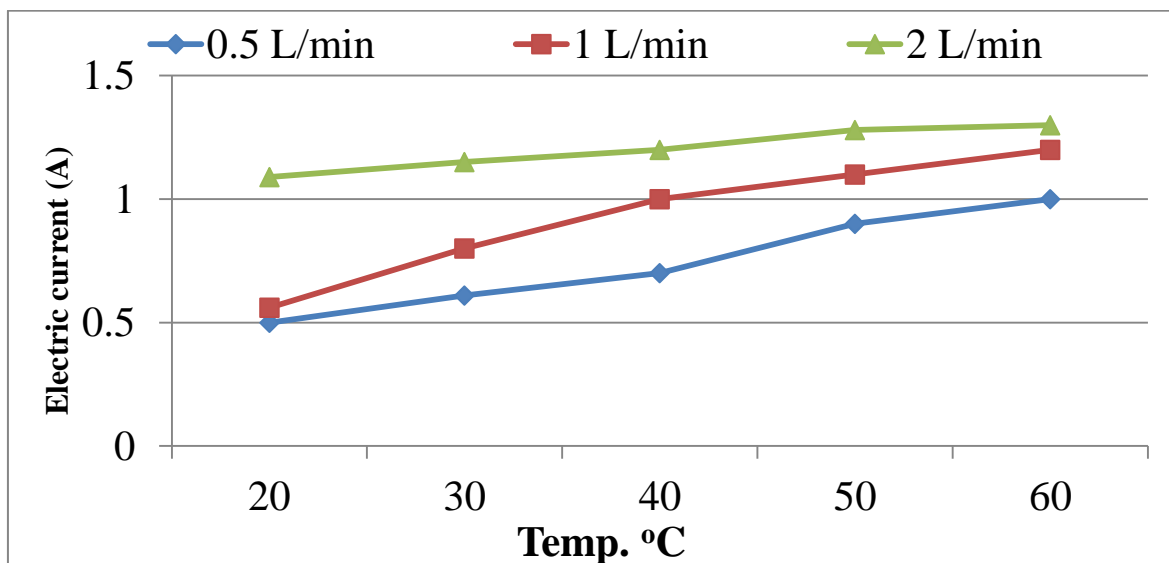


Figure (5.21) Electric current resulted.

Figure (5.22) exhibits behaviour that is comparable to that of the previous drawing in terms of the increase and its underlying cause. The electrical potential differential (TEG) for three different water flow rates is depicted in the graph. It is clear from the same pattern that the electric potential difference increases at the maximum flow rate.

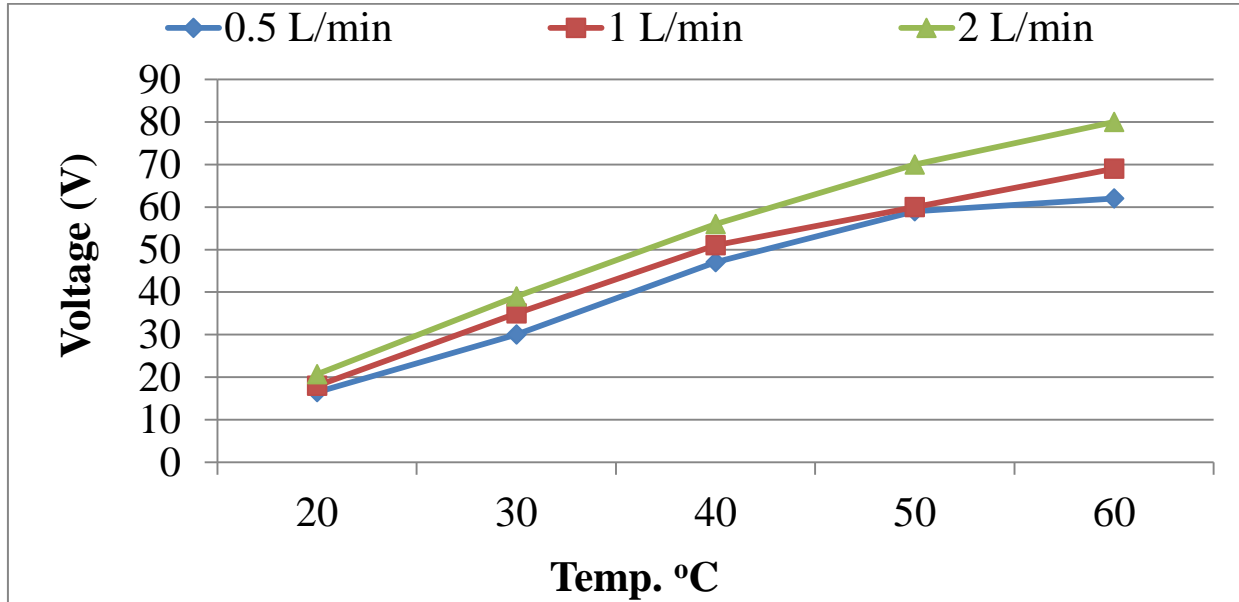


Figure (5.22) Voltage Resulted from TEG by Solar Pond

Calculating the electrical potential difference and the current caused by the flow of hot and cold water on both sides of the TEG at a rate of 2 liters per minute leads to the production of electrical energy, as shown in Figure (5.23). In the same figure, the electrical efficiency of the (TEG) is estimated by calculating the electrical energy generated by the work of the (TEG) and also at a flow rate of 2 liters per minute. It can also be seen that E. P. increases with increasing temperature, reaching 104 W at a temperature of 60 Celsius degrees.

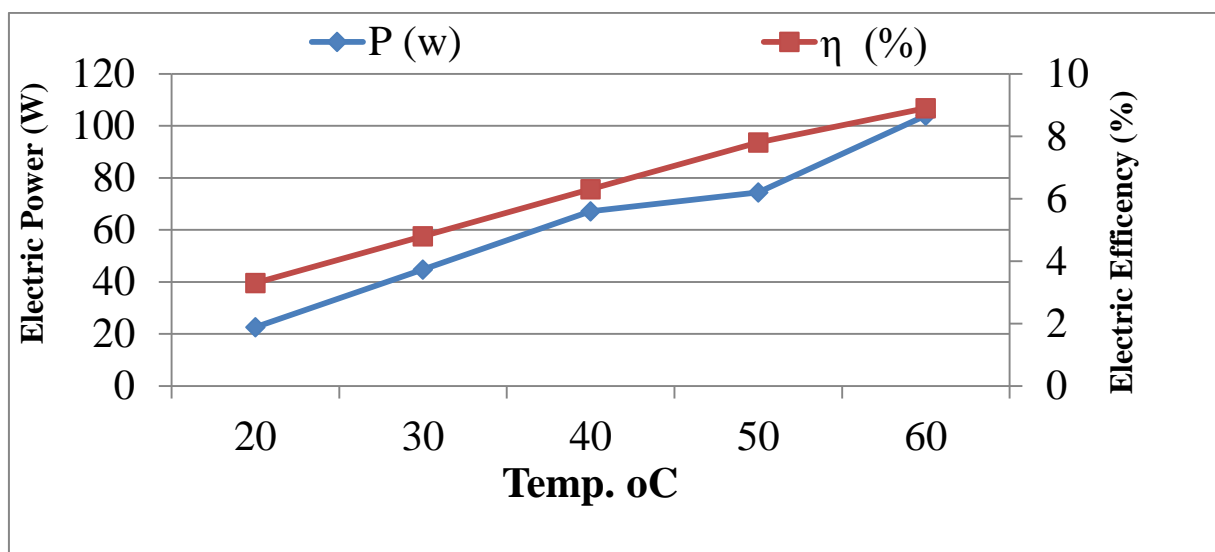


Figure (5.23) Power and Efficiency Resulted from Solar Pond

5.4 Comparison between the experimental and theoretical results

The comparison of the experimental and theoretical findings from the voltage produced by the TEG using hot pond water is shown in Figure (5.24). Same behaviour with regard to voltage and current. An increase in the amount of voltage can be observed as the temperature difference increases on both sides of TEG. The percentage 74% between the highest and lowest temperature in both experimental and theoretical readings.

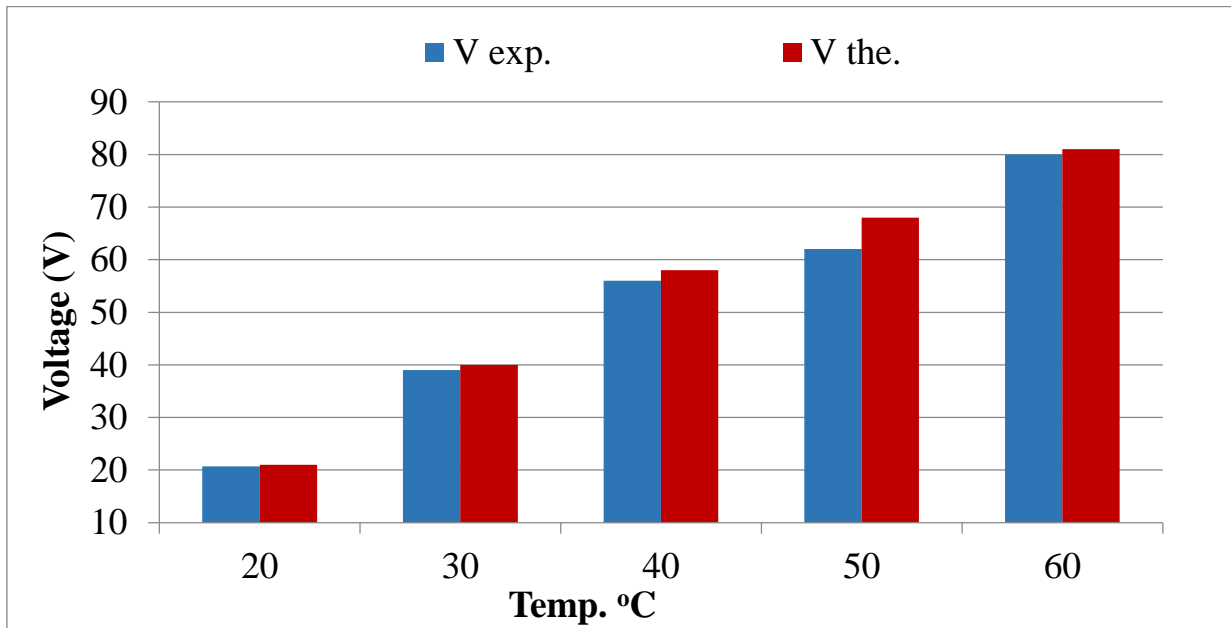


Figure (5.24) Comparison of the experimental and theoretical findings of the voltage produced by the TEG

The comparison of the actual and predicted values of the electric Current by the TEG using hot pond water is shown in Figure (5.25).

It was showed through the figures that the outcomes from theoretical and experimental are close by drawing the current resulting of TEG at different temperatures, the percentage increase estimated at 26% and 16% for theoretical and experimental method, respectively.

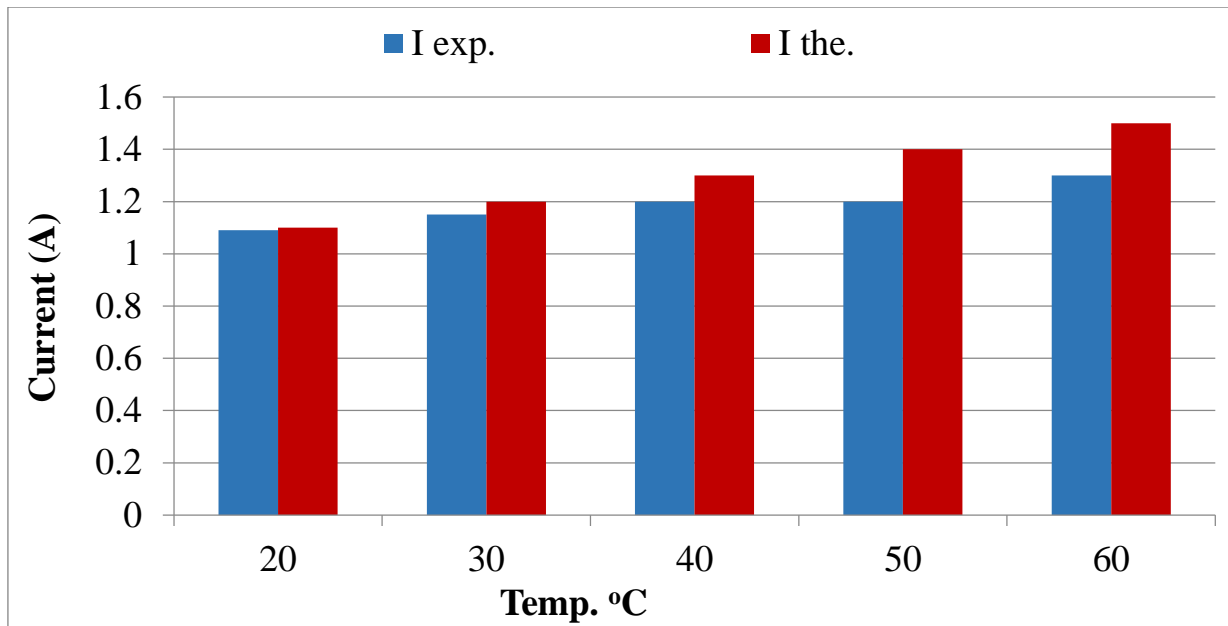


Figure (5.25) Comparison of the experimental and theoretical findings of the Electric Current by the TEG.

There is an increase of approximately 80% between the value of electrical energy obtained by experimental and theoretical method of the highest and lowest temperature resulting from solar basins with a salt gradient, with the addition of cover, reflective mirrors and gravel for the purpose of producing energy from the thermoelectric generator. Figure (5.26) indicates the extent to which these additions affect the performance of the solar pond and improve its productivity, thus increasing the production of energy generated by the thermoelectric generator will be is crossed.

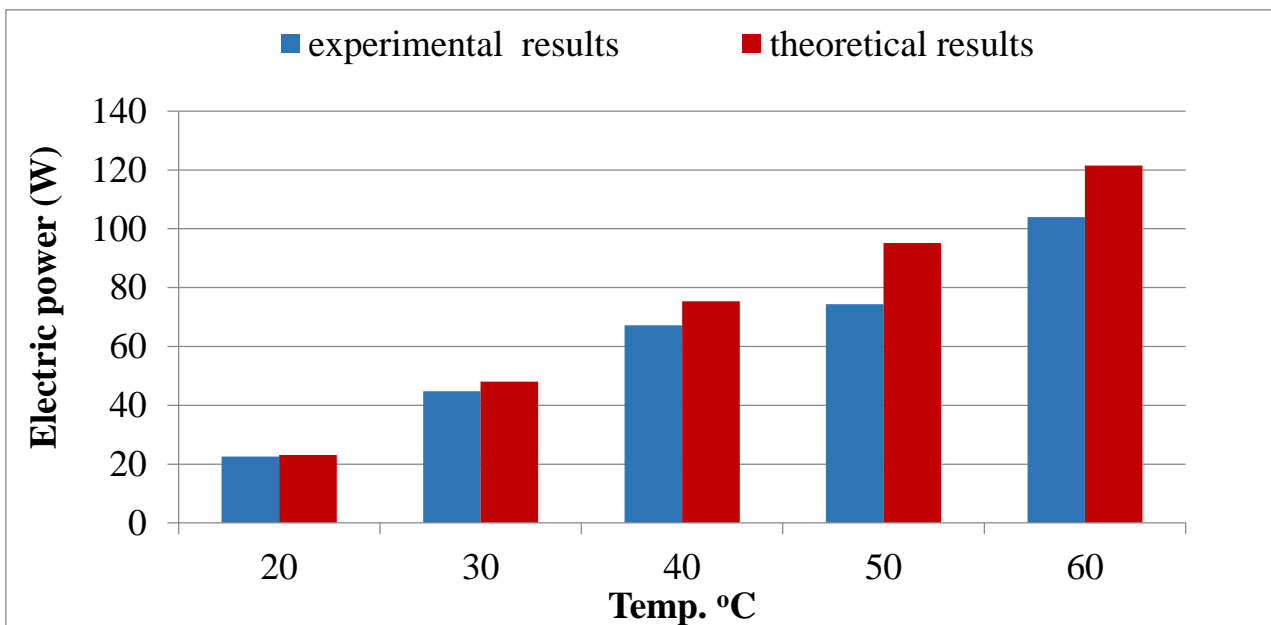


Figure (5.26) Comparison of the experimental and theoretical findings of the Electric power by the TEG.

5.5 Validation with previous work

A validation of the current work is conducted with the research (M H Abbood et al. 2021) [30] and Prasad 2016 [17] on performing the solar pond, considering the substrate's thickness, the pond's surface area, and the temperature of the lower layer produced by the solar pond.

The Authors	Year	Thickness Of LCZ m	Area Of Solar Pond m ²	Efficiency %	Solar Radiation W/m ²	Description
Prasad	2016	0.8	4	11.2	1100	salinity gradient solar pond conducted a computational simulation to understand a behavior of a solar pond and a direction of heat diffusion based on assumptions
Abbood et al	2021	0.4	7.29	18.3 %	1135	salinity gradient solar pond using (NaCl) with reflecting mirrors and solar tracking system.
Current work	2022	0.5	6.25	32%	1155	Solar pond with a salinity gradient made of magnesium sulfate salt, reflective mirrors, a glass cover, and black gravels .

When putting the comparison results in a graph as shown in figure (5.27), it is possible to note the increase resulting from the current work in the efficiency of the solar pond. This can be explained by the effect of several factors, including the insulating material used to isolate the walls of the pond from the surroundings, and the cover on the surface of the pond, which greatly contributed to reducing the losses from the pond. The reasons are the wind or evaporation of water from the surface of the pond, in addition to the type of salt used and its properties.

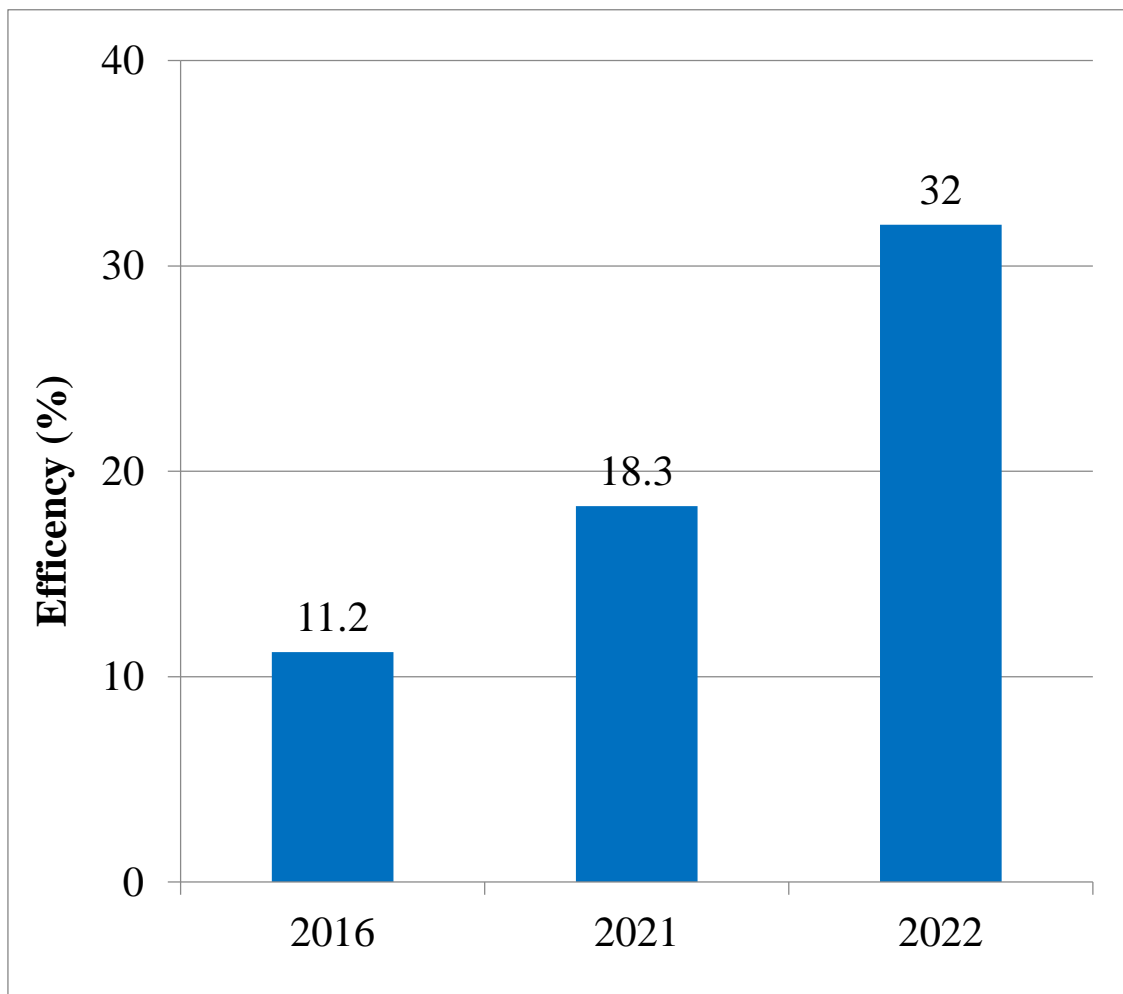


Figure (5.27) A comparison of the efficiency of the solar pond for the current work (2022) and other researches for the years from 2016 to 2021.

CHAPTER SIX
CONCLUSIONS AND RECOMMENDATIONS

Chapter Six

Conclusions and Recommendations

6.1 Conclusions

The following conclusions were drawn from the experimental and theoretical results of the current work:

1. Solar pond's thermal properties and storage capacity are enhanced by adding salt, and solar pond's thermal properties can be improved by adding reflecting mirrors to the edges of the structure.
2. The plastic cover has improved the efficiency of the pond's operation.
3. When installing salt (magnesium sulfate), cover (plastic and glass), reflectors and black gravel for the solar pond, the experimental efficiency of the pond reached 28%, and the theoretical efficiency increased by 12% compared to the experimental results.
4. At a temperature of 60 degrees Celsius, the electric power and efficiency generated by TEG for the solar pond were 104 and 9% watts for the experimental, respectively, and increased by 14% and 25% for the theoretical compared to the experimental results.
5. When adding salt, cover, mirrors, and black gravel to the pond, the amount of useful energy increased by 90% for the experimental, and with the same percentage of increase, the amount of useful energy increased for the theoretical. Compared to the normal pond.

5.2 Recommendations

1. Using phase change materials to store heat is desired so that it may be used for as long as possible.
2. Adding nanomaterials to the bottom layer to improve thermal energy storage is also beneficial.
3. Using TEG to generate electricity between the upper and lower layer of the solar pond.

References

References

1. Singh, B., Tan, L., Date, A., & Akbarzadeh, A. (2012, December). Power generation from salinity gradient solar pond using thermoelectric generators for renewable energy application. In 2012 IEEE International Conference on Power and Energy (PECon) (pp. 89-92). IEEE
2. Sayer, A. H. (2017). An experimental and theoretical investigation of novel configurations of solar ponds for use in Iraq. University of Surrey (United Kingdom).
3. Aramesh, M., Kasaeian, A., Pourfayaz, F., & Wen, D. (2017). Energy analysis and shadow modeling of a rectangular type salt gradient solar pond. *Solar Energy*, 146, 161-171.
4. Mahdi, J. T., & Jebbar, Y. A. (2019, August). A theoretical investigation of solar radiation and heat transfer in a solar pond in Kerbala city. In *AIP Conference Proceedings* (Vol. 2144, No. 1, p. 030019). AIP Publishing LLC.
5. Rizvi, R. Z., Jamal, Y., Ghauri, M. B., Salman, R., & Khan, I. (2015). Solar pond technology for brine management and heat extraction: a critical review. *Journal of Faculty of Engineering & Technology*, 22(2), 69-79.
6. . Abdulsalam, A., Idris, A., A. Mohamed, T., & Ahsan, A. (2015). The development and applications of solar pond: a review. *Desalination and Water Treatment*, 53(9), 2437-2449.
7. Assari, M. R., Tabrizi, H. B., Nejad, A. K., & Parvar, M. (2015). Experimental investigation of heat absorption of different solar pond shapes covered with glazing plastic. *Solar energy*, 122, 569-578.
8. Okhrimenko, L., Favergeon, L., Johannes, K., Kuznik, F., & Pijolat, M. Thermodynamic study of MgSO₄-H₂O system dehydration at low pressure in view of heat storage [Author links open overlay](#).
9. Abbood, M. H., Alhwayzee, M., & Sultan, M. A. (2021, February). Experimental investigation into the performance of the solar pond in Kerbala. In *IOP Conference Series: Materials Science and Engineering* (Vol. 1067, No. 1, p. 012098). IOP Publishing.
10. Aljibory, M. W., Hashim, H. T., & Abbas, W. N. (2021, February). A review of solar energy harvesting utilising a photovoltaic-thermoelectric integrated hybrid system. In *IOP Conference Series: Materials Science and Engineering* (Vol. 1067, No. 1, p. 012115). IOP Publishing.

11. J. O'Callaghan, "Thermoelectric energy harvesting," *Sensors* (Peterborough, NH), vol. 28, no. 6, doi: 10.5772/intechopen.85670, 2011.
12. D. M. C. Rowe, *Handbook of Thermoelectric*. 1995.
13. S. Twaha, J. Zhu, Y. Yan, and B. Li, "A comprehensive review of thermoelectric technology: Materials, applications, modelling and performance improvement," *Renew. Sustain. Energy Rev.*, vol. 65, pp. 698–726, doi: 10.1016/j.rser.2016.07.034, 2016.
14. B. I. Ismail, and W. H. Ahmed, "Thermoelectric power generation using waste-heat energy as an alternative green technology," *Recent Patents on Electrical & Electronic Engineering (Formerly Recent Patents on Electrical Engineering)*, 2(1), 27-39, 2009.
15. Bezir, N. C., Dönmez, O., Kayali, R., & Özek, N. (2008). Numerical and experimental analysis of a salt gradient solar pond performance with or without reflective covered surface. *Applied Energy*, 85(11), 1102-1112.
16. Singh, B., Gomes, J., Tan, L., Date, A., & Akbarzadeh, A. (2012). Small scale power generation using low grade heat from solar pond. *Procedia engineering*, 49, 50-56.
17. Tundee, S., Srihajong, N., & Charmongkolpradit, S. (2014). Electric power generation from solar pond using combination of thermosyphon and thermoelectric modules. *Energy Procedia*, 48, 453-463.
18. Singh, B., Remeli, F., Oberoi, A., Tan, L., Date, A., & Akbarzadeh, A. (2014). Electrical power generation from low grade heat of salinity gradient solar pond using thermoelectric generators. In *Proceedings of the 52nd annual conference, Australian Solar Energy Society (Australian Solar Council), Melbourne*. ISBN (pp. 948-0).
19. Assari, M. R., Tabrizi, H. B., Nejad, A. K., & Parvar, M. (2015). Experimental investigation of heat absorption of different solar pond shapes covered with glazing plastic. *Solar energy*, 122, 569-578.
20. Qarroot, A. W. (2015). *Using Solar Evaporation Ponds for the Treatment of the Desalination Plants Brine*.
21. Singh, B., Saoud, A., Remeli, M. F., Ding, L. C., Date, A., & Akbarzadeh, A. (2015). Design and construction of a simple thermoelectric generator heat exchanger for power generation from salinity gradient solar pond. *Jurnal Teknologi*, 76(5).
22. Balaji, B. (2016). Experimental Investigation On A Mixed Salt Salinity Gradient Solar Pond. *International Journal*, 8(1), 252-261.
23. Al-whoosh, K., Aljaradin, M., Bashitialshaaer, R., & Balawneh, H. (2017). Establishing Small-Scale Salt-Gradient Solar Pond Experiment, Dead Sea-Jordan. *Sustain. Resour. Manag. J*, 2, 1-10.

24. Goswami, R., & Das, R. (2019, July). Investigation of thermal and electrical performance in a salt gradient solar pond. In *Journal of Physics: Conference Series* (Vol. 1240, No. 1, p. 012111). IOP Publishing.
25. Goswami, R., & Das, R. (2020). Experimental analysis of a novel solar pond driven thermoelectric energy system. *Journal of Energy Resources Technology*, 142(12).
26. Jouhara, H., Żabnieńska-Góra, A., Khordehgah, N., Doraghi, Q., Ahmad, L., Norman, L., ... & Dai, S. (2021). Thermoelectric generator (TEG) technologies and applications. *International Journal of Thermofluids*, 9, 100063.
27. Rizvi, R. Z., Jamal, Y., Ghauri, M. B., Salman, R., & Khan, I. (2015). Solar pond technology for brine management and heat extraction: a critical review. *Journal of Faculty of Engineering & Technology*, 22(2), 69-79.
28. Monjezi, A. A., & Campbell, A. N. (2016). A comprehensive transient model for the prediction of the temperature distribution in a solar pond under mediterranean conditions. *Solar energy*, 135, 297-307.
29. Mahdi, J. T. (2012). Solar Pond is a New Technique of Supplying Thermal Energy. *Journal of kerbala university*, 10(3), 339-347.
30. Alenezi, I. (2012). Salinity gradient solar ponds: Theoretical modelling and integration with desalination. University of Surrey (United Kingdom).
31. Kanan, S., Dewsbury, J., & Lane-Serff, G. (2014, January). A simple heat and mass transfer model for salt gradient solar ponds. In *International Conference on Energy and Environmental Sciences* (pp. 27-33). World Academy of Science, Engineering and Technology
32. A. Akbarzadeh, J. Andrews, I.A. Burston, I. Oanca, U-Y. Wong, A. Ngoh, S. Wong, *Solar Ponds at RMIT: Renewable energy plus salinity mitigation* (2015)
33. Goswami, R., & Das, R. (2019, July). Investigation of thermal and electrical performance in a salt gradient solar pond. In *Journal of Physics: Conference Series* (Vol. 1240, No. 1, p. 012111). IOP Publishing.
34. Abbood, M. H., Alhwayzee, M., & Sultan, M. A. H. (2021). Experimental Investigation for the Solar Pond Performance with and Without Reflector Mirrors and Tracking System in Kerbela City of Iraq. *Design Engineering*, 7247-7254.
35. Mahdi, J. T., & Jebbar, Y. A. (2019, August). A theoretical investigation of solar radiation and heat transfer in a solar pond in Kerbala city. In *AIP Conference Proceedings* (Vol. 2144, No. 1, p. 030019). AIP Publishing LLC.
36. Jassim, M. M., Abbood, M. H., & Rashid, F. L. (2022). Design and Construction Solar Oven Sterilizer. *Journal homepage: <http://iieta.org/journals/ijht>*, 40(2), 641-645.
37. Duffie, J. A., & Beckman, W. A. (2013). *Solar engineering of thermal processes*. John Wiley & Sons.

38. O.A. Al-Musawi, A.A. Khadom, B. Fakhru" l-Razi, D.R. Ahmadun, R. Biak, Water distillation in a combined solar still and solar pond system: Iraq as a case study, *EuroMediterranean J. Environ. Integ.* 3, 20 (2018)
39. T. M. Tritt and M. A. Subramanian, "Thermoelectric Materials, Phenomena, and Applications : A Bird ' s Eye View," vol. 31, no. March 2006, 2018.
40. Tundee, S., Srihajong, N., & Charmongkolpradit, S. (2014). Electric power generation from solar pond using combination of thermosyphon and thermoelectric modules. *Energy Procedia*, 48, 453-463.
41. <https://www.weather-atlas.com/en/iraq/Kerbala-climate>.
42. Goedecke, G., Toussaint, V., & Cooper, C. (2012). On energy transfers in reflection of light by a moving mirror. *American Journal of Physics*, 80(8), 684-687.
43. Al Alawin, A.(2014). Performance of Solar pond Greenhouse Heating System in Jordan. *Iosr journal of mechanical and civil engineering* volume 11, issue 5 ver. Ii, pp 30-35
44. Saifullah, A. Z. A., Iqbal, A. S., Saha, A., Mesda, Y., Isik, B., Okoro, A. U., & Ndubueze, V. O. (2012). Solar pond and its application to desalination. *Asian Transactions on Science & Technology*, 2(03), 01-25.
45. Zohuri, B. (2017). Heat exchanger types and classifications. In *Compact Heat Exchangers* (pp. 19-56). Springer, Cham.
46. Ito, M., & Azam, S. (2019). Feasibility of Saline Gradient Solar Ponds as Thermal Energy Sources in Saskatchewan, Canada. *Journal of environmental informatics letters*, 1(2), 72-80.
47. AL-Musawi, O. A., Khadom, A. A., Manhood, H. B., & Mahdi, M. S. (2020). Solar pond as a low grade energy source for water desalination and power generation: a short review. *Renewable Energy and Environmental Sustainability*, 5, 4
48. Husan, J. M., Khalaf, H. A., & Hashem, A. L. (2007). Study the Performance of the Solar Ponds for Iraq Marshes. *Univesity of Thi-Qar Journal*, 3(3).
49. Bozkurt, I., & Karakilcik, M. (2012). The daily performance of a solar pond integrated with solar collectors. *Solar Energy*, 86(5), 1611-1620.
- 50.c Alcaraz, A., Montalà, M., Valderrama, C., Cortina, J. L., Akbarzadeh, A., & Farran, A. (2018). Thermal performance of 500 m² salinity gradient solar pond in Granada, Spain under strong weather conditions. *Solar Energy*, 171, 223-228
51. Aramesh, M., Kasaeian, A., Pourfayaz, F., & Wen, D. (2017). Energy analysis and shadow modeling of a rectangular type salt gradient solar pond. *Solar Energy*, 146, 161-171.
52. Chaichan, M. M. T., & Abaas, K. I. (2012). Productivity amelioration of solar water distillator linked with salt gradient pond. *Tikrit Journal of Engineering Sciences*, 19(4), 24-34.

53. Simic, M., & George, J. (2017). Design of a system to monitor and control solar pond: a review. *Energy Procedia*, 110, 322-327.
54. Mohamed, A. F., Hegazi, A. A., Sultan, G. I., & El-Said, E. M. (2019). Enhancement of a solar still performance by inclusion the basalt black gravels as a porous sensible absorber: Experimental study and thermo-economic analysis. *Solar Energy Materials and Solar Cells*, 200, 109958
55. Leblanc, J., Akbarzadeh, A., Andrews, J., Lu, H., & Golding, P. (2011). Heat extraction methods from salinity-gradient solar ponds and introduction of a novel system of heat extraction for improved efficiency. *Solar Energy*, 85(12), 3103-3142.
56. El-Sebaei, A. A., Ramadan, M. R. I., Aboul-Enein, S., & Khallaf, A. M. (2011). History of the solar ponds: a review study. *Renewable and Sustainable Energy Reviews*, 15(6), 3319-3325.
57. da Jornada, D. H., ten Caten, C., & Pizzolato, M. (2010). Guidance documents on measurement uncertainty: An overview and critical analysis. *NCSLI Measure*, 5(1), 68-76.

Appendix

Solar Irradiation Calculations in Karbala city

In the recent years, the data of solar irradiation are usually measured and recorded for almost every region in almost every state on the world. The solar irradiation estimates and predictions are often required to obtain a good approximation of incident radiation. The solar radiation path in the atmosphere is seasonally various depending on the position of a solar pond so, the sun's altitude, daily sunshine period and azimuth angle will be also various. This may be due to the earth's rotation or/and the angle of deviation. This might have a direct impact (positively or adversely) on the amount of incident radiation on the pond surface and, consequently, on the solar pond's performance.

The dust and fog in the atmosphere reflect a slight part of the solar radiation which enters the atmosphere and the residual part falls on the earth's surface.

The quantity of the solar radiation arrived into the solar pond (H_x) can be found at any depth (x) of the pond as follows [3]: -

$$H_x = H_o \{ 0.36 - 0.08 \ln(x / (\cos \theta_1)) \}$$

Where: (H_o) is the quantity of global incident solar radiation on the solar pond surface and θ_1 is the light refraction angle inside the solar pond. H_o can be found by the next equation [6]: -

$$H_o = [0.29 \times \cos(\varphi) + 0.52 \times (\underline{n} / \underline{N})] H_{ex}$$

Where: φ is the latitude angle and its value is 32.55° for Kerbala city, $(\underline{n} / \underline{N})$ is the percentage of the sunshine period and H_{ex} is the incident daily solar radiation on the solar pond.

The light refraction angle (θ_1) can be found by the following equation [25]:

$$\cos \theta_1 = 1.333 \cos \theta_2$$

Where: θ_2 is the direct radiation incidence angle on the surface of pond.

H_{ex} can be determined by the following equation [3]: -

$$H_{ex} = 24/\pi \times I_{on} \times [\cos(\varphi) \cos(\delta) \cos(\omega_s) + 2\pi \omega_s / 360 \sin(\varphi) \sin(\delta)]$$

Where: I_{on} is the daily intensity of constant irradiation and depends on the days number of the year. δ is the angle of solar declination and ω_s is the angle of sunset hour.

The incidence angle (θ_2) can be calculated as follow as [6]:

$$\cos \theta_2 = [\cos(\varphi) \cos(\delta) \cos(\omega) + \cos(\varphi) \cos(\delta)]$$

Where: ω is the hour angle which can be found from the noon depending on the local time (h). ω in the morning be negative and in the evening be positive.

The angle of solar declination (δ) can be found by the next equation [30]:

$$\delta = 23.45 \sin \left[\frac{360}{365} (283 + n) \right]$$

Where: n is the number of days of the year.

The angle of hour (ω) can be determined by the next equation [25]:

$$\omega = 360 \cdot (h - 12) / 24$$

The daily intensity of the constant irradiation (I_{on}) can be calculated by the following equation [25]:

$$I_{on} = 1367 \times [1 + 0.033 \times \cos \left(\frac{360 \times n}{365} \right)]$$

The angle of sunset hour (ω_s) can be calculated by the next equation [6]:

$$\omega_s = \cos^{-1} \left[(-\tan \phi \times \tan \delta) \right]$$

The percentage of absorbed radiation, H_x , decreases as we go deeper into the layers of the solar pond to a certain depth, x. The value of H_o is different from H_x because the value of the refractive index in air is different from the value in water.

Table (3.1) contains the monthly input quantities for Kerbela city for April month. These quantities are the average daily ambient temperature (T_a), wind velocity (v), relative humidity (γ), and the percentage of sunshine interval ($\frac{n}{N}$) [35].

Table (3.1) Weather Data for the City of Kerbala in Year of 2022 [43].

Month	T_a (°C)	γ (%)	v (m/s)	$\frac{n}{N}$
April	23.8	28	4	0.69

The water flow meter that measures the flow rate of the water volume is calibrated using a graduated bottle. Keep track of how long it takes the water to travel to various locations in the bottle. The average results were plotted against the flowmeter data in a curve. after this method was completed three times with an error rate 0.058, as shown in Fig(4.17).

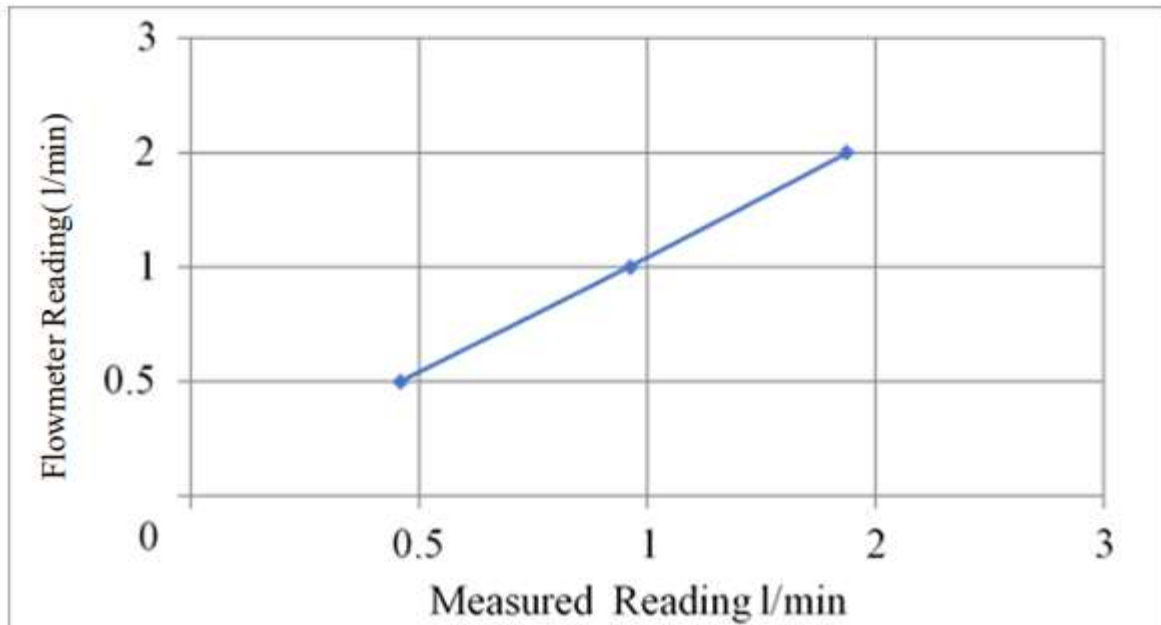
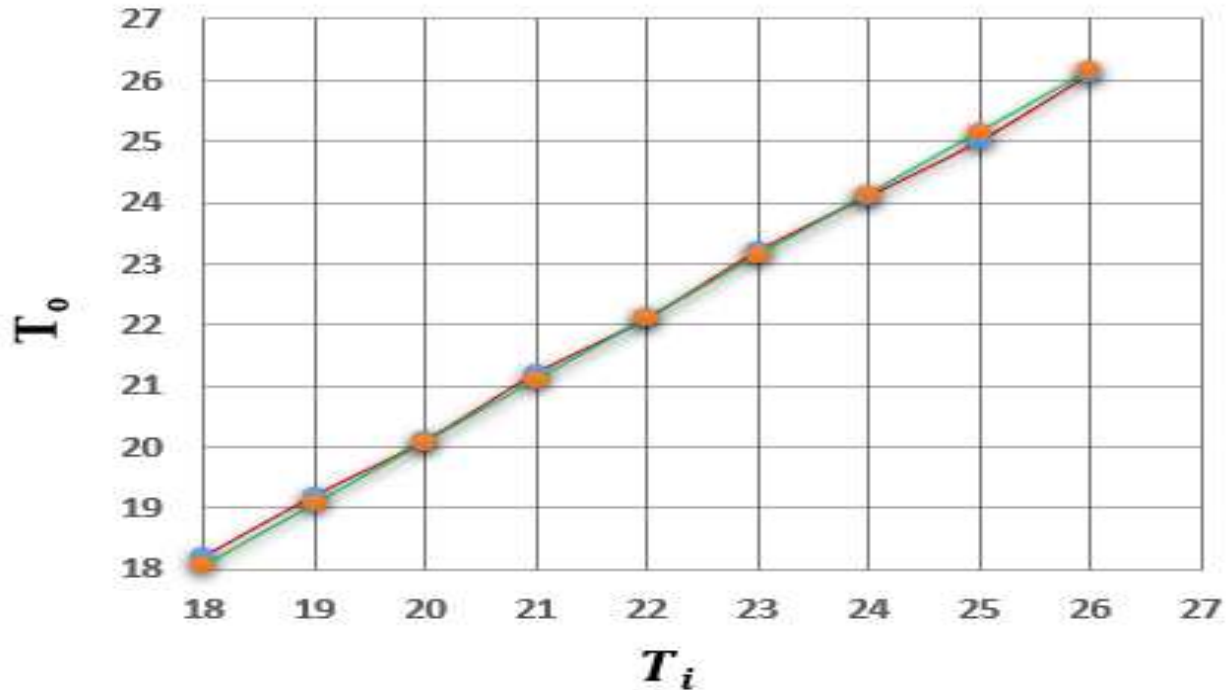


Figure (4.17): The Calibration of the Water Flow Meter

Table . The Calibration of thermocouples of the two devices

No.	Multifunction Calibration (T_i) °C	Temperature Recorder (T_o) °C
1.	18	18.2
2.	19	19.2
3.	20	20.1
4.	21	21.2
5.	22	22.1
6.	23	23.2
7.	24	24.1
8.	25	25
9.	26	26.1

Calibration curve of an instrument



Experimental Calculations

Equations for solar radiation, useful thermal energy, and the thermal effectiveness of the solar pond are included in this section. The experimental outcomes for the aforementioned parameters would be determined using these equations. Physical characteristics (density, heat capacity, and thermal conductivity) of the water and salt used in this process would be on the supposition that they are constant. The solar pond's surface would also be regarded as a horizontal surface.

Useful Energy

To get an equation determining the useful thermal energy of the solar pond (Q_u), an energy balance of the control volume of the solar pond mixture (solution) is made. According to the following equation, Duffie [34].

$$(M_s * C_{ps} * T)_t - (M_s * C_{ps} * T)_{t+\Delta t} = \Delta t Q_u \quad \dots (4.1)$$

Where M_s and C_{ps} are the mass and the heat capacity of the solution of the solar pond, respectively. t and Δt are the time and time duration limits for calculating the control volume's energy balance.

By dividing the equation (4.1) on t, the following equation is obtained:

$$((M_s * C_{ps} * T)_t - (M_s * C_{ps} * T)_{t+\Delta t}) / \Delta t - Q_u = 0 \quad \dots (4.2)$$

When the time duration (Δt) approaches zero, the limit can be taken for the equation (t) as follow as:

$$\lim_{\Delta t \rightarrow 0} ((M_s * C_{ps} * T)_t - (M_s * C_{ps} * T)_{t+\Delta t}) / \Delta t - Q_u = 0 \quad \dots (4.3)$$

$$M_s * C_{ps} * dT/dt - Q_u = 0 \quad \dots (4.4)$$

The useful heat energy of the solar pond (Q_u) can be calculated as:

$$Q_u = M_s C_{ps} \Delta T \quad \dots (4.5)$$

where: M_s is the solution mass of the solar pond, C_{ps} is the heat capacity of the pond solution and ΔT is the difference in the temperature between the lower convective zone and ambient air.

The solution mass of the solar pond (M_s) can be calculated by the following equation: -

$$M_s = VLCZ * \rho_s \quad \dots (4.6)$$

Where: $VLCZ$ and ρ_s are the volume and density of the solution of the lower layer of the solar pond respectively. $VLCZ$ equals 0.650 m³ and ρ_s equals 1329 kg/m³ is determined by the next equation: -

$$\rho_s = \rho_w * (1 - C) + \rho_{salt} * C \quad \dots (4.7)$$

The heat capacity of the pond solution (C_{ps}) equal 2.572 kJ/kg.C° can be calculated by the following equation: -

$$C_{ps} = [(\rho_w * C_{pw} * (1 - C) + \rho_{salt} * C_{Psalt} * C)] / \rho_s \quad \dots (4.8)$$

Where: C is the concentration of the salt in the solar pond water. ρ_w and C_{pw} are the density and the heat capacity of the water and equal 997 kg/m³ and 4.18, kJ/kg.C° respectively. ρ_{salt} and C_{Psalt} are the density and the heat capacity of the salt and equal (2660 kg/m³) and (1255 J/kg. k) for the salt of MgSo₄, respectively.

Thermal Efficiency of Solar Pond

The thermal efficiency of the solar pond can be found by dividing the useful thermal energy (Q_u) by the amount of incident solar radiation on the surface of the pond (I), Saifullah [47]:

$$[\eta = Q]_{u/I} \quad \dots (4.9)$$

The incident solar radiation on the pond surface (I) can be determined by the following equation.

$$I = I_0 * A \quad \dots (4.10)$$

Where: A is the surface area of the solar pond equal 6.25 m².

4.2 Experimental Calculations for Thermoelectric(TEG):

- Electric power and Efficiency of TEG: -

The electrical power generated is given as [5].

$$P_{TEG} = IV \quad \dots (4.1)$$

$$V_{TEG} = \alpha \Delta T \quad \dots (4.2)$$

where $(\alpha_p - \alpha_n) = \alpha$ and $(T_h - T_c) = \Delta T$, T_h and T_c represent the hot and cold junction temperature respectively. α_p and α_n are the Seebeck coefficient of P and N type TEG leg respectively.

For TEG containing N number of couples, the following equation can be used for open circuit and short circuit relations.

$$V_{TEG} = 2N\alpha\Delta T \quad \dots (4.3)$$

$$I_{TEG} = (\alpha/\rho) (A_{TEG}/L) \Delta T \quad \dots (4.4)$$

ρ Ω cm =Electrical resistivity of thermo element material,

A=TEG Area of thermo element (mm²).

L= Length of thermo element(mm).

The thermoelectric power is related to dimensionless figure of merit given by

$$ZT = \alpha^2 \sigma T / k \quad \dots (4.5)$$

Where α is the Seebeck coefficient of TEG, σ and k are the electrical and thermal conductivity respectively and T is the absolute temperature.

For calculating the efficiency of TEG, the following equation is used.

$$\eta_{TEG} = \frac{T_h - T_c}{T_h} \left[\frac{(1 + ZT)^{0.5} - 1}{(1 + ZT)^{0.5} + \left(\frac{T_c}{T_h}\right)} \right] \quad \dots (4.6)$$

REPUBLIC OF IRAQ
MINISTRY OF SCIENCE & TECHNOLOGY
RENEWABLE ENERGY DIRECTORATE



جمهورية العراق
وزارة العلوم والتكنولوجيا
دائرة الطاقات المتجددة
معاينة فواتير المسحقة الهائلة لحجر الإبراهيم
العدد: ط م / ٢٦٥
التاريخ: ٢٠٢٢/٣/١٢

الى / جامعة كربلاء/ كلية الهندسة
م/أبداء مساعدة

تحية طيبة :

اشارة الى كتابكم العدد د ع /٦/٦٣٦ في ٢٠٢٢/٢/١٥ الخاص بابداء المساعدة لطالب الماجستير (محمد محسن جاسم) في قسم الهندسة الميكانيكية نرفق لكم طيا نتائج الفحص والمعايرة الخاصه ببحثه .
١- تم اجراء فحص ومعايرة لجهاز قياس شدة الاشعاع الشمسي من خلال المقارنة بين قراءات شدة الاشعاع الشمسي لجهاز قياس شدة الاشعاع الشمسي المطلوب فحصه (+10%): es132Data (T logging solar power meter accuracy) والذي يحمل الرقم التسلسلي (160001732) مع قراءات جهاز قياس شدة الاشعاع الشمسي معتمد لدينا علما ان القراءات كانت بوضع الاجهزة الافقي ووجد ان هناك فروقات في القراءات بعد انجاز المعايرة تعزى الى نسبة الخطا المصنعية للجهاز البالغة (+10%) وكما موضح في الجدول رقم (1) المرفق طيا .

٢- تم فحص جهاز (12channels SD Data Logger) الذي يحمل الرقم (H.297840) من خلال مقارنة القراءات مع جهاز معتمد لدينا ومن خلال استخدام فرن حراري حيث وجد ان القراءات كانت متقاربة الى حد ما والفرق البسيط يعزى الى الاختلاف في مدى نسبة الخطا من جهاز الى اخر وكما موضح في الجدول رقم (2) المرفق طيا . علما ان انتاج هذا النوع من الاجهزة لا يمكن معايرته حيث يخضع لمعايير دولية قياسية .



مع التقدير

د.فلاح ابراهيم العطار
معاون المدير العام
٢٠٢٢/٣/٩

لنفسه مله/الى
اسم التخطيط والمتابعة/شعبة المعلومات مع الاوليات

Table (1) : Comparison between Standard solar Power meter and TES 132 Data Logging Solar power meter Accuracy: (\pm (10 %) under testing

No.	Time	Solar Power meter W/m ² Standard	TES 132 Solar Power meter W/m ² under testing
1	10:06	648	649
2	10:48	735	733
3	11:30	765	776
4	11:54	795	801
5	12:25	790	784

Table (2): Comparison between two Data Logger ; the Standard Data logger and Data Logger under the testing



Time	Data Logger under testing (° C)	Data Logger Standard (° C)
10:30:59	307.3	308.3
10:35:59	299.3	300.1
10:40:59	283	283.6
10:45:59	266	266.5
10:50:59	249.4	249.7
10:55:59	233.4	234
11:00:59	218.9	219.4
11:05:59	205.4	205.8
11:10:59	192.8	193.4
11:15:59	181.2	181.9
11:20:59	170.4	171.2
11:25:59	160.3	161.3
11:30:59	126.1	123.3
11:35:59	102.6	102.6
11:40:59	86.4	86.6
11:45:59	74.9	75.3
11:50:59	66.2	66.4
11:55:59	59.1	59.4
12:00:59	53.6	53.9
12:05:59	49	49.2
12:10:59	45.3	45.6
12:15:59	42.2	42.4
12:20:59	39.4	39.8
12:25:59	26.4	26.5
12:30:59	23.9	25.3
12:35:59	20.1	21.2

Republic of Iraq
Ministry of Higher Education
And Scientific Research
University of Karbala
College of Engineering
Postgraduate

جمهورية العراق
وزارة التعليم العالي والبحث العلمي
جامعة كربلاء
كلية الهندسة
الدراسات العليا

No :
Date :

العدد : ١٥٥٩ / ٦ / ٤
التاريخ : 2022 / 4 / 18

الى /مديرية الانواء الجوية في كربلاء المقدسة
م / إبداء مساعدة

تحية و د احترام ...

انطلاقاً من مبدأ التعاون العلمي بين مؤسسات التعليم العالي والقطاعات الأخرى خدمة للمسيرة العلمية في بلدنا العزيز ، راجين التفضل بإبداء المساعدة لطالب الدراسات العليا / الماجستير (باسم ساجت عطيه) في قسم الهندسة الميكانيكية بكليتنا لغرض الحصول على بيانات الانواء الجوية لإكمال متطلبات رسالة الماجستير الخاصة به.

شاكرين تعاونكم معنا .. مع التقدير .

أ.م.د. ميثاق نعمة رحيمة
معاون العميد للشؤون العلمية والدراسات العليا
2022 / 4 / 18

نسخة منه إلى ///

- قسم الهندسة الميكانيكية / للتفضل بالعلم ... مع التقدير .
- شعبة الدراسات العليا / مع الأوليات .
- الصادرة .

جمهورية العراق . كربلاء . حي الموظفين
Email : engineering@eng.uokerbala.edu.iq
pgr.eng@uokerbala.edu.iq



العدد: ٣٩٦١
التاريخ: ٦ / تشرين / ١٤٤٣ هـ
٨ / ٥ / ٢٠٢٢ م

إلى / الباحث باسم ساجت عطية الموضوع / تقرير

نرفق لكم نتائج الفحوصات (نسبة الاملاح الكلية) للعينات التي تم نمذجتها وجلبها من قبلكم ليوم الثلاثاء الموافق (٢٦/٤/٢٠٢٢).

مع التقدير ...

المرفات :-
- تقرير

المهندس
ع. ضياء مجيد عياض الصالح
رئيس القسم
٥٠٨ / ٢٤٤
ع. ضياء مجيد عياض الصالح
RABULHAQI - LLC - 2014

نسخة منه الى //

- مختبر مياه العتبة العباسية المقدسة / مطالعتكم المرقمة ١٧٨٠ في ٥/٨/٢٠٢٢ / للتفضل بالعلم والمتابعة. مع التقدير...
- الصادر العام .



العدد : ٣٤٥٦
التاريخ : ٥ / ٥ / ١٤٤٣ هـ
٢٠٢٢ / ٥ / ٧ م

الموقع / عينة ماء خارجية

مكان اخذ النموذج/ عينة ماء

جامع النموذج / تم جنب العينة من قبلهم

تاريخ اخذ النموذج :- ٢٦ / ٤ / ٢٠٢٢

ت	العينات	الوحدة	كمية الملح
١	عينة رقم 1	غم/لتر	382.097
٢	عينة رقم 2	غم/لتر	330.358
٣	عينة رقم 3	غم/لتر	74.538
٤	عينة رقم 4	غم/لتر	48.866
٥	عينة رقم 5	غم/لتر	39.685
٦	عينة رقم 6	غم/لتر	0.132



استشاري العتبة العباسية المقدسة
للشؤون البيئية

سجاد ضياء عباس

(مساعد فاحص)

تقرير الانواء الجوية لشهر نيسان لسنة 2022

ت	التاريخ	كمية الامطار	معدل درجة الحرارة	درجة الحرارة العظمى	درجة الحرارة الصغرى	الرطوبة النسبية العظمى	الرطوبة النسبية الصغرى	مجموع الاشعاع الشمسي	معدل سرعة الرياح	اعلى سرعة رياح
	Date	Rain mm	AT Avg C°	AT Max C°	AT Min C°	RH Max%	RH Min%	SLR Total Mj/m2	WS Avg m/s	WS Max m/s
1	3/1/2022	0.10	16.08	21.72	10.43	75.74	20.44	18.27	3.29	10.90
2	3/2/2022	0.00	11.13	16.62	5.64	63.19	19.39	19.08	3.58	10.09
3	3/3/2022	0.00	10.46	18.19	2.73	64.93	26.35	18.60	1.01	5.43
4	3/4/2022	0.00	12.61	21.09	4.12	81.90	17.89	18.95	0.48	4.51
5	3/5/2022	0.00	13.03	21.29	4.77	83.90	23.76	13.41	0.68	6.04
6	3/6/2022	0.00	14.99	23.89	6.08	81.80	17.54	16.91	0.68	4.14
7	3/7/2022	0.00	16.85	22.62	11.08	72.84	23.11	18.62	1.26	7.47
8	3/8/2022	0.00	14.87	21.84	7.90	78.11	30.41	18.69	1.09	9.49
9	3/9/2022	0.80	10.77	15.16	6.38	85.60	46.18	11.01	2.00	7.47
10	3/10/2022	0.00	13.98	22.89	5.06	90.30	18.80	20.44	1.54	6.53
11	3/11/2022	0.00	14.30	23.02	5.57	73.98	14.97	20.95	1.40	6.68
12	3/12/2022	0.00	14.40	22.96	5.84	77.49	18.02	20.15	0.96	9.25
13	3/13/2022	0.00	14.39	23.38	5.40	73.07	18.87	18.17	0.64	4.06
14	3/14/2022	0.00	17.80	26.33	9.26	74.20	14.55	17.36	1.16	7.02
15	3/15/2022	6.50	17.52	25.17	9.86	95.10	31.11	14.58	2.05	14.27
16	3/16/2022	0.00	14.63	20.85	8.41	94.60	32.51	20.89	1.23	4.86
17	3/17/2022	0.00	16.93	25.64	8.21	94.20	21.04	21.11	1.23	6.82

Improving the Performance of a Solar Pond Using TEG: An Experimental Investigation

Mohammed Hasan Abood[✉], Hayder Noori Mohammed[✉], Basim Sacht Atiyah[✉]

Mechanical Engineering Department, College of Engineering, University of Kerbala, Kerbala 56001, Iraq

Corresponding Author Email: basim.s@uokerbala.edu.iq



<https://doi.org/10.18280/ijht.410223>

ABSTRACT

Received: 24 August 2022

Accepted: 15 February 2023

Keywords:

salinity gradient, solar pond, magnesium sulfate, reflectors

A study has created a solar pond model. The pond's performance in terms of heat storage and electric power generation using TEG is analyzed using this model. The impact of various parameters, such as covering the pond's surface with plastic and using reflectors to focus on the intensity of solar radiation, will be investigated. A pyramidal pond with a base size of 0.64 square meters was used to validate the model. And it has a 6.25 square meter surface area. There's also a 1.35-meter depth. The walls are inclined at a 60-degree angle. TEG was also used to determine the pond's electrical capacity. The addition of a plastic cover and reflectors enhanced the efficiency of the pond's operation from 12.1% to 27.5%, according to the findings. At a lower layer temperature of 60 degrees Celsius, the electrical capacity reached 104 watts with a TEG operating efficiency of 8.9%.

1. INTRODUCTION

Energy plays a critical role in all aspects of a country's economic development. A nation's living levels can be correlated with its per person energy use. There is an energy crisis because of the rapid increase in the human population and the standard of living. Oil supplies will not meet rising population demand. To fulfill future energy demands, an alternative energy source had to be identified. Several green technologies, as well as methods for extracting energy, have been identified. Solar energy is one of the most extensively distributed and clean renewable energy supplies, and it is one of the most effective solutions to pollution and fossil fuel scarcity. An abundant and sustainable source of energy is solar energy [1]. There has been a surge in attention to environmental protection, resulting in using energy transference and thermal energy storage technologies (TES) that use renewable energy sources like solar energy. Thermal energy storage systems are employed in applications where the needed energy demand and supply do not coincide. There are two types of energy storage systems: sensible and latent. The fluid temperature is constant, when heat is kept or removed in the phase change part of the storing and charging duration in a sensible TES, including a solar pond, where the medium of storage does not undergo a phase transition and is added or subtracted, such as those systems that use a liquid combination of water and ice as the storage medium, where the fluid temperature is constant and heat is removed or stored in latent form in the phase change part of the charging and storing period. Solar ponds, often referred to as renewable storage systems for thermal energy (TES), are used for both storing and collecting solar energy and are gaining popularity in various thermal uses such as water desalination, space heating, and the use of biological cycles to generate power [2, 3].

The transfer process that takes place when a mixture is subjected to a heat gradient is known as thermos diffusion in physical terms [4]. It is referred to as "the Soret Effect," and a great deal of theoretical and experimental research has been

done to interpret it. This article briefly discusses a one-dimensional theoretical and numerical approach to the concentration distribution of NaCl in a solar pond with a salinity gradient that is based on the first law of thermodynamics. Its fluid-thermodynamic factors are intended to be framed by the theoretical developments. Al Alawin [5] constructed a solar pond in Jordan with a 56 m² surface area and a 1.8 m depth. Three primary strata were present, UCZ, NCZ, and LCZ, according to the salinity scale and temperature that were measured. In the LCZ layer, the lowest specific gravitational value was 1.16. According to Al Alawin [5], the wind and the dust that accumulated on the pond's surface had a considerable impact on the pond's performance. Ongoing cleaning improved the efficiency of the pond, while the installation of a network of ropes lessened the effect of the wind. The solar pond's reflection mirrors were used to concentrate solar radiation.

Khalilian [6] has conducted both theoretical and practical research on heat transfer in a brackish-gradient solar pond. The model investigates how transit energy interacts in each area of the pond, considering several processes that affect the solar pond's effectiveness. Both theoretical and actual measurements of the storage area's temperature were taken. The results showed that evaporation—rather than convection or radiation—handles most heat loss from the pond surface. According to the application, the thickness of the lower load zone can be changed; however, the top load area should have the thinnest thickness possible. Wall shadow was shown to have a considerable impact on a pond's stored temperature, whereas a big pond had less of an impact. Al-whoosh et al. [7] constructed a 5 m³ salty graded solar pond near the Dead Sea, which shows that after 100 hours of operation, the lower layer's maximum temperature is 85°C. Heat extracted from the solar pond can generate electric power or for desalination plants that operate under 100 degrees Celsius. Bezir et al. [8] constructed a solar pond with a surface area of 3.5x3.5 m² and a depth of 2m. The results revealed that reflectors during the day increased the heating area, and that these reflectors are

foldable and serve as a cover at night to decrease heat loss, and that they have a great performance for the solar pond, as the heat increases by 25%. Theoretically, the larger the solar pond, the more efficient it is because heat loss from the walls and bottom is reduced per unit area. In order to prevent power supply interruptions caused by the temporary unavailability of a suitable heat source, Ding [9] discusses how most thermoelectric generator applications generate electricity from a non-stored heat source and the solar pond (SP) has been proposed as a heat source for a thermal storage system that can continuously supply enough heat for electricity generation. A low-grade heat source between 50°C and 100°C can be obtained from sun ponds, which also serve as thermal storage. The thermoelectric generator and the solar pond are also both extremely scalable in terms of size. In order to maximize the potential of the solar thermoelectric power generating system for the pond, the performance of the thermoelectric cells was integrated with the temporary heat transfer of the solar pond. An experimental solar pond model to heat water was built by Abbood et al. [10]. The pond measured 1 m in depth and 7.29 m² in surface area, and walls inclined at a 45° angle. In this study, potassium chloride and sodium chloride were employed as salts. Two reflecting mirrors were utilized to concentrate radiation of solar on the pond's surface. The highest temperature in the pond was 44 degrees Celsius when sodium chloride was used, while potassium chloride yielded a maximum temperature of 40 degrees Celsius. Thermal efficiency and usable energy were discovered to be 28.2 MJ/h and 11.6 percent, respectively, in the experiment. This study [11] presented a design and model for a low-cost solar sterilizer that uses hot, dry air to clean medical equipment. Sterilization of dry objects using hot air takes 60 minutes at 160°C. A box made of stainless steel measuring 60 cm × 30 cm × 12 cm is part of the design, and is used to carry surgical supplies. The system has been tested in many ways. Surgical instruments and reflective panels are present and absent. In 121 minutes, the system produced hot air at 160°C. When surgical instruments weighing 1.2 kg added, this time it increased by 23.9%. Reflective panels reduce the time required to generate the required heat by 9%.

The best method for capturing and storing solar energy is a solar pond with changeable salt density [12]. sunlight-based ponds that are permeable and impermeable are tested under various environmental situations. A 30-day period of readings was used to examine the salt density concentration, thermal energy storage measurement, and temperature cycle. Two identical 0.02 m³ and 0.32 m tall solar basins were constructed for testing. Broken glass, weld spray, and fragments of black granite were utilized in the lowest convective zone (LCZ) as a permeable medium. The impermeable solar pond and the detachable solar pond had the greatest temperatures of 42.3 and 40.6, respectively. Temperature increased by 4.18% in the permeable median solar pond. The difference in the thermal energy reserves is 4.54 kilojoules. Compared to the impermeable solar pond, the medium permeable solar pond stores higher heat energy, according to optimization carried out using the acquired parameters [13]. Energy use increases together with the amount of underdeveloped or unusable land in developing nations. For these nations, solar energy presents a positive prospect. Solar Pond is a long-term heat storage and solar collector that can be used in open, sunny spaces. Numerous applications that call for low-grade thermal energy can be heated using solar pond technology, which can also be used to generate electricity. It is required to use systems fed by

low enthalpy sources, such as thermoelectric generators (TEG) and the organic Rankine cycle, in order to generate electrical energy from solar ponds (ORC). In this study, the organic Rankine cycle and a solar pond model for power production are examined.

Goswami et al. [14], presented research in India on an experimental analysis of a new solar pond-driven thermal power system. The aim of the experimental study was to charge a 12V battery using a 4m² and 1m deep solar pond insulated with ethylene black and covered with propylene. The salt used is sodium chloride in the lower area at a concentration of 24.01%. An octagonal stainless steel reflector is installed to direct solar radiation. The pond's bottom layer had a temperature of 55C, when the radiation intensity was 976 w/m², and here comes the role TEG, which is a material made of bismuth semiconductor, in converting thermal energy into electrical energy. Volts 1.5 were obtained at a temperature of 23°C.

The aim of this study was to examine how effectively a solar pond with a salinity gradient functioned as a source of hot water intending to use it to generate energy using TEG. In order to compare the addition of magnesium sulfate salt regarding its qualities and efficacy in thermal storage, the pond is built to use the solar radiation that falls on its surface. This has been made easier by using reflective surfaces and a plastic cover system to track how the sun affects the pond's effectiveness. The performance of a thermoelectric generator in these circumstances is another goal of the research.

2. EXPERIMENTAL SETUP

2.1 Construction of a solar pond system

A solar pond in the shape of a pyramid with a base area of 0.64 square meters. And it has a 6.25 square meter surface area. There's also a 1.35-meter depth as shown in Figures 1 and 2. The walls are inclined at a 60-degree angle. Foam is used to insulate the walls in two layers, each 5 cm thick. Nylon covered in black is used as a lining. A plastic cap is placed on top of the container. On both sides, reflectors are mounted. Thermocouples are inserted at various depths inside it. Magnesium sulfate salt was used at a 28 percent concentration, with 400 grams of salt per liter.

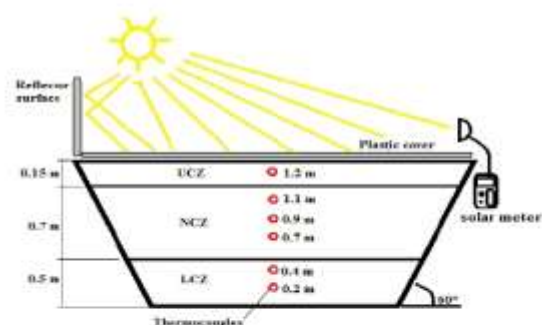


Figure 1. Schematic of the solar pond

The pond was exposed to natural solar radiation and also other weather conditions after construction. A thermocouple type 8 k were used: six of these were placed at 0.2, 0.4, 0.7, 0.9, 1.1, and 1.2 m from the lowest of the pond, with one at the

pond bottom, the last thermocouple was placed to measure the outside temperature. Throughout the pond testing period, solar radiation measurements were made every day from 8 a.m. to 5 p.m. During the testing period, the temperatures of the pond layers were recorded over a 24-hour period. Reflecting mirrors were used with a cover plastic as shown in Figure 3, to lower the required surface area by increasing the sun's radiation intensity on the pond's surface.



Figure 2. Solar pond with plastic cover and reflective mirrors



Figure 3. Instruments for measuring: 1-thermocouples, 2-temperature meter, 3-solar power meter

2.2 Measurements

The intensity of solar radiation, water salt concentration, and temperature were all measured using the following equipment.

- 1) K-type thermocouples.
- 2) Temperature meter the temperature readings range of this device is from -20 to +250°C with an error ratio of ±0.4% (±0.5°C).
- 3) Solar power meter with a manufacturing error rate of 0.4% to 0.50%, the greatest radiation range that may be detected by this instrument is 2000 W/m².

2.3 The procedure for the test

In February and March 2022, two months were dedicated to the present experiment. Each beta test lasts from 8 a.m. until 7 a.m. the next morning in the city of Karbala, Iraq. Table 1 contains the monthly input quantities for Kerbela city for April month. These quantities are the average daily ambient temperature (Ta), wind velocity (v), relative humidity (Y), and the percentage of sunshine interval (n/N) [15].

Table 1. Weather data for the city of Kerbala in year of 2022 [15]

Month	Ta (°C)	Y (%)	v (m/s)	n/N
April	23.8	28	4	0.69

The following steps can be used to characterize the experimental process of the current work:

- 1) Examining a group of salts using beakers to know the efficiency of each salt in collecting heat. The highest temperature is reached by any type of salt.
- 2) After determining the best salt (magnesium sulfate), use the same flasks to test three salt concentrations until reaching the state of saturation at a concentration of 28% with an amount of salt of 400 grams per liter.
- 3) After determining the best salt and the best concentration, the solar pond was worked by adding water and salt, waiting for it to settle, and recording the temperatures.
- 4) Installing reflective mirrors on the pond's sides, waiting for the pond to settle, and recording temperatures.
- 5) Add a transparent plastic cover and record the temperatures after the pond has settled.
- 6) After reaching the highest possible temperature in the previous steps, we now use TEG slices.
- 7) Installing TEG slides inside the pond and recording the voltage and the resulting amperage as shown in Figure 4.

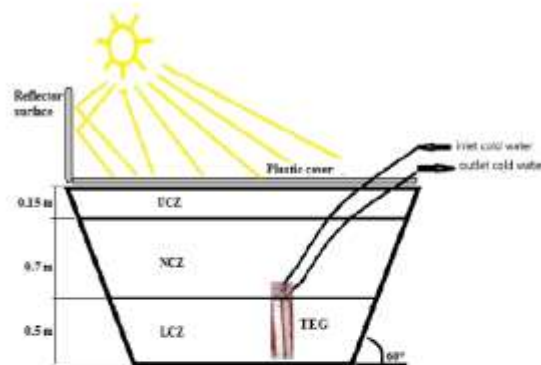


Figure 4. The location of the TEG fixation inside the pond

3. THERMAL EFFICIENCY AND USEFUL ENERGY CALCULATIONS

The amount of useable energy, computed as [16]:

$$Q_u = M_s * c_{p_s} * \Delta T \quad (1)$$

where,

$$M_s = V_{LCZ} * \rho_s \quad (2)$$

$$\rho_s = \rho_w * (1 - C) + \rho_{salt} * C \quad (3)$$

$$c_{p_s} = [(\rho_w * c_{p_w} * (1 - C) + \rho_{salt} * c_{p_{salt}} * C)] / \rho_s \quad (4)$$

The following equation may be used to determine the thermal effectiveness of a solar pond [17]:

$$\eta = Q_u / I \quad (5)$$

$$I = H_o * A \quad (6)$$

where,

C is the amount of salt in the water; V_{LCZ} is the LCZ layer's volume; ρ_w=997 kgm⁻³, c_{p_w}=4.18 kJkg⁻¹. K⁻¹, ΔT is the

difference in temperature between the lower convective zone and the surrounding air, While H_0 is the solar irradiance on the solar pond and I is the solar energy incidence on the pond.

The electrical energy produced by TEG is provided as [18]:

$$P_{TEG} = I_{TEG} * V_{TEG} \quad (7)$$

where,

P_{TEG} , I_{TEG} , V_{TEG} is power, current and voltage of TEG,

$$V_{TEG} = \alpha * \Delta T \quad (8)$$

$$I_{TEG} = \left(\frac{\alpha}{\rho}\right) * \left(\frac{A_{TEG}}{L}\right) * \Delta T_b \quad (9)$$

where,

α is the Seebeck coefficient of TEG, A_{TEG} is area of TEG.

The following equation is used to determine TEG's efficiency: [19-21].

$$\eta_{TEG} = \frac{T_h - T_c}{T_h} \left[\frac{(1 + ZT)^{0.5} - 1}{(1 + ZT)^{0.5} + \frac{T_c}{T_h}} \right] \quad (10)$$

where,

$$ZT = \alpha^2 * \sigma * T / K \quad (11)$$

where,

T is the absolute temperature, while k and σ are the thermal and electrical conductivities, respectively.

4. RESULTS AND DISCUSSION

Figure 5 demonstrates that the pond levels have become warmer overall, but particularly in the bottom layer. The effect of salting the water, which produces a brine solution that absorbs solar energy and converts it into thermal energy inside the pond, is what causes this.

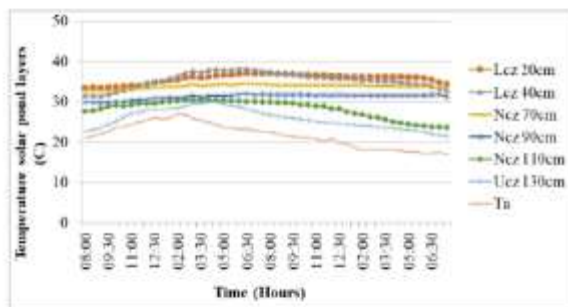


Figure 5. Three-layer salinity solar pond's temperatures

The temperature distribution on the pond levels and at different depths is depicted in Figures 7 and 8. Figure 6 shows the temperatures when using magnesium sulfate salt with the plastic cover and without mirrors. As shown in the diagram, the highest temperature in the lower layer, at a depth of 40 cm, reaches 45 degrees Celsius.

When magnesium sulfate, a cover, and mirrors are used, the temperature distribution is shown in Figure 7. The temperature rises in all layers, reaching 59 degrees Celsius in the storage

layer at the bottom. The increase in temperature is because of the use of mirrors, which enhance the quantity of radiation falling on the pond's surface, hence increasing the heat energy stored in the pond.

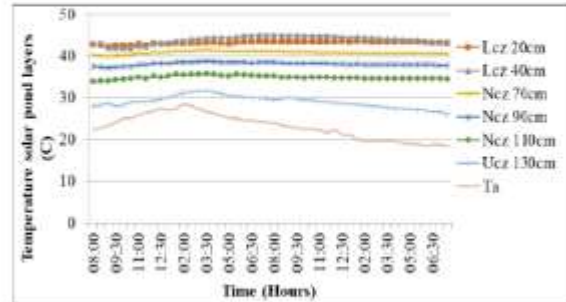


Figure 6. Temperature of the three layers of the covered salty solar pond

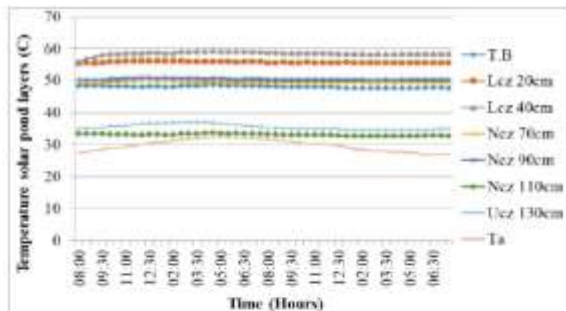


Figure 7. Temperature of the three layers of the covered salty solar pond with the reflectors

Figure 8 presents the useful energy (Q_u) and thermal efficiency for three experiments: the first using simple salt (magnesium sulfate), the second using salt (magnesium sulfate) plus a plastic cover on the pond's surface, and the third adding reflectors to the pond. The quantity of useful energy was shown to be a factor in the practical results. In the first experiment, the usefulness was 6.92 kw, while in the second experiment, it was 10.35 kw, with the plastic cover helping to reduce heat losses by limiting reflection beyond the pond. The reflectors contributed to increasing the solar radiation intensity, which increased the quantity of heat absorbed and so raised the heat selected in the third experiment. The usable heat transfer is 17.32 kilowatts. This gain was reflected in the pond's efficiency, which increased to 27.5 percent when salt (salt), a plastic cover, and reflectors were used.

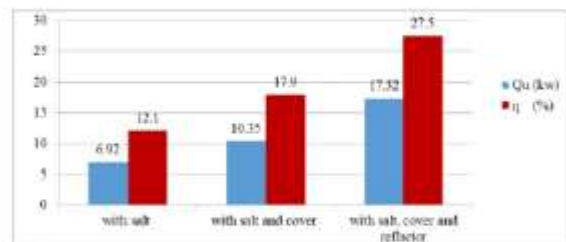


Figure 8. Thermal efficiency (η) and output useful energy (Q_u) of solar pond

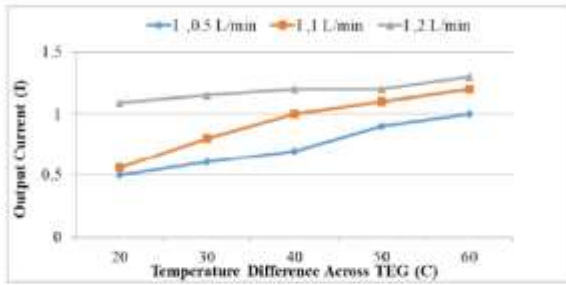


Figure 9. The output current, I_{out} [A] for temperature difference across TEG, ΔT [C]

Figure 9 displays the current produced by TEG because of temperature differences and for three water flow rates via the tubes in contact with the electrodes (TEG). It should be noted that the current value increases along with the flow rate. Because all the water in contact with the TEG at high speeds is of the same intensity, all the TEG chips function at the same productivity.

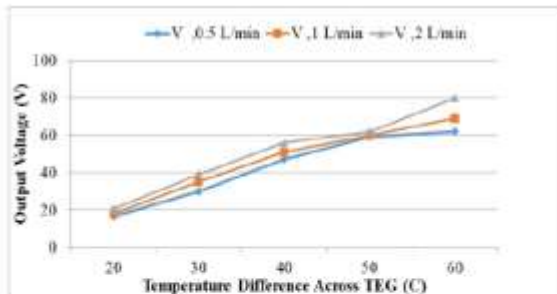


Figure 10. The output voltage, v_{out} [V] for temperature difference across TEG, ΔT [C]

Figure 10 shows behavior similar to that of the prior graph. The electrical potential differential (TEG) for three different water flow rates is depicted on the graph. According to the same principle, the increased flow rate happens as the electric potential difference widens.

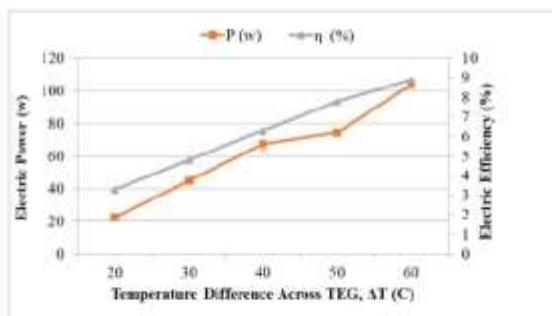


Figure 11. The Output Electric Power, P_{out} [w] and Electrical Efficiency [%] for temperature difference across TEG, ΔT [C]

Figure 11 depicts the electrical power generated by TEG and its work efficiency at five different temperatures (20, 30, 40, 50, and 60 degrees Celsius). It was showed through actual

results that raising the temperature stored in the lower layer leads to an increase in electrical power production to its greatest value of 104 watts, therefore boosting the efficiency of TEG's work to 8.9%.

5. CONCLUSIONS

(1) Experiments show that the temperature in the pond's lower layer is influenced by several elements, the most important of which are the intensity of solar radiation, the kind and concentration of salt used, and good pond insulation to limit heat loss.

(2) The use of the plastic cover has helped to improve the pond's efficiency work by limiting heat loss from the pond's surface.

(3) Reflectors improved the quantity of heat received and stored in the pond by concentrating the intensity of solar radiation on it.

(4) Using the plastic cover and reflectors, the pond's bottom layer attained a maximum temperature of 59 degrees Celsius.

(5) When salt (magnesium sulfate), a plastic cover, and reflectors were installed, the pond's operational efficiency reached 10.3 percent.

(6) At 60°C temperature and a flow rate of 2 liters per minute, the current, voltage, and capacitance produced by TEG from the solar pond were 1.3 A, 80 V and 104 W respectively, and the efficiency of TEG was 8.9%.

REFERENCES

- [1] Goutham, K., Krishna, C.S. (2013). Solar pond technology. *International Journal of Engineering Research and General Science*, 1(2): 12-22.
- [2] Dehghan, A.A., Movahedi, A., Mazidi, M. (2013). Experimental investigation of energy and exergy performance of square and circular solar ponds. *Solar Energy*, 97: 273-284. <https://doi.org/10.1016/j.solener.2013.08.013>
- [3] Aizaz, A., Yousaf, R. (2013). Construction and analysis of a salt gradient solar pond for hot water supply. *European Scientific Journal*, 9(36).
- [4] Sleiman, K., Van Vaerenbergh, S., Hamieh, T. (2021). Progress in Solar Energy and Engineering Systems. *Journal homepage*, 5(1): 26-34. <http://iicta.org/journals/PSEES>
- [5] Al Alawin, A. (2014). Performance of Solar pond Greenhouse Heating System in Jordan. *IOSR Journal of Mechanical and Civil Engineering*, 11(5): 30-35.
- [6] Khalilian, M. (2017). Experimental investigation and theoretical modelling of heat transfer in circular solar ponds by lumped capacitance model. *Applied Thermal Engineering*, 121: 737-749. <https://doi.org/10.1016/j.applthermaleng.2017.04.129>
- [7] Al-whoosh, K., Aljaradin, M., Bashitialshaaer, R., Balawneh, H. (2017). Establishing small-scale salt-gradient solar pond experiment, Dead Sea-Jordan. *Sustainable Resources Management Journal*, 2(4): 1-10. <http://doi.org/10.5281/zenodo.803396>
- [8] Bezir, N.C., Dönmez, O., Kayali, R., Özek, N. (2008). Numerical and experimental analysis of a salt gradient solar pond performance with or without reflective

- covered surface. *Applied Energy*, 85(11): 1102-1112. <https://doi.org/10.1016/j.apenergy.2008.02.015>
- [9] Ding, L.C. (2017). Power generation from salinity gradient solar ponds using thermoelectric generators (Doctoral dissertation, RMIT University).
- [10] Abbood, M.H., Alhwayzee, M., Sultan, M.A. (2021). Experimental investigation into the performance of the solar pond in Kerbala. In *IOP Conference Series: Materials Science and Engineering*, IOP Publishing, 1067(1): 012098. <https://doi.org/10.1088/1757-899X/1067/1/012098>
- [11] Abbood, M.H., Alhwayzee, M., Sultan, M.A.H. (2021). Experimental investigation for the solar pond performance with and without reflector mirrors and tracking system in Kerbela City of Iraq. *Design Engineering*, 7247-7254.
- [12] Hassan Abbood, M., Rashid, F.L., Jassim, M.M. (2022). Design and construction solar steam sterilizer. *International Journal of Nonlinear Analysis and Applications*, 13(1): 2535-2547. <https://doi.org/10.22075/IJNAA.2022.5955>
- [13] Rangaraju, P., Sivakumar, S. (2021). Comparative experimental analysis of temperature distribution in mini size permeable and non-permeable varying salt density solar pond. *International Journal of Heat and Technology*, 39(2): 486-492. <https://doi.org/10.18280/ijht.390218>
- [14] Goswami, R., Das, R. (2020). Experimental analysis of a novel solar pond driven thermoelectric energy system. *Journal of Energy Resources Technology*, 142(12). <https://doi.org/10.1115/1.4047324>
- [15] La Rocca, V., Morale, M., Peri, G., Scaccianoce, G. (2017). A solar pond for feeding a thermoelectric generator or an organic Rankine cycle system. *International Journal of Heat and Technology*, 35(1): S435-S441. <https://doi.org/10.18280/ijht.35Sp0159>
- [16] Weather forecast and temperature for today Kerbala, Iraq. <https://www.weather-atlas.com/en/iraq/Kerbala-climate>.
- [17] Vichare, R.V. (2015). Design of a solar pond as an energy storage system for the pasteurization process in dairy industry. *International Journal of Science and Research (IJSR)*, 6(11). <https://doi.org/10.21275/ART20177872>
- [18] Duffie, J.A., Beckman, W.A. (2013). *Solar engineering of thermal processes*, Fourth Edition. Chapter 1: 37.
- [19] Kumar, A., Singh, K., Verma, S., Das, R. (2018). Inverse prediction and optimization analysis of a solar pond powering a thermoelectric generator. *Solar Energy*, 169: 658-672. <https://doi.org/10.1016/j.solener.2018.05.035>
- [20] Singh, B., Remeli, F., Oberoi, A., Tan, L., Date, A., Akbarzadeh, A. (2014). Electrical power generation from low grade heat of salinity gradient solar pond using thermoelectric generators. In *Proceedings of the 52nd Annual Conference, Australian Solar Energy Society (Australian Solar Council)*, Melbourne, ISBN, 948-0.
- [21] Hashim, H.T., Rashid, F.L., Kadham, M.J. (2021). Concentration solar thermoelectric generator (CSTEG): Review paper. *Journal of Mechanical Engineering Research and Developments*, 44(1): 435-447.

Performance of Solar Pond Integrated with Thermoelectric Generator: A Theoretical Study



Hayder Noori Mohammed[✉], Mohammed Hassan Abboud[✉], Basim Sachet Atiyah[✉]

Mechanical Engineering Department, College of Engineering, University of Kerbala, Karbala 56001, Iraq

Corresponding Author Email: basim.s@uokerbala.edu.iq

<https://doi.org/10.18280/mmep.100217>

ABSTRACT

Received: 7 August 2022

Accepted: 20 January 2023

Keywords:

solar pond, magnesium sulphate, reflectors, TEG

This article intends to theoretically propose and investigate the construction of a solar pond with a salinity gradient and the generation of electrical energy from it using a thermoelectric generator. It is possible to gradually add salt (magnesium sulfate salt) to the lower layer, increasing the quantity of thermal energy supplied to the pond. According to the theoretical findings, increased heat storage in the pond's bottom layer is enhanced by the addition of salt, and reflecting mirrors help to raise the quantity of solar radiation that is directed at the pond's surface, increasing the amount of thermal energy that is absorbed through the layers of the pond. Thermal energy losses are decreased by the plastic cover that has been applied to the pond's surface. When salt, a cover, and mirrors were added to the conventional pond, the amount of useable energy increased from (2 kilowatts) to (20 kilowatts), and these modifications helped the pond's thermal efficiency rise from (5 percent) to (28.4 percent). TEG Electric Efficiency was 12% at a temperature of 65°C and a mass flow rate of 2 L/min.

1. INTRODUCTION

The importance of solar energy as being one of the major renewable energies is well known to scientists and researchers. Solar energy, which is available in the world's majority countries, can meet humanity's future energy needs. Solar energy does not, however, always exist, which is one of its limitations. It is necessary to have solar energy storage technologies because this energy is not present during overcast weather at or night. Finding a means to store this energy is required before exploring and using solar power. As a result, one technique used to store solar energy is the solar pond, which has a variety of uses [1-3]. A solar pond is a sizable body of water designed to store solar energy in heat reservoirs on the pond's bottom side, where it can later be used for practical reasons. Solar ponds are used to gather heat from the sun's rays, and the energy they contain will eventually be used for other purposes. It can run constantly all year round. A salinity gradient solar pond (SGSP) uses saltwater to capture, store, and conserve the thermal energy of the sun's descending rays. It comprises three layers: the upper convective area (surface zone), which has little salt content; solar radiation absorption; and with the excess energy being transported to the intermediate zone underneath (gradient zone). This zone can be identified by the gradient concentration of salty water, which varies with depth as measured from the upper convective zone boundaries to the lower convective zone limits. The region with the highest salt density is the lower convective zone (store zone). At the zone boundary, there is no difference in salt content. Its uniformly high salinity water is heated by solar radiation, which permeates the water's surface and saves intermediate zones at the pond's lowest point. The solar pond can be used for many purposes, including heating and cooling homes; providing heat for industrial processes; producing electricity; drying crops for

business or agriculture; desalination; heating swimming pools and greenhouses; etc. [4, 5]. TEGs have been identified as a method for both large-scale electric power generation and a different source for low power generation. According to the life cycle analysis that was done, alternative power generation methods will become more popular because of their economic benefits and their environmental friendliness as fuel prices rise. Including taking externalities into account will undoubtedly favor the use of TEG as an addition for the generation of electric power. Seebeck effect and the Peltier effect are the basis for the TEG's operation because there is a temperature gradient. The former occurrence relates to the temperature differential associated with the Seebeck coefficient (V/K), and the thermoelectric potential under open-circuit conditions [6-10]. Many studies have investigated theoretical and practically the performance and productivity of solar ponds with additions, including: Heat transmission in a brackish-gradient solar pond has been theoretically and empirically investigated by Khalilian [11]. The model examines how transit energy behaves in each section of the pond, including many procedures that impact the solar pond's efficiency. The temperature in the storage region was measured both theoretically and practically. The findings showed that evaporation, rather than convection and radiation, accounts for most heat loss from the pond surface. The thickness of the lower load region can be adjusted depending on the application, while the thickness of the top load area should be as thin as possible. The stored temperature of a pond was found to be significantly impacted by wall shade, whereas a large pond's effect was determined to be minimal. The impact of the solar pond's design when covered with plastic glazing was examined by Assari et al. [12]. Solar ponds similar in size and area to one another but with a distinct geometric shape—rectangular as opposed to circular—have been examined. At the conclusion of the research, it was discovered

that the maximum temperature in the rectangular pond was higher. The equations also show how variables like geographic location, radiation angle, pond size, and the day and time of year affect the shadow area produced in each of the solar ponds. So, The rectangular solar pool was shaded less than a result, according to the results. The rectangular solar pond's shaded area appears to have shrunk. The solar pond in UCZ had a temperature that was considerably different from the surrounding air because of the glass, plastic used in solar pond construction. Heat couldn't escape from the pond's surface because of the glass cover. As a result, heat was kept in the ponds, raising the temperature in the UCZ. At the conclusion of the test, it was also noted that there was a 13°C temperature differential between the UCZ in the solar ponds and the ocean. The plastic glass handled the temperature discrepancy. The difference in temperature between the circular and rectangular solar ponds at the conclusion of the testing period was 12 degrees and 9 degrees Celsius, respectively. A mathematical model was designed to simulate the performance of a solar pond used to collect thermal energy in the Iraqi city of Kerbela by Mahdi [13]. Calculating the incident solar radiation on the pond's surface required the usage of Fortran software. The water temperature was then calculated using the finite difference approach. The findings corroborated earlier meteorological data. The lower layer of the pond's water reached a maximum temperature of 90°C, and more solar radiation than 7 kW/m² was received. The findings suggest that the city of Kerbela is suited for creating a solar pond and using it for a variety of purposes. Sogukpinar 2019's [14] used COMSOL software to determine how a solar pond with a salinity gradient and a square surface area operates and how much energy it produces. It was discovered that there was a good agreement between the numerical outcomes of this work and the experimental outcomes of earlier investigations. These findings show that the solar pond system is a successful method for supplying hot water for many uses, including the production of electricity, and that the highest temperature of the water in the solar pond is approximately 55 degrees Celsius. Rizvi et al. [15] describe how adding reflectors to the solar pond's sides and covering the water's surface with a cover can improve the solar pond's efficiency and the amount of radiation it receives. The maximum water temperature reached was about 65°C, which is a rise of about 28% over the average situation (without installing reflectors or covering the pond deck). Kumar [16] studied Theoretically, the performance evaluation and boost of a salt-gradient solar pond incorporates a thermoelectric generator in its top layer. A genetic algorithm was used to solve an inverse optimization issue in order to determine the ideal size of various zones while taking into account the minimal temperature differential throughout the TEG. To show the thermal performance and power generation under various circumstances, parametric simulations of different meteorological data from India were looked at. The developed system enabled improved performance in comparison to the literature while having an about 18.11 percent lower height. A net heat transfer coefficient was used by Verma and Das [17] to study heat extraction from the gradient layer of a solar pond with a more realistic perspective. The thermal efficiency of the solar pond was studied for research purposes, the temperature distribution in the gradient layer was established by an analytical method. The outcomes demonstrated that the idealized assumptions under-predicted the exergy destruction rate and gradient zone optimum thickness.

The current work aims to provide a theoretical study to improve the performance of the solar pond with salt (magnesium sulfate) and the addition of reflective mirrors, this to conserve thermal energy in the solar pond's bottom layer. As well as verifying the possibility of benefiting from the thermal energy of the pond to produce electrical energy using a thermoelectric generator (TEG). This is done by feeding TEG from one side with hot water produced from the solar pond in theory, while cold water is pumped from the other side TEG to create a temperature difference on both ends TEG to produce an electrical potential difference to be used in certain applications. This work is theoretically carried out in the city of Karbala, Iraq.

2. SOLAR POND CONSTRUCTION

The test rig for the current investigation is a solar pond with a salinity gradient. The solar pond's construction was raised by the following measures: Reflective mirrors are added once the plastic covering applies to the pond's sides. Finally, the inside and edges of the pond were covered with glass, mirrors, and black stones. In Figure 1, the schematic diagram is shown. The pyramidal design and salt gradient were used in the production of the solar pond. The pond is 6.25 square meters on top, 1.35 meters deep, and 0.64 square meters at its bottom. There is a 60-degree tilt in the pond's walls.

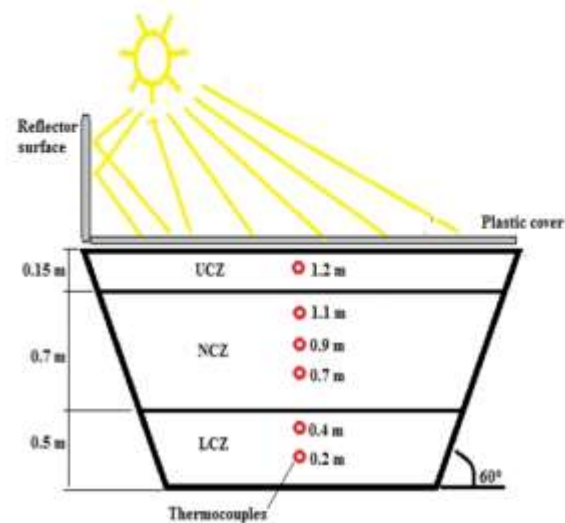


Figure 1. A solar pond schematic with secondary, measurement, and modification devices

3. MATHEMATICAL MODELLING

Heat Analysis of Lower Convective Zone:

$$H_L = Q_{cond,4} + \left(\frac{\partial T}{\partial t} * \rho_{LCZ} * C_{pLCZ} * X_{LCZ} \right) \quad (1)$$

where, H_L is the thermal energy entered into the lower convective zone $Q_{cond,4}$ is the thermal energy exited from the lower zone $\frac{\partial T}{\partial t} * \rho_{LCZ} * C_{pLCZ} * X_{LCZ}$ is the thermal energy kept in the lowest zone of the solar pond.

$$Q_{cond.A} = -K_{LCZ} \frac{\partial T_n^t}{\partial x} \quad (2)$$

The finite difference of brine temperature of the pond lower zone (LCZ) can be determined by the next equation:

$$T_L^{t+1} = T_L^t + \frac{\Delta t}{\rho_{LCZ} \cdot C_{PLCZ} \cdot X_{LCZ}} \left[(H_L) + \frac{K_{LCZ}(T_L^t + T_n^t)}{X_{LCZ}/2} \right] \quad (3)$$

The solar pond useful thermal energy (Qu) can be determined by the following equation [18]:

$$Q_u = M_s C p_s \Delta T \quad (4)$$

where, M_s is the solar pond brine mass of, $Caps$ is the pond brine heat capacity of and ΔT is the average temperature difference between the ambient and lower zone.

The solar pond thermal efficiency (η) can be calculated by division of the useful energy (Qu) on the quantity of incident sun light on the pond surface (I) as follows [18]:

$$\eta = Q_u / I \quad (5)$$

The incident sun light on the pond surface (I) can be found by the following equation:

$$I = I_0 \cdot A \quad (6)$$

where, A is the solar pond surface area.

TEG electrical power generated is given as studies [19-23]:

$$P_{TEG} = I \cdot V \quad (7)$$

$$V_{TEG} = \alpha \cdot \Delta T \quad (8)$$

where, $(ap-an)=a$ and $(Th-Tc)=\Delta T$, Tc and Th denote the cold and hot junction temperature. ap and an are the Seebeck coefficient of P and N type TEG leg respectively.

The following equation may represent short circuit and open circuit relationships in a TEG with N number of couples.

$$V_{TEG} = 2 \cdot N \cdot \alpha \cdot \Delta T \quad (9)$$

$$I_{TEG} = \left(\frac{\alpha}{\rho} \right) \cdot \left(\frac{A_{TEG}}{L} \right) \cdot \Delta T \quad (10)$$

Electrical resistivity of thermo element material, ($\rho \Omega \text{ cm}$). Area of thermo element, ($A_{TEG} \text{ mm}^2$). Length of thermo element, $L \text{ mm}$.

The thermoelectric power is related to dimensionless figure of merit given by:

$$ZT = \alpha^2 \cdot \sigma \cdot T / K \quad (11)$$

where, α is the TEG Seebeck coefficient, k and σ are the thermal conductivity and electrical and T is the absolute temperature.

For calculating the efficiency of TEG, the following equation is used.

$$\eta_{TEG} = (T_h - T_c) / T_h \cdot \frac{(1 + ZT)^{0.5} - 1}{(1 + ZT)^{0.5} + \left(\frac{T_c}{T_h} \right)} \quad (12)$$

4. THEORETICAL RESULTS

In theory, the study is carried out using the MATLAB program to resolve the governing equations and constrained flowcharts in this program such as theories of solar radiation falling on the solar pond surface and the mathematical calculations to compute it. It also includes analyzes of heat transfer through the lower layer of the solar pond. In addition, the mathematical equations for calculating the heat loss and the energy saved in the solar pond are shown, the mathematical equations are revealed to determine the thermal efficiency and the solar pond useful energy, the thermoelectric generator, the energy generated from it and its efficiencies. Here, magnesium sulfate salt is used at a concentration of 28 percent with the use of a plastic cover with reflective mirrors. The following results indicating the water temperatures in the pond layers in three different scenarios, were obtained by applying special equations to two types of ponds: Standard pond and salt gradient pond with addition of cover and reflective mirrors.

Water can convert solar radiation into heat energy when exposed to it, which it then stores inside its layers. Figure 2 displays numerically the water temperatures in the salt-free pond throughout a 24-hour period. The results show that during the period of solar radiation, as more radiation enters the water, the temperature rises; after sun set, as the angle of the sun's light as it strikes the pond's surface changes, the temperature falls.

Figure 3 demonstrates that the pond layer has become warmer overall, but particularly in the bottom layer. The effect of salting the water, which produces a brine solution that absorbs solar energy and converts it into thermal energy inside the pond, is what causes this.

In contrast to the previous case, where the salinity gradient pond was left exposed to the elements, Figure 4 illustrations the effects of covering the solar pond's surface with plastic. The lowest layer of the pond's temperature is clearly rising, as seen by the graph. Because of the cover's large reduction in water evaporation and consequent reduction in heat loss from the pond, the pond's functionality is affected.

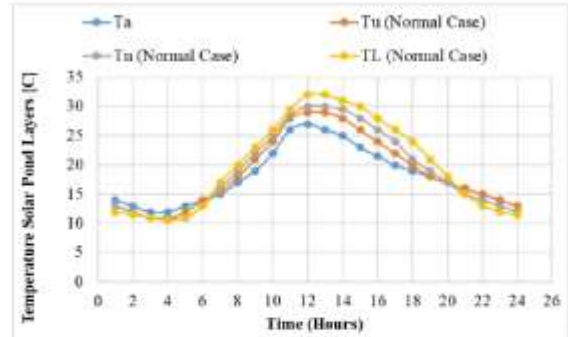


Figure 2. Temperature of the three layers of the normal solar pond

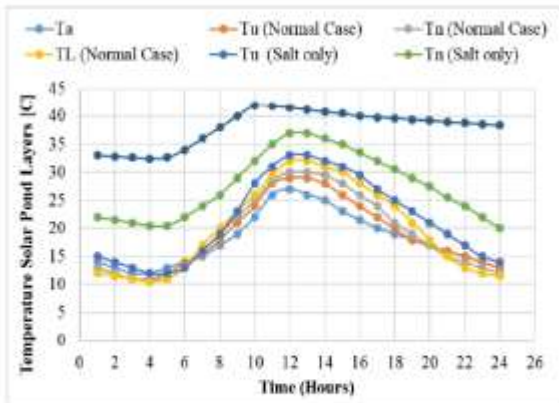


Figure 3. The three-layer salinity solar pond's temperatures

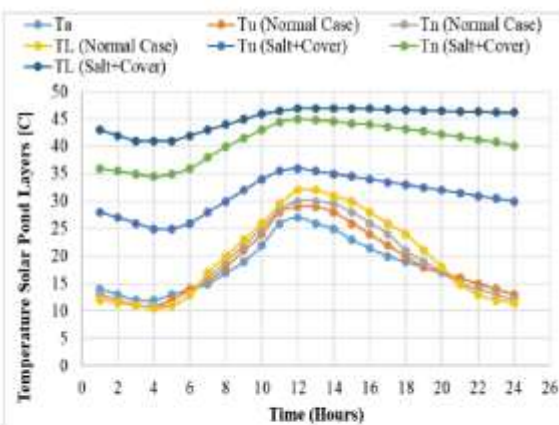


Figure 4. Temperature of the three layers of the covered salty solar pond

Because the solar radiation amount on the surface of the pond affects the quantity of thermal energy kept in the layers of the pond, any increase in the radiation shed on the pond's surface shows a growth in the thermal energy stored in the pond. This is where the reflective mirrors on the sides of the pond come into play, boosting the amount of radiation by redirecting the sun's rays away from its surface and toward the surface of the pond. This is depicted in Figure 5.

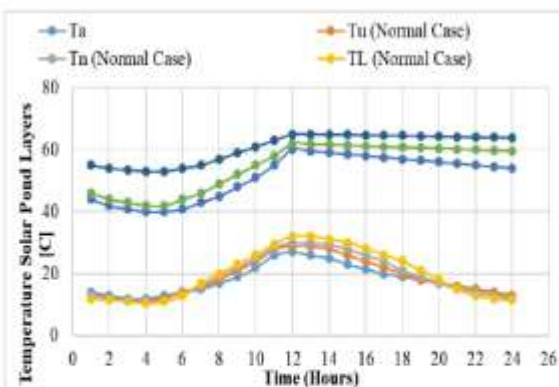


Figure 5. Temperature of the three layers of the covered salty solar pond with the reflectors

Theoretical results using additive methods are shown in Figure 6 for usable energy in a solar pond with a normal pond and a salt gradient pond. Given that the reflective mirrors and cover raised the pool's temperature, more usable energy would almost certainly be generated. This is because it is directly related to temperature. According to the theoretical results, the pond has a usable power of 2 kW. Salts are added to this quantity to reach 7.5 kilowatts. The highest value of usable energy during the study is close to 20 kW due to the increase in radiation that reaches the pond surface caused by the addition of salts, reflecting mirrors and cover. The substrate's internal heat storage system benefits from the addition of salts as well.

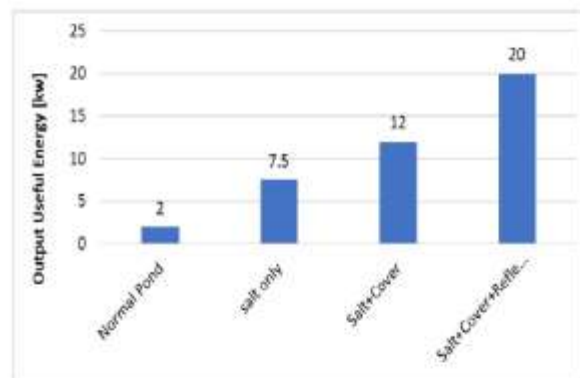


Figure 6. Output useful energy of solar pond [kw]

Figure 7 displays the efficiency outcomes of the solar-powered pond with a salinity gradient and the standard pond. Adding gravel, cover, and reflective mirrors has made the pond more efficient. The efficacy of the ponds is increased by this technique because it improves the amount of energy that can be used by the solar pond, which is directly proportional to the solar pond's thermal efficiency. The solar pond's efficiency increased with improvements, going from 5% to 28.4%.

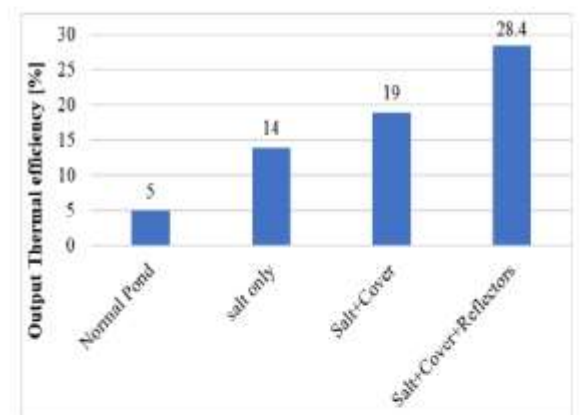


Figure 7. Output overall thermal efficiency of solar pond [%]

Figure 8 displays the current produced by TEG because of temperature differences and for three water flow rates via the tubes in contact with the electrodes. (TEG). It should be noted that the current value increases along with the flow rate. Because all the water in contact with the TEG at high speeds

is of the same intensity, all the TEG chips function at the same productivity. Regarding the growth and its cause, Figure 9 shows behavior similar to that of the prior graph. The electrical potential differential (TEG) for three different water flow rates is depicted on the graph. According to the same principle, the increased flow rate happens as the electric potential difference widens. The electric power is calculated from the current and electrical potential difference induced by the flow of hot and cold water at three different flow rates on both sides of the TEG (TEG). This is depicted in Figure 10.

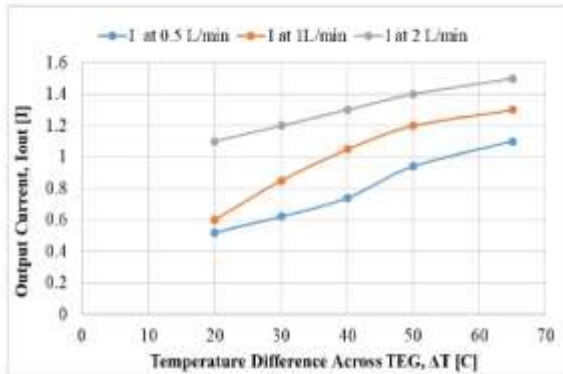


Figure 8. The output current, I_{out} [A] for temperature difference across TEG, ΔT [C]

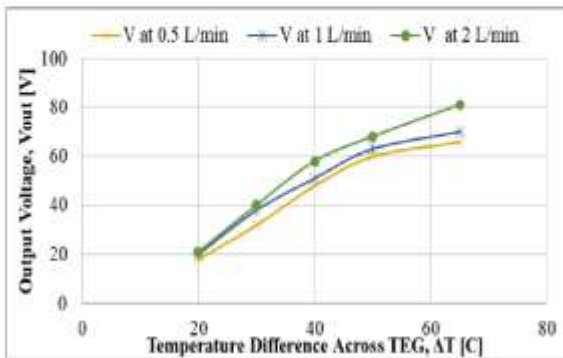


Figure 9. The output voltage, V_{out} [V] for temperature difference across TEG, ΔT [C]

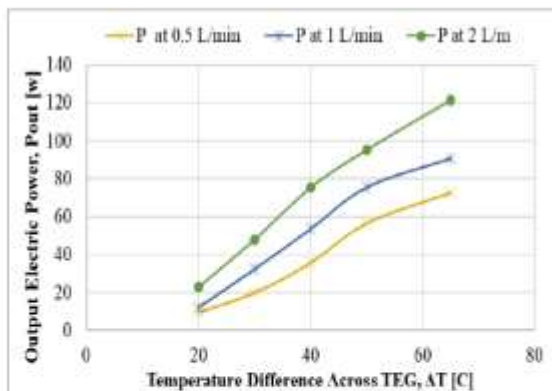


Figure 10. The output electric power, P_{out} [w] for temperature difference across TEG, ΔT [C]

The electrical efficiency of the TEG is calculated using the electrical energy produced by the TEG and three flow rates, as shown in Figure 11. Since it can be seen in the figure that increasing mass flow rate enhances thermal efficiency, the best mass flow rate throughout the tests was 2 liters per minute.

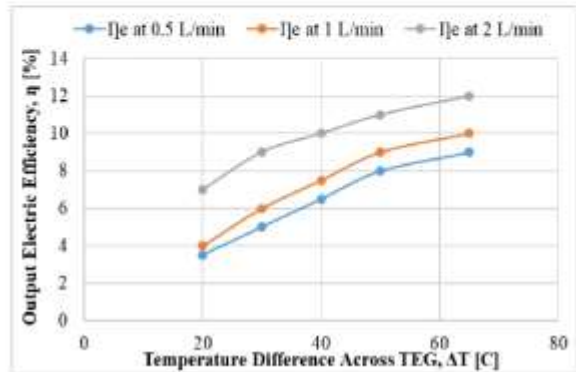


Figure 11. The output electric efficiency, η [%] for temperature difference across TEG, ΔT [C]

5. CONCLUSIONS

According to the theoretical findings got with the help of the Matlab software:

(1) While reflective mirrors help to raise the intensity of solar radiation directed at the pond's surface, which serves to raise the amount of heat energy absorbed through the pond's layers, the addition of salt helps to increase the amount of heat energy stored in the lower layer.

(2) The plastic cover that has been added to the pond's surface helps to cut down on thermal energy losses.

(3) When salt, a cover, and mirrors were added, the quantity of useful energy increased from 2 kilowatts to 20 kilowatts when compared to the conventional pond.

(4) These improvements allowed the pond's thermal efficiency to rise from 5 percent to 28.4 percent.

(5) TEG efficiency was 12% at a temperature of 65°C and a mass flow rate of 2 L/min.

REFERENCES

- [1] Ali, M.M., Ahmed, O.K., Abbas, E.F. (2020). Performance of solar pond integrated with photovoltaic/thermal collectors. *Energy Reports*, 6: 3200-3211. <https://doi.org/10.1016/j.egy.2020.11.037>
- [2] Jassim, M.M., Abbood, M.H., Rashid, F.L. (2022). Design and construction solar oven sterilizer. *International Journal of Heat and Technology*, 40(2): 641-645. <https://doi.org/10.18280/ijht.400235>
- [3] Rasheed, R.M., Jabbar, S.A.A.S., AL Hussiny, N.M., Rasheed, A.M. (2021). Study of optimum performance of solar still process under weather conditions of Baghdad. *International Journal of Nonlinear Analysis and Applications*, 12(Special Issue): 1355-1366. <https://doi.org/10.22075/ijnaa.2021.5712>
- [4] Al-Musawi, O.A., Khadom, A.A., Manhood, H.B., Mahdi, M.S. (2020). Solar pond as a low grade energy source for water desalination and power generation: A

- short review. *Renewable Energy and Environmental Sustainability*, 5: 4. <https://doi.org/10.1051/rees/2019008>
- [5] Panchal, H., Sadasivuni, K.K., Essa, F.A., Shanmugan, S., Sathyamurthy, R. (2021). Enhancement of the yield of solar still with the use of solar pond: A review. *Heat Transfer*, 50(2): 1392-1409. <https://doi.org/10.1002/htj.21935>
- [6] Mamur, H., Dilmaç, Ö.F., Begum, J., Bhuiyan, M.R.A. (2021). Thermoelectric generators act as renewable energy sources. *Cleaner Materials*, 2: 100030. <https://doi.org/10.1016/j.clema.2021.100030>
- [7] Ding, L.C., Akbarzadeh, A., Tan, L. (2018). A review of power generation with thermoelectric system and its alternative with solar ponds. *Renewable and Sustainable Energy Reviews*, 81: 799-812. <https://doi.org/10.1016/j.rser.2017.08.010>
- [8] Hakim, I.I., Putra, N., Ananda, Y.O. (2020). Investigation on the use solar thermoelectric generator for open pond cultivation with heat pipe cooling. *Engineering Journal*, 24(4): 295-304. <https://doi.org/10.4186/ej.2020.24.4.295>
- [9] Wicaksono, R.M., Yunesti, P. (2021). Study of thermoelectric generator utilization to recover heat at low temperature grade application: A review. *Journal of Science and Applicative Technology*, 5(2): 313-318.
- [10] Özbaş, E. (2019). Experimental investigation of passive water cooling in solar heating thermoelectric generator. *Politeknik Dergisi*, 23(4): 1231-1236. <https://doi.org/10.2339/politeknik.613095>
- [11] Khalilian, M. (2017). Experimental investigation and theoretical modelling of heat transfer in circular solar ponds by lumped capacitance model. *Applied Thermal Engineering*, 121: 737-749. <https://doi.org/10.1016/j.applthermaleng.2017.04.129>
- [12] Assari, M.R., Tabrizi, H.B., Nejad, A.K., Parvar, M. (2015). Experimental investigation of heat absorption of different solar pond shapes covered with glazing plastic. *Solar Energy*, 122: 569-578. <https://doi.org/10.1016/j.solener.2015.09.013>
- [13] Mahdi, J.T., Jebbar, Y.A. (2019). A theoretical investigation of solar radiation and heat transfer in a solar pond in Karbala city. In *AIP Conference Proceedings*, 2144(1): 030019. <https://doi.org/10.1063/1.5123089>
- [14] Sogukpinar, H. (2019). Seasonal temperature variation of solar pond under Mediterranean condition. *Thermal Science*, 23(6 Part A): 3317-3326. <https://doi.org/10.2298/TSCI180518060S>
- [15] Rizvi, R.Z., Jamal, Y., Ghauri, M.B., Salman, R., Khan, I. (2015). Solar pond technology for brine management and heat extraction: A critical review. *Journal of Faculty of Engineering & Technology*, 22(2): 69-79.
- [16] Kumar, A., Singh, K., Verma, S., Das, R. (2018). Inverse prediction and optimization analysis of a solar pond powering a thermoelectric generator. *Solar Energy*, 169: 658-672. <https://doi.org/10.1016/j.solener.2018.05.035>
- [17] Verma, S., Das, R. (2020). Revisiting gradient layer heat extraction in solar ponds through a realistic approach. *Journal of Solar Energy Engineering*, 142(4): 041009. <https://doi.org/10.1115/1.4046149>
- [18] Abbood, M.H., Allwayzee, M., Sultan, M.A. (2021). Experimental investigation into the performance of the solar pond in Kerbala. In *IOP Conference Series: Materials Science and Engineering*, 1067(1): 012098. <https://doi.org/10.1088/1757-899X/1067/1/012098>
- [19] Jouhara, H., Żabnieńska-Góra, A., Khordehgah, N., Doraghi, Q., Ahmad, L., Norman, L., Dai, S. (2021). Thermoelectric generator (TEG) technologies and applications. *International Journal of Thermofluids*, 9: 100063. <https://doi.org/10.1016/j.ijft.2021.100063>
- [20] Allouhi, A. (2019). Advances on solar thermal cogeneration processes based on thermoelectric devices: A review. *Solar Energy Materials and Solar Cells*, 200: 109954. <https://doi.org/10.1016/j.solmat.2019.109954>
- [21] Hashim, H.T., Rashid, F.L., Kadham, M.J. (2021). Concentration solar thermoelectric generator (CSTEG): Review paper. *Journal of Mechanical Engineering Research and Developments*, 44(1): 435-447.
- [22] Hassan Abbood, M., Rashid, F.L., Jassim, M.M. (2022). Design and construction solar steam sterilizer. *International Journal of Nonlinear Analysis and Applications*, 13(1): 2535-2547. <https://doi.org/10.22075/ijnaa.2022.5955>
- [23] Rashid, F.L., Fayyadh, I.K., Hashim, A. (2012). Design of solar pond for electricity production. *British Journal of Science*, 3(2).

Error Analysis

A study of errors is the first step toward determining the accuracy of the final test result and finding solutions to reduce them

Random Errors

Random mistakes, in addition to Human errors, are errors that are outside the control of the researcher, such as fluctuating temperatures, and so on, and cannot be quantified precisely. The random mistakes in an experiment are usually estimated using statistical methods based on the repeatability of the data

Systematic Errors

Systematic errors can be generated by employing an uncalibrated instrument or wrongly ignoring the impacts of an influencing parameter. Under the same measurement conditions, these errors will have the same size and direction. In practice, the magnitude of systematic mistakes is impossible to estimate

Uncertainty

Uncertainty is a measurement of the degree of uncertainty regarding a measurement result. To calculate a measurement's uncertainty, first identify the sources of uncertainty in the measurement, then estimate the amount of the uncertainty from each source. Corrections from calibration certificates address known errors, but any error whose amount we don't know is a cause of uncertainty Holman [60]

:[The absolute error can be calculated by from below .

$$E_a = X^i - X^t$$

$$E_r = \left(\frac{X^i - X^t}{X^t} \right) * 100$$

Where

E_a is absolute error.

X^i is true value.

X^t is measured value.

E_r is Percentage or relative error.

الخلاصة

تعتبر الشمس مصدر طاقة نظيفاً ومجانياً ويمكن الوصول إليه بسهولة. تعد مجمعات الطاقة الشمسية والبرك الشمسية المقطرات الشمسية أمثلة قليلة على الاستخدامات المتنوعة للطاقة الشمسية. أصبحت الطاقة الشمسية شائعة في السنوات الأخيرة لمعالجة مشكلة ندرة الطاقة العالمية.

في الدراسة الحالية ، تم استقطاب الطاقة الشمسية وتخزينها في بركة شمسية ملحية متدرجة (تم استخدام ملح كبريتات المغنيسيوم في هذه الدراسة). باستخدام TEG ، تم الاستفادة من هذه الطاقة المنتجة في البركة الشمسية لتوليد الكهرباء. كما تم فحص ما إذا كانت إضافة الحصى ستزيد من كمية الحرارة المحتجزة في البركة. بالإضافة إلى وضع مرآيا عاكسة وبسلك 3 سم لتركيز شدة الإشعاع الشمسي على سطح البركة.

تم التحقق من صحة النموذج باستخدام بركة هرمية مساحتها 0.64 م². إلى جانب ذلك تبلغ مساحة السطح 6.25 م² ، ويبلغ عمقها 1.35 م. تميل جدران البركة بزاوية 60 درجة.

أظهرت النتائج النظرية (باستخدام برنامج MATLAB version 2014) أن إضافة الملح يحسن تخزين الحرارة في الطبقة السفلية للبركة وأن كمية الإشعاع الشمسي التي تنعكس بواسطة المرآيا العاكسة تزيد من كمية الطاقة الحرارية التي يتم امتصاصها من خلال طبقات البركة. يقلل الغطاء البلاستيكي أو الزجاجي الذي تم وضعه على سطح البركة من فقد الطاقة الحرارية. ارتفعت كمية الطاقة القابلة للاستخدام من 2 كيلوات إلى 22 كيلوات بعد إضافة الملح والغطاء والمرآيا والحصى إلى البركة التقليدية. ساعدت هذه التغييرات في رفع درجة حرارة البركة مما زاد الكفاءة من 5 في المائة إلى 32 في المائة. مع معدل تدفق يبلغ 2 لتر في الدقيقة ودرجة حرارة 60 درجة مئوية ، بلغت الطاقة والكفاءة الكهربائية لـ TEG 121.5 واط و 12% على التوالي.

ووفقاً للنتائج التجريبية ، فإن إضافة غطاء بلاستيكي أو زجاجي ومرآيا عاكسة وحصى أدى إلى زيادة الكفاءة التشغيلية للبركة من 3% إلى 28%. زادت كمية الطاقة المفيدة من 2 كيلوات إلى 20.94 كيلوات. حققت كل من القدرة الكهربائية والكفاءة التشغيلية 104 واط و 9% لـ TEG ، عند درجة حرارة الطبقة السفلى البالغة 60 درجة مئوية.

وقد تبين من خلال النتائج المتحصلة وتحليل نسبة الخطأ أن النتائج النظرية والعملية متقاربة بنسبة 6%.

الكلمات المفتاحية: بركة شمسية ، ملح كبريتات المغنيسيوم ، مولد كهربائي حراري.



جمهورية العراق
وزارة التعليم العالي و البحث العلمي
جامعة كربلاء
كلية الهندسة
قسم الهندسة الميكانيكية

فحص أداء المولد الكهروحراري المقترن بالبركة الشمسية.

رسالة مقدمة الى مجلس كلية الهندسة / جامعة كربلاء وهي جزء من متطلبات نيل درجة الماجستير في علوم الهندسة
الميكانيكية

المؤلف:

باسم ساجت عطية

بإشراف :

ا.م.د. محمد حسن عبود

د. حيدر نوري محمد